Thesis for doctoral degree (PhD)

February, 2019

Development of an Efficient Test for Autoimmune disease using Gold Nanoparticles

Anantdeep Kaur

Faculty of Science

15 Broadway, Ultimo NSW 2007

CERTIFICATE OF ORIGINAL AUTHORSHIP

I, Anantdeep Kaur declare that this thesis, is submitted in fulfilment of the requirements for the award of PhD degree, in the Faculty of Science at the University of Technology Sydney.

This thesis is wholly my work unless otherwise reference or acknowledged. In addition, I certify that all information sources and literature used are indicated in the thesis.

This document has not been submitted for qualifications at any other academic institution. This research is supported by an Australian Government Research Training Program Scholarship.

Anantdeep Kaur

Production Note:
Signature removed prior to publication.

15/2/2019

ACKNOWLEDGEMENTS

Foremost I would like to express my sincere gratitude to my supervisor's Dr Olga Shimoni and Prof Michael Wallach for believing in me and giving me the opportunity to work on this project. It has been a great learning experience that was made possible by their continuous encouragement and support. I will forever be grateful to them for their continuous support and guidance. I'm thankful to you for being such a wonderful mentors for guiding me through the research.

I would also like to thank Dr Jason Tye-Din, Chair Coeliac Australia, MBBS, PhD, FRACP, Immunology Division, The Walter and Eliza Hall Institute of Medical Research, Parkville, Victoria, Australia, for providing clinical samples as well for his constant support, guidance and words of wisdom. I am thankful for his suggestions and guidance during the course of the study. I am thankful to the University of Technology Sydney Research Ethics committee for providing ethical approval for the clinical research.

The time I have spent in lab with such a wonderful and kind team has left me with very fond memories of my PhD study. I would like to express my sincere thanks to Ying, David, Alex, Yvonne, Wei, Jacquilene for promoting a stimulating and welcoming social environment in the lab and for their continuous support and kind words. I am also thankful to Buket Demrici for her support and encouragement.

My sincere thanks to my family for their extended support throughout this journey. My parents, my brother have given me their unequivocal support throughout, as always, for which mere expression of thanks likewise does not suffice. I am thankful to you for believing in me and providing me with this beautiful chance to make my dreams come true.

Last, but by no means least, I would like to acknowledge the financial support of the Australian Government and the Science Faculty at UTS, particularly in the award of an Australian Government Research Training Program Scholarship and travel grants that provided necessary financial support for this project.

List of patents and papers

Patent Entitled: Nanoparticles adsorbed with gliadin molecules

Patent date Issued Feb 15, 2018

Patent issuer and number: AU International Patent Application PCT/AU2018/050125. This work has been published with International Publication No. WO 2018/148801.

Kaur, A., Shimoni, O. & Wallach, M. 2017, 'Coeliac disease: from etiological factors to evolving diagnostic approaches', Journal of Gastroenterology, vol. 52 (9), pp. 1001–1012. https://doi.org/10.1007/s00535-017-1357-7*.

Kaur, A., Wallach, M. & Shimoni, O. 2018, 'A novel diagnostic test for coeliac disease using gliadin coated gold nanoparticles' (under review).

Kaur, A., Shimoni, O. & Wallach, M. 2018, 'A novel screening test for coeliac disease using peptide functionalised gold nanoparticles', World Journal of Gastroenterology, vol. 24(47), pp. 5379-5390*.

* Papers reprinted with permission from Publishers

Statement of contribution of authors

Paper I: Coeliac disease: from etiological factors to evolving diagnostic approaches

Author contributions: I (Anantdeep Kaur) researched and reviewed the literature and analysed data. I (Anantdeep Kaur) wrote the paper with critical revisions related to the intellectual content of the manuscript from Prof Michael Wallach and Dr Olga Shimoni.

Paper II: Novel diagnostic assay for coeliac disease using gliadin coated gold nanoparticles

Author contributions: Dr Olga Shimoni and Prof Michael Wallach designed research, I (Anantdeep Kaur) performed research and analysed data. I (Anantdeep Kaur) wrote the paper with critical revisions related to the intellectual content of the manuscript from Prof Michael Wallach and Dr Olga Shimoni.

Paper III: A novel screening test for coeliac disease using peptide functionalised gold nanoparticles

Author contributions: Dr Olga Shimoni and Prof Michael Wallach designed research, I (Anantdeep Kaur) performed research and analysed data. I (Anantdeep Kaur) wrote the paper with critical revisions related to the intellectual content of the manuscript from Prof Michael Wallach and Dr Olga Shimoni.

Awards and Prizes

UTS Academic Excellence Grant, 2013

University of Technology Sydney

The Australian Government Research Training Program Scholarship, 2015

Department of Industry, Innovation Science, Research and Tertiary Education

Australian Government

Runner up UTS Science 3 Minute Thesis (3MT) Competition, 2017

3MT Topic: 'To go gluten free or not?'

University of Technology Sydney

Table of Contents

List of Tables and Figures

List of Abbreviations

CD	Coeliac Disease
AGA	Anti-gliadin antibody
RCD	Refractory Coeliac Disease
HLA	Human Leukocyte Antigen
MHC	Major Histocompatibilty Complex
TG2	Tissue Transglutaminase
FADD	Fas associated via death domain
DED	Death Effector Domain
IL	Interleukin
NK	Natural killer
TCR	T cell receptor
LMW	Low molecular weight
CDR	Complementarity determining region
DGP	Deamidated gliadin peptides
Ig	Immunoglobulin
Anti-EMA	Anti-endomysial antibodies
Anti-tTG	Anti-transglutaminase antibodies
Anti-DGP	Anti-Deamidated gliadin peptide
MMR	Mumps and Rubella vaccine
HAV	Hepatitis A Virus
EGF	Epidermal Growth Factor
NCGS	Non Coeliac Gluten Sensitivity
IFA	Indirect immunofluorescence

RIA	Radioimmunoassay
GFD	Gluten free diet
SPR	Surface plasmon resonance
DIG	Diffusion in gel
IBD	Inflammatory bowel disease
GIP	Gluten immunogenic peptides
AuNP	Gold Nanoparticle
LSPR	Localised Surface Plasmon Resonance
PEG	Polyethylene glycol
ELISA	Enzyme linked immunosorbent assay
HCG	Human Chorionic Gonadotrophin
Mab	Monoclonal antibody
CTAB	Cetyl trimethylammonium bromide
IPA	Isopropyl Alcohol
BSA	Bovine Serum Albumin
HEPES	4-(2-hydroxyethyl)-1-piperazineethanesulfonic acid
PBS	Phosphate Buffer Saline
DLS	Dynamic Light Scattering
℃	Celsius
Å	Angstorm
kDa	kiloDalton

ABSTRACT

Coeliac disease results because of an unusual immune response to the digestion of gliadin protein. Patients suffering from the disease show varying degrees of chronic inflammation within the small intestine ranging from mild lesions to completely flat mucosa. The immune response in turn, leads to the production of a number of cytokines and antibodies that are linked to the disease and its pathological effects. The released antibodies can be used as specific biomarkers for developing reliable diagnostic tests. Over the years, different approaches like the use of mucosal biopsy, genetic typing of the disease associated gene, gliadin induced cytokines, antibodies and auto-antibodies have been used to develop diagnostic tests for coeliac disease. However, in spite of the encouraging initial results in terms of sensitivity and specificity, the existing tests have limited scope as point-of-care tests.

The current study was aimed at developing a coeliac diagnostic assay based on the properties of the gold nanoparticles combined with the specificity of the antibodies from serum as well as saliva. In this study, I developed a novel diagnostic test for coeliac disease based on the coating of gold nanoparticles with gliadin, the highly antigenic protein responsible for inducing the symptoms of coeliac disease. A novel protocol for binding the hydrophobic gliadin protein on the surface of the gold nanoparticles was developed in this study. This was followed by the development of a simple, single antibody serology based diagnostic test.

Finally, I used the assay on thirty patient serum samples in a blinded assessment and compared the results with the data from previously run serological and pathological tests on these patients. When tested on real patient samples, the data showed that the developed assay had an overall accuracy of over 96%.

Furthermore, I developed an assay based on the coating of gold nanoparticles with a peptide sequence derived from gliadin. To develop the serological assay based on the peptide functionalised nanoparticles, I first established a stable suspension of peptide coated gold nanoparticles and then tested the assay on spiked serum samples. I then used the assay to test thirty patient serum samples and found that the peptide functionalised nanoparticle-based assay could distinguish coeliac disease from non-coeliac disease patients with an accuracy of 86.6%.

This study demonstrates the potential of gold nanoparticle-based approach to be adapted for developing a point-of-care screening assay for diagnosis for CD. The developed assay could be a part of an exclusion based diagnostic strategy and prove beneficial for testing high coeliac disease risk populations.

CHAPTER I

Coeliac disease: from etiological factors to evolving diagnostic approaches

1.1 General introduction to coeliac disease

Coeliac disease (CD) is a chronic disorder that damages the small intestine and is caused by consuming gluten proteins that are present in wheat and other cereals [Ludvigsson et al. 2013]. Patients with CD show varying degrees of chronic inflammation within the small intestine due to an aberrant immune response to gluten. Gliadin is one of the two major protein groups that comprises gluten and plays a key role in causing the disease. CD is described as an immune mediated response to the antigen-gliadin. The innate immune response is initiated following the T cells recognition of the gliadin epitopes that further stimulates the release of T cell surface molecules such as CD4, CD8 as well as natural killer (NK) cells. The release of pro-inflammatory cytokines in turn damages the small intestine. As a result, cytokines and antibodies are produced in patients with CD that can be used as specific biomarkers to develop diagnostic tests.

There has been an increasing number of developments of a wide range of diagnostic tests for CD following the advances in pathophysiology, immuno-molecular biology and diagnostic technologies. The existing detection test methods on the market, however, have limited narrow adaptability for use for the early, rapid identification and quantification of CD. As the number of sufferers with CD are rapidly increasing, there has become an immediate need to develop cheap, accurate, simple and safe diagnostic tools that would be widely available to the general public.

This thesis is divided into various chapters; chapter I describes CD pathogenesis and current diagnostic tests, chapter II discusses the properties of gold nanoparticles and their applicability in developing novel biosensors, chapter III discusses the materials and methods used in the

experiments. Chapter IV discusses the development of a novel diagnostic assay for CD using gliadin coated gold nanoparticles while chapter V explains the development of a novel screening test for CD using peptide functionalised gold nanoparticles. Chapter VI concludes the results obtained in the study and provides an outlook to the future work.

Chapter I has been published as a review paper, titled, 'coeliac disease: from etiological factors to evolving diagnostic approaches' in the Journal of Gastroenterology, 2017.

This chapter describes CD in terms of its etiological cause, pathological effects, current diagnostic tests based on mucosal biopsy and the genetic basis for the disease. In addition, it discusses the use of gliadin induced cytokines, antibodies and auto-antibodies as a diagnostic tool for CD. In spite of good initial results using these diagnostic tests in terms of sensitivity and specificity, when these immunological tests were used on a large scale even in combination with genetic testing, the results were found to have a lowered sensitivity value. I address the issue of low sensitivity value and provide an outlook on the future work using new sensing platforms namely, gold nanoparticles that can be applied to develop novel diagnostic tests to help in the diagnosis for CD. The development of such an efficient diagnostic test is required to achieve an accurate diagnosis to predict CD in the general public avoiding invasive tests, such as endoscopy and mucosal biopsy.

1.2 CD Prevalence

Epidemiological studies have provided evidence on the world-wide distribution of CD. During the past few decades, the incidence of the disease has increased significantly. In developed countries such as USA, a high prevalence rate of CD ranging from 0.7 per cent has been reported while in Europe a prevalence rate of one per cent was indicated in a population-based study [Lionetti et al. 2015]. In South America, where CD had been considered historically as a

rare disease, a Brazilian prevalence study disclosed an affected rate of 1:214 [Oliveira et al. 2007] and an Argentinian prevalence rate of 1:167 [Gomez et al. 2001]. In a study conducted in Western Australia, (0.4%) of the population was found to be affected by CD, the disease frequency being one in two hundred and fifty people [Hovell et al. 2001]. In a study conducted in Asia based in North Western India, where there has been a history of wheat cultivation from before 1000 BC, a significant increase in patients diagnosed with CD has been observed. The growth rate of the disease was noted as 79.43% with a trend equation increase of 15.49 cases/year and the disease was shown to be affecting 1 in 310 children and affected 1.04% of adults [Sood et al. 2001, Ramakrishna et al. 2016].

In a study comparing serum stored from 1948–54 to current serum samples from the USA, an increasing prevalence of CD with time was shown with a reported 4–4·5 times increase when samples were compared from 1948–54 to the present day [Lohi et al. 2007].

In addition, CD cases are shown to be increasing in numbers every two decades and in this process, CD has advanced from a medical rarity to a highly prevalent disease [Kang et al. 2013]. This has been supported by a study of two cross-sectional adult population cohorts in Finland at two different time points. The first sampling and study design was performed in 1978-1980 and second was in 2000-2001. The results showed an increase in prevalence rates of CD from 1.05% (1978-1980) to 1.99% in 2000-2001 [Lohi et al. 2007]. A recent study on the Finnish population also showed that incidence of CD autoimmunity increased in the early 2000s and may have reached a plateau in recent years [Kivela et al. 2015].

One of the possible reasons for the increased disease frequency that has been observed in most of the autoimmune diseases is the improved hygiene and environmental changes in the industrialised world that has led to reduced microbiota content at an early age. This has been described as the hygiene hypothesis of atopic diseases [Rautava et al. 2004]. It has been proposed that the gut microbiota of infants lacks critical interaction strains involved in

developing the anti-inflammatory and tolerogenic responses that are further maintained by the cytokines, TGF-β and IL-10. Both these cytokines work in a synergistic manner and play an important role in promoting intestinal microbiota [Khoo et al. 1997]. Other factors that have contributed to the increased risk of CD include gastrointestinal infections, [Canova et al. 2014], rotavirus in children and campylobacter infection in adults, have been reported as risk factors, [Stene et al. 2006, Riddle et al. 2013] with rotavirus vaccination seeming to provide a protective effect [Kemppainen et al. 2017].

1.3 CD: Iceberg Model

A high number of the CD sufferers worldwide remain undiagnosed. In a study conducted by the Gastroenterological Society of Australia, approximately 75 per cent of sufferers of CD remained undiagnosed [Gastroenterological Society of Australia 2019, Australia, accessed 8 February 2019, <http://www.gesa.org.au>] whereas in the United States, up to 83 per cent of cases go unsuspected [Rubio-Tapia et al. 2012]. CD epidemiology has been competently described by the iceberg model [Lionetti et al. 2011]. The size of the iceberg is determined by the overall number of CD cases. These are dependent not only on the frequency of the HLA-DQ genotypes in the population, but also on the pattern of gluten consumption. While the visible part of the iceberg represents the top of the disease made up by the typical CD cases, on average for each diagnosed case of CD, five cases remain undiagnosed (the submerged iceberg part) because of the atypical and minimal symptoms [Catassi et al. 2014]. The problem of a significantly high number of undiagnosed cases has the potential to cause serious economic burden to health care systems in the Asia-Pacific region where an estimated 10 million people in India as well as in China remain undiagnosed [Catassi et al. 2012].

1.4 CD pathology and histology

The normal small intestine shows the presence of finger like villi on its surface. These villi help in nutrient absorption enabled by an increased surface area. In contrast, the pathological features of CD demonstrate varying degrees of intestinal damage, from mild abnormalities to completely flat mucosa (Figure 1). The severity of mucosal damage has been described by the Marsh-Oberhuber classification, which is a scoring system that relies on the diagnosis of upper intestinal pathology to categorise CD associated lesions, such as varying levels of crypt hyperplasia, intraepithelial lymphocytes and villous atrophy [Oberhuber et al. 1999, Marsh et al. 2015]. The distinct categories of CD associated mucosal lesions are shown in Table 1.

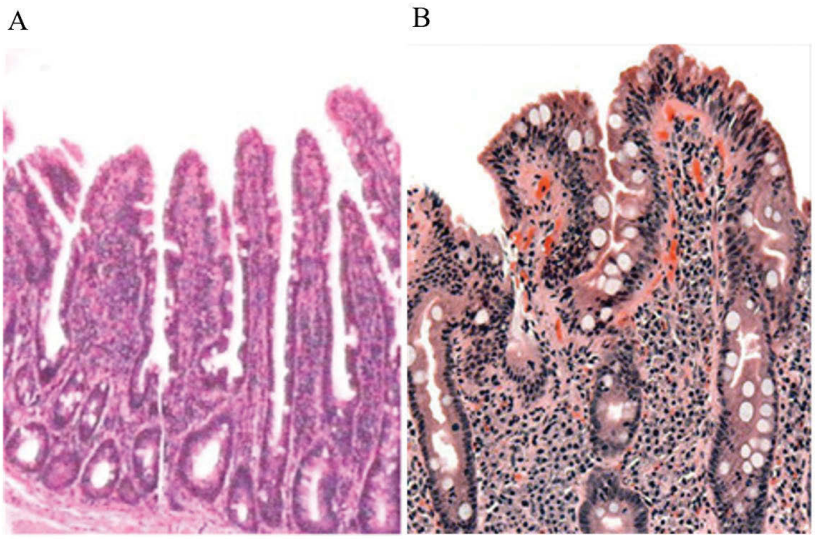

Figure 1: Pathological features of CD (A) *surface of the normal small intestine (jejunum) folded into finger like villi.* (B) *surface of jejunum with CD showing blunt villi, crypt hyperplasia and lymphocyte infiltration of crypts (Marsh Classification III).*

Table 1. Histological scoring system for CD [Marsh et al. 2015, Tonutti and Bizzaro 2014]

Stage of the disease	Histological Observation
Stage 1	Infiltrative
Stage 2	Infiltrative-Hyperplastic
Stage 3	3a) Mild Villous atrophy 3b) Moderate Villous atrophy 3c) Complete absence of villi
Stage 4	Total mucosal atrophy

The Marsh-Oberhuber system is mainly valid under optimal clinical conditions. However, given the presence of a broad spectrum of lesions as well as low inter-observer and intra-observer agreement particularly for low-grade histopathological abnormalities may result in failure to diagnose CD [Mohamed et al. 2008].

A new system comprising a simplified grading system with uniform diagnosis and improved validity of the pathological diagnosis of CD was developed by using only three categories (A, B1 or B2). Category 'A' represents normal villous with lymphocytic infiltration. Categories B1 and B2 represent partial and complete villous atrophy, respectively [Corazza et al. 2007]. Further, the lesions were classified into grades A and B [Corazza and Villanacci 2005]. Grade A (non-atrophic) is characterised by the isolated increase of intraepithelial lymphocytes (IELs) (>25/100 enterocytes), while grade B (atrophic) was differentiated into B1, wherein the villous/crypt ratio is less than 3/1, with detectable villi, and B2, in which the villi are no longer detectable.

In addition, changes in duodenal morphology, including quantitative measurements of villous height, apical and basal villous widths, and crypt length are being reported particularly after

adherence to a gluten free diet along with serology changes. A comparison between the different systems of CD classification is represented in Table 2 below.

Table 2. Comparison of different histological scoring systems for CD

Marsh System	Marsh-Oberhuber System	New Grading System
Type I	Type 1	Grade A
Type II	Type 2	
Type III	Type 3a	Grade B1
	Type 3b	
	Type 3c	Grade B2

1.5 Clinical Presentations of CD

The clinical manifestations of CD depend greatly on the age of the patient, the duration of the disease as well as the presence of extra intestinal pathology. Depending on the observed histological and immunological features, CD can be sub-divided into the following clinical forms: classical, atypical, silent and undiagnosed CD.

1.5.1 Classical (Typical) Form

The beginning of symptoms in the classical form generally occurs between 6 and 18 months of age. The active form is typically characterised by chronic diarrhea, failure to thrive, muscle wasting and anorexia. While growth is usually normal during the first months of life, symptoms

begin weeks to a few months after introduction of weaning foods that contain prolamins. This leads to a progressive decrease in the child's percentile for weight and weight for height. On observation, such children are usually pale and noticeably thin with a protuberant abdomen, decreased subcutaneous fat, and reduction in muscle mass. Laboratory signs of malabsorption include anaemia, hypocalcemia, hypoalbuminemia and vitamin deficiencies. The pathological changes are mostly visible in the duodenum and upper jejunum, but the extent of mucosal damage is variable with at times the entire small intestine being involved. The histological changes include minor villous blunting to subtotal or total villous atrophy, decreased villous height-to-crypt depth ratio, crypt hyperplasia with increased mitosis, increased lymphocyte infiltration in the lamina propria as well as increased number of intraepithelial lymphocytes. [Ludvigsson et al. 2013].

1.5.2 Atypical Form

In recent years, there has been a notable change in the age of onset of symptoms as well as the clinical presentations of CD. Epidemiological studies have indicated that up to 50% of patients with newly diagnosed CD do not present with gastrointestinal symptoms and prevalence cannot be explained by the known genetic and environmental risk factors [Lebwohl et al. 2018].
Other than intestinal damage, some of the other common signs and symptoms observed in CD sufferers particularly those defined as occult or atypical cases include iron-deficiency, anorexia, weight loss, abdominal pain, diarrhea, short stature, irritability, chronic fatigue, constipation and increased levels of liver enzymes and joint pain [Tonutti and Bizzaro 2014]. CD can also lead to severe neurological conditions, such as gluten ataxia and peripheral neuropathy [Hadjivassiliou et al. 2008]. The clinical manifestations of CD are described in Table 3.

Table 3. Major clinical manifestations of atypical CD in children and adults

Children	Adults
Poor Appetite	Diarrhoea/Weight loss
Failure to thrive	Cutaneous disease such as Dermatitis herpetiformis
Abdominal distension	Peripheral neuropathy
Muscle Wasting	Gluten Ataxia
Diarrhoea	Liver Dysfunction
Anaemia	Irritable bowel Syndrome
Malabsorption	Thyroid Dysfunction (hypo/hyper)
Lethargy	Reproductive Disease including abnormalities in menarche and menopause

In addition, a number of disorders are found to be associated with increased risk of developing CD. Some of the strongly associated disorders are listed in Table 4.

Table 4. Disorders associated with CD

Autoimmune	Idiopathic	Chromosomal
T1DM	Dilated cardiomyopathy	Down Syndrome
Hashimoto thyroiditis	Cerebellar ataxia	Turner Syndrome
Grave's Disease	Peripheral neuropathy	Williams Syndrome
Autoimmune hepatitis	Multiple Sclerosis	

Primary biliary cirrhosis	Inflammatory bowel disease	
Dermatitis herpetiformis	Sarcoidosis	
IgA deficiency	Atopy	

1.5.3 Asymptomatic (Silent) Form

The silent form of the disease is identified by the presence of histologic changes, limited mainly to the proximal intestine, that occur in the individuals and are apparently asymptomatic [Auricchio et al. 1988] and it manifests itself as a decreased psychophysical well-being. Common indicators in such individuals include iron deficiency with or without anaemia, behavioural disturbances, such as tendency to depression, irritability, easy fatigue and impaired physical fitness, reduced bone mineral density [Ferguson et al. 1993]. Early diagnosis and gluten free treatment improves the wellbeing of the sufferers whereas ignoring the symptoms may lead to long-term complications and disease progression.

1.5.4 Undiagnosed, Potential Coeliac

Another category of CD are the CD sufferers comprising the undiagnosed and potential CD sufferers. Undiagnosed sufferers of CD may contain the HLA-DQ genotype but show mild intestinal lesions to normal intestinal features along with an increased number of other pathological signs such as intraepithelial lymphocytes (IELs). On continued gluten exposure, mucosal atrophy was observed while adherence to a gluten free diet resolved the intestinal issues and improved mucosal damage in sufferers.

Potential coeliac sufferers are people with a normal small intestinal mucosa who are at increased risk of developing CD. These include first-degree relatives of CD sufferers that are HLA-DQ2/8 positive. The small intestine is characterised by a normal villous architecture along with a demonstration of histological feature such as increased $\gamma\delta^+$ intraepithelial lymphocytes (IELs). IELs can lead to mucosal inflammation, these individuals show the presence of gliadin specific antibodies, usually at low titres (<1:40) and are serologically positive [Weinstein 1974].

Another CD concept is observed in patients particularly above 50 years of age, who even after following a strictly gluten free diet, continue to show intestinal damage and are known to suffer from refractory CD. Refractory CD (RCD) is further divided into two types; RCD I and RCD II. This classification is based on the presence of IELs in both the types and the presence of either a polyclonal T cell phenotype (considered as normal) or oligoclonal/monoclonal T cell phenotype (considered as abnormal) [Ludvigsson et al. 2013].

Of both these refractory CD subtypes, RCD II is the most severe form of CD. RCD II sufferers show mainly the symptoms of malnutrition, ulcerative jejunitis and lymphocytic gastritis.

1.5.5 High at-risk persons

In addition to the coeliac sufferers there are high risk groups that may have higher CD prevalence rates. It has also been reported that patients suffering from certain other disorders such as Hashimoto's thyroiditis, type 1 diabetes, IgA deficiency and Down's syndrome have a higher risk of developing CD than the normal population [Freeman 2008]. Some of the disorders associated with increased risk of developing CD are listed in Table 4.

The most determining factor is familial history of biopsy proven CD with estimates of up to 20% or more of first-degree relatives having CD [Freeman 2010]. Another high-risk group are

those with the insulin dependent diabetes (type 1 diabetes), as well as those having liver disorders particularly, autoimmune hepatitis and primary biliary cirrhosis.

While the overall prevalence of CD is highly dependent on the HLA DQ2/8 typing and gluten consumption, the population with positive HLA typing for CD along with diabetes, relatives of coeliac sufferers as well as with autoimmune disorders have even higher risks for development of CD.

1.6 Role of α-Gliadin as the trigger for CD

Gluten is the storage protein of wheat and accounts for its viscoelastic properties. Gluten can be further classified, into the ethanol-insoluble glutenin's and alcohol soluble gliadins. Based on the mobility in 2D-PAGE at low pH, the gliadins were identified as a large family of proteins and were initially classified into four sub- fractions, α, γ, ω and δ type gliadins [Woychik et al. 1961, Bushuk and Zillman 1978]. Characterisation based on biochemical properties led to re-classification of gliadins into four families: α, γ, ω and low molecular weight (LMW) gliadins [Metakovsky et al. 1997, Anderson et al. 2012]. There is continued research on the classification of gliadins, as the gliadin family is much larger, complex and diverse.

The α-gliadins have an average molecular weight of 31 kDa, represent 15-30% of the total protein in wheat grain and contain a total of 282-286 amino acids [Kasarda et al. 1984]. The α-gliadin protein is one of the most abundant proteins in wheat and is also believed to be one of the main initiators of CD. It is comprised of a signal peptide, a large repetitive domain, two poly-glutamine regions and two unique domains with a relatively conserved number of cysteine residues [Anderson and Greene 1997] (Figure 2). Most of the α-gliadin genes have been found to contain six cysteine amino acids that form three intramolecular disulphide bonds thereby,

forming a globular protein. The α-gliadin family genes have been mapped on the short arm of chromosome 6 of wheat and have a high copy number [Noma et al. 2016].

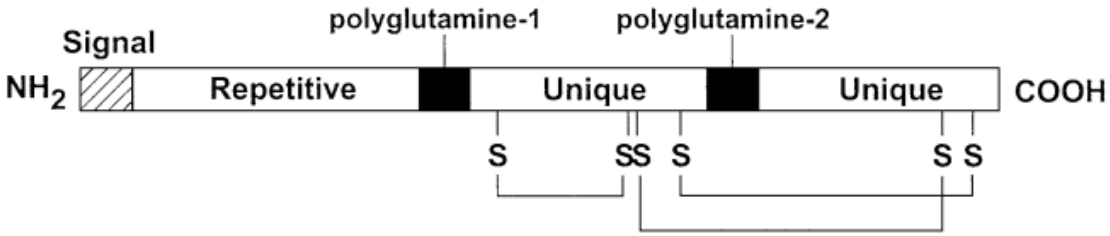

Figure 2: The general structure of α-Gliadin protein [Adapted from Anderson and Greene 1997].

1.6.1 γ-Gliadins

γ-gliadins from wheat are also a notable source of CD epitopes. It has been shown that T cell reactive lines from γ-gliadins show more variability as compared to reaction to the α-gliadin derived peptides. This is because of the greater number of immunogenic peptides found in γ-gliadins as compared to α-gliadin [Camarca et al. 2009].

The amino acid sequence of the γ-gliadin transcript begins with a 20-residue signal peptide sequence, followed by a short N-terminal non-repetitive domain (I), as well as a highly variable repetitive region (domain II). The length of the domain II varies between 138 to 537 base pairs. This is followed by another non-repetitive domain containing cysteine residues (Region III), a glutamine rich region (IV) and a C terminal non-repetitive domain containing two conserved cysteine residues (V) [Qi et al. 2009]. Most of the sequence variants can be assigned to one of the three genomic γ-gliadin loci, Gli-A1, Gli-B1 and Gli-D1. One of the main CD epitopes is DQ2-γ-1 epitope (PQQSFPQQQ) and is recognised by at-least one–third of the patients [Vader et al. 2002].

1.7 Pathogenesis of CD

CD develops because of an aberrant immune response to wheat gluten and related cereal proteins in genetically predisposed individuals. This immune response in turn leads to the production of a number of auto-antibodies that are linked to the disease and its pathological effect. It has been observed that increased concentrations of auto-antibodies can be associated with progressive degrees of villous atrophy based on the Marsh classification [Kruppa 2012] (see Table 1).

CD development involves environmental, genetic as well as immunological factors [Kagnoff 2002]. In patients showing susceptibility to the disease, the immune system recognises gliadin epitopes as an antigen. This leads to recognition by the T cells, increased production of CD4, CD8 and natural killer cells which release pro-inflammatory cytokines that results in tissue destruction and damage to the small intestine.

Gliadin severely alters the intestinal immune system and can access the basal surface of the epithelium via both the trans- and paracellular routes of absorption (Figure 3). The paracellular permeability of gliadin is supported by the identification of Zonulin, a 47 kDa protein (recently identified as perhaptoglobin-2) in the mammalian intestine that plays the significant role of modulating intercellular tight junctions [Fasano 2011]. Following gliadin binding to the chemokine receptor CXCR3 [Lammers et al. 2008], myeloid differentiation primary response protein 88 (MyD88) in enterocytes, induces release of zonulin that causes increased epithelial permeability and gliadin passage to the gut mucosa.

The transcellular passage of gliadin peptides has been reported to be stimulated by IFN-γ, a cytokine produced in patients with CD [Schumann et al. 2008]. Transport of intact gliadin peptides has been reported by retro-transport via CD71, the transferrin receptor. CD71 is over-expressed in coeliac affected patients and is expressed at the enterocyte apex where it can bind

secretory IgA (SIgA), to form SIgA-gliadin complexes. This binding enables intact translocation of gliadin peptides by escaping lysosomal degradation [Matysiak-Budnik et al. 2008].

1.7.1 Activation of Immune Response

The activation of the innate immune response helps in the stimulation of the adaptive immune response (HLA-DQ2 or HLA-DQ8 mediated) and initiation of the T cell and B cell specific response. The adaptive immune response is comprised of the T cells that contain the T cell receptor (TCR) on the cell surface. The CD4 T cells that express the CD4 glycoprotein on the cell surface are known as T helper cells. MHC Class II molecules act as the antigen presenting cells (APC) and in turn lead to activation of the T helper cells, following interaction with the gliadin peptides. Upon activation, $CD4^+$ T cells secrete cytokines and may differentiate to several sub types such as T_H17. It is suggested that T_H17-derived interleukins (IL-17, IL-21, IL-22 and interferon-γ) act on immunocompetent cells and cause an inflammatory cascade resulting in tissue damage and the destruction of the cellular matrix structure. It also acts synergistically with Tumor Necrosis Factor (TNF). Activated $CD4^+$ T cells secrete pro-inflammatory cytokines and stimulate cytotoxic T cells and fibroblasts to produce zinc dependent endopeptidases called matrix metallo-proteinases (MMP) that can degrade all kinds of extracellular membrane proteins [Di Sabatino and Corazza 2009, Sollid and Jabri 2013].

A second pathway used by Cytotoxic T cells (Tc) cells to promote apoptosis is through the release of Fas ligand on Tc cells that binds to Fas molecules expressed on mucosal epithelial cells. Killing of mucosal epithelium cells by Fas ligand begins by binding of the death domain of Fas to the death domain of an adaptor protein FADD (Fas associated via death domain). The clustered death effector domains (DED) of FADD recruit pro-caspase 8 that induces apoptosis

and also releases interleukin-15 from intestinal cells. IL-15 further helps in the stimulation of T_H1 $CD4^+$ T cells, T $CD8^+$ and natural killer cells. The activation of $CD8^+$ T cells is dependent on several simultaneous interactions which includes stimulation by IL-15 and activation by their NKG2D receptors. These receptors belong to the C-type Lectin family and helps in the activation of NK cells. Once the NKG2D receptors recognise the ligand MHC class I chain-related gene A (MIC-A), a transmembrane glycoprotein, they can kill MIC-A expressing epithelial cells through the same NKG2D receptors [Bulfone-Paus et al. 1997, Waldmann 2006].

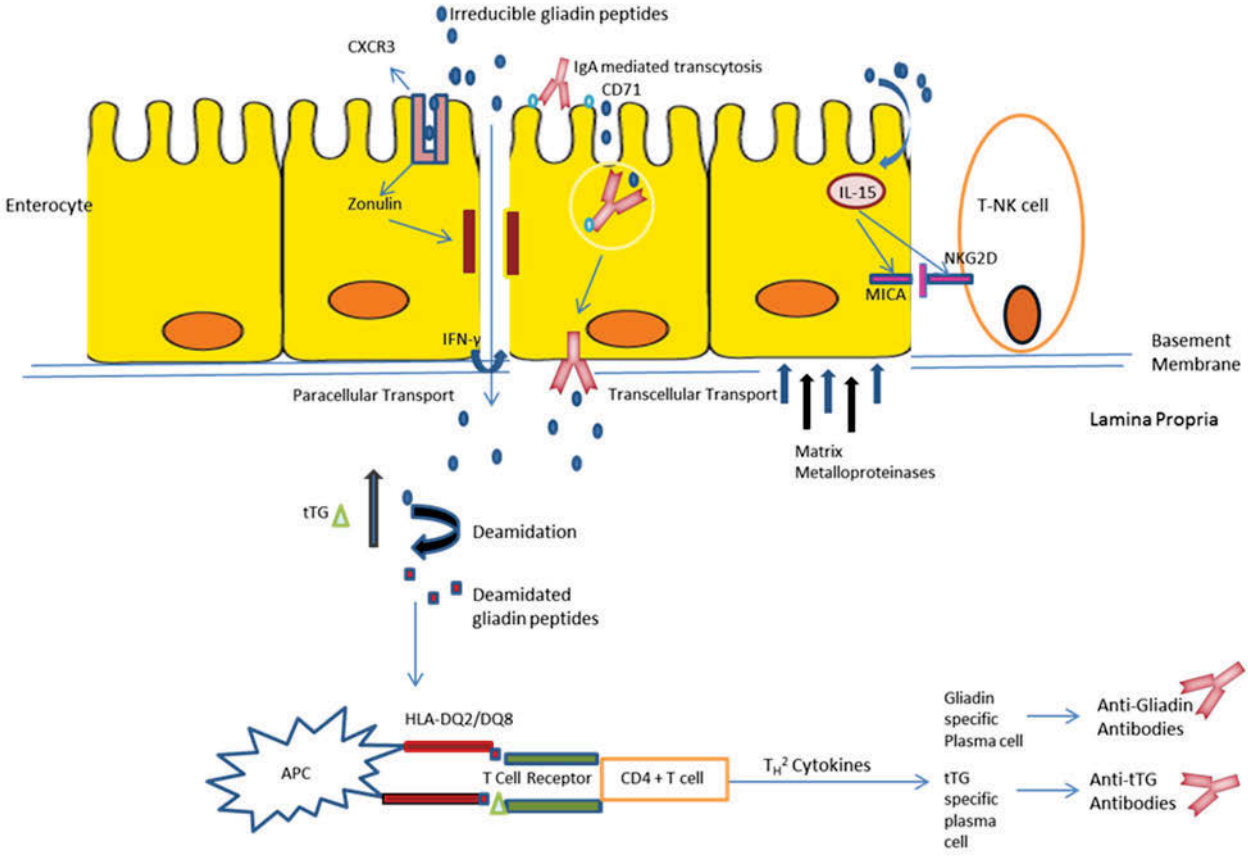

Figure 3: Schematic diagram showing the pathway for release of anti-gliadin and anti-transglutaminase antibodies. *Gliadin peptides cross the enterocyte by the paracelluar tight junctions following the release of Zonulin upon binding of gliadin peptide to the CXCR3 receptor or by IgA mediated retro transcytosis through the transferrin receptor CD71. Tissue transglutaminase (tTG) deamidates gliadin, which is recognised by human leukocyte antigen*

(HLA)-DQ2 or DQ8 molecules on the surface of antigen presenting cells (APC). The APC presents the deamidated peptide to CD4$^+$ T cells, which upon activation produce elevated levels of pro-inflammatory cytokines. These cytokines promote increased cytotoxicity of natural killer cells, T cells and intraepithelial lymphocytes, which cause apoptotic death of enterocytes. The production of T-helper2 (TH2) cytokines induces clonal B cell expansion followed by differentiation into anti-gliadin and anti-transglutaminase antibody secreting plasma cells. [adapted and modified from Di Sabatino and Corazza 2009, Sollid and Jabri 2013].

1.7.2 Role of Intra-epithelial lymphocytes in CD

Along with an increase in the number of gliadin specific CD4$^+$ T cells, CD is also characterised by an increase in the number of pro-inflammatory cytokines such as IFN-γ [Bodd et al. 2010]. IL-21 drives the production and release of IFN-γ as well as plays a key role in activation of intraepithelial lymphocytes (IEL) [Peluso et al. 2007]. An increase in the level of IL-15, results in the release of other stress-inducible molecules, such as MIC and HLA-E (which are ligands that activate recognition receptors NKG2D and CD94/NKG2C on IEL's) [Hue et al. 2004, Meresse et al. 2006]. These transmembrane recognition receptors that play a key role in imparting tissue damage that takes place in the enterocytes expressing IL-15 and stress-induced ligands for natural killer (NK) receptors. The cytotoxic IEL's thereby, show the tendency to kill intestinal epithelial cells as a response to epithelial stress, i.e. 'altered self', rather than a trigger by a specific antigen. In this regard, IEL's have been regarded as self-reactive CD [Sollid and Jabri 2013].

1.7.3 Role of tissue transglutaminase enzyme in CD

The pivotal step in the immune identification of gliadin as a foreign antigen is the deamidation of the protein by the tissue transglutaminase enzyme (tTG), a 76 kDa calcium dependent enzyme comprised of 686 amino acids. The transglutaminases are distributed widely in various organs, tissues and body fluids. Apart from tTG, other transglutaminase enzymes include, liver tissue transglutaminase, hair follicle transglutaminase, epidermal transglutaminase, prostrate transglutaminase and coagulation factor XIII from blood [Griffin et al. 2002]. These enzymes differ from each other in their physical properties as well as in their distribution in the body.

tTG is present in the liver and erythrocytes as a monomer of M_r 75,000-80,000. It can be isolated from the cytoplasm of cells and does not require even minor proteolysis for enzyme activation. The enzyme activity is Ca^{2+} dependent with two regions rich in glutamine residues (around amino acids 450 and 470) identified as the most probable Ca^{2+} binding sites in the enzyme [Ikura et al. 1988]. Further analysis based on hydropathy revealed that the active site in the human as well as the guinea pig transglutaminase are located at a transition region between the hydrophilic and hydrophobic regions [Folk and Gross 1971].

Immunohistochemical studies have suggested that the expression of tTG is elevated in the small intestine of untreated patients with CD as compared to normal individuals [Thomazy and Fesus 1989]. As the enzyme tTG belongs to the trans-amidating class of enzymes, it catalyses Ca^{2+} dependent acyl transfer reaction, the covalent linking of two proteins, one with a glutamine amino acid and the other with a lysine residue to form a ε-(γ-glutamyl)-lysine isopeptide bond (Figure 4) [Sabatino et al. 2012, Evans et al. 1988]. Most of the deamidation occurs in the brush border cells of the small intestine, where the pH is about 6.6 [Evans et al. 1988].

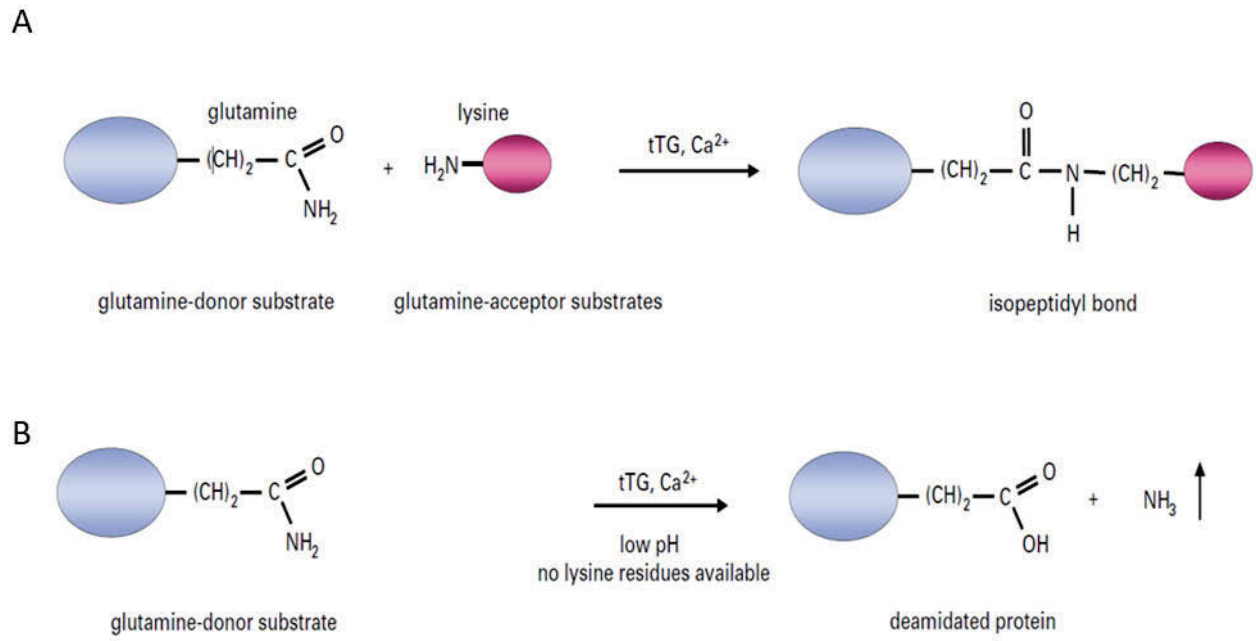

Figure 4: Gliadin modifications by enzyme tissue transglutaminase (tTG) (adapted from Dieterich et al. 2003). *(A) tTG catalyses the cross-linking of protein bound glutamine donor with the lysine residue of second protein resulting in the formation of an irreversible isopeptidyl bond. (B) In the absence of glutamine acceptors or at low pH, deamidated peptides are formed followed by release of ammonia.*

The deamidation effect of tTG on wheat gliadin, helps in increasing the immunostimulatory effect and affinity for HLA-DQ2 and HLA-DQ8 as well as act as a target for disease-specific antibodies that results in mucosal damage in CD (Fig. 5). The peptides released show a left handed polyproline II helical conformation which is preferred by HLA class II ligands [Sjostorm et al. 1998]. About 36% of glutamine residues of wheat gliadin are available to tTG catalysis as investigated by gliadin deamidation by polyamine incorporation or by ammonia liberation. It has been demonstrated that the secondary structure of the peptide affects the affinity of the enzyme as the presence of proline residues after glutamine results in the peptide not being deamidated [Piper et al. 2002].

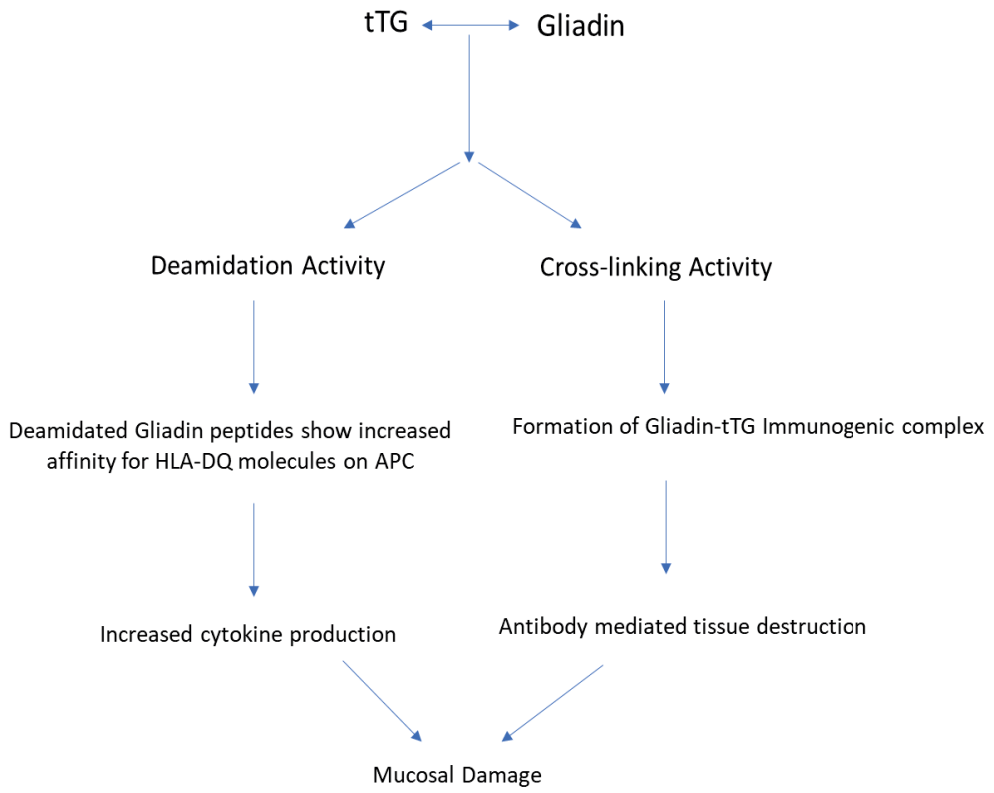

Figure 5: Role of tTG in the progression of mucosal damage in CD

1.7.4 Release of auto-antibodies in CD

The release and formation of specific anti-gliadin and anti-transglutaminase antibodies that are considered as the serological biomarkers for CD is based on the stimulation of $CD4^+$ T cells that leads to lymphocyte B cell differentiation into plasma cells [Dieterich et al. 1998]. The autoantibody formation depends on the existence of tTG-specific naïve B cells in the secondary lymphoid tissue in patients with CD. Following the binding of tTG to the B cell receptor, a gliadin-tTG complex is formed with a covalent link between gliadin peptide and the B cell receptor [Sollid 2000]. Internalisation of the gliadin-tTG complex results in the release of deamidated gliadin peptides that further activate the $CD4^+$ T cells in the intestinal mucosa of

patients with support by the gluten reactive helper T cells [Du Pre' and Sollid 2015] (refer Figure 3).

1.7.5 Coeliac Toxicity and amino acid composition of gliadin

Early studies to assess coeliac toxicity of wheat were carried out using gliadin digested with the enzyme's pepsin, trypsin and pancreatin. This peptide mixture, with an average molecular mass of approximately 1000 Da, was introduced into the duodenum of patients with CD where it was found to be toxic [Bronstein et al. 1966]. In addition, a study was carried out to test individual gliadin peptides and assess their coeliac toxicity. Peptides that were found to be toxic had a relatively high amino acid content of glutamine and proline.

The relationship between amino acid composition and coeliac toxicity was further demonstrated in a study that compared the alcohol soluble proteins (prolamins) of different cereals [Weiser 1996]. That study showed that prolamins of wheat (gliadin), rye (secalin) and barley (hordein), all of which contain an elevated content of glutamine (~36%) and proline (17-23%) assembled in a repetitive pattern, induced coeliac toxicity. In contrast, prolamins of cereals such as maize, millet and rice, which have a lower percentage of glutamine and proline but are higher in leucine and alanine, do not induce coeliac toxicity [Weiser 1996]. The FASTA sequence showing the complete amino acid composition of the alpha-gliadin protein is presented in Figure 6.

MKTFLILVLLAIVATTATTAVRFPVPQLQPQNPSQQQPQEQVPLVQQQQFLGQQQPF
PPQQPYPQPQPFPSQLPYLQLQPFPQPQLPYSQPQPFRPQQPYPQPQPQYSQPQQPISQ
QQQQQQQQQQQQQQQQILQQILQQQLIPCMDVVLQQHNIAHGRSQVLQQSTYQLL

QELCCQHLWQIPEQSQCQAIHNVVHAIILHQQQKQQQQPSSQVSFQQPLQQYPLGQG

SFRPSQQNPQAQGSVQPQQLPQFEEIRNLALQTLPAMCNVYIPPYCTIAPFGIFGTN

Figure 6: FASTA sequence of alpha-gliadin *(>sp|P02863|GDA0_WHEAT Alpha/beta-gliadin OS=Triticum aestivum OX=4565 PE=2 SV=2)*

A proline and glutamine rich 33-mer peptide with the following amino acid sequence: LQLQPFPQPQLPYPQPQLLPYPQPQLPYPQPQPF (α_2-gliadin 56-88) was found to be highly toxic and immunodominant. Within this peptide, 13 of the 33 amino acids are proline, which also makes this fragment highly resistant to digestion by intestinal proteases [Shan et al. 2002]. Furthermore, most of the T-cell stimulatory peptides are located in the repetitive domains of the protein one of which is the 33-mer peptide [Qi et al. 2013]. These T-cells act to induce the autoimmune response caused by exposure to gliadin in the intestine.

1.8 Diagnosis for CD

To date, the accurate diagnosis of CD has mainly depended upon gastrointestinal endoscopy to acquire a tissue sample that can show any potential abnormalities. Apart from endoscopy, current methods for diagnosis include serological testing for gliadin induced antibodies using an enzyme-linked immunosorbent assay (ELISA). These methods are expensive, confined to centralised pathology labs and require highly specialised operational and analytical expertise. In addition, due to the need to take a blood sample and go on a gluten diet for 6-8 weeks particularly when a definitive diagnosis is required, it is often difficult to get young children as well as even some adults to go for voluntary testing.

1.8.1 Intestinal Biopsy for testing CD

Biopsy has been considered the gold standard for identifying CD patients. Over the years, it has been recognised that CD patients show an entire spectrum of histological changes ranging from increase in villous intraepithelial lymphocyte count to villous flattening. Endoscopy has been useful to report some of the unique intestinal features such as loss or reduction of duodenal folds, scalloping of duodenal folds, and, less commonly, a mosaic pattern and prominent vasculature [Ravelli et al. 2001]. Over the years; however, several challenges have limited the practice of relying on pathology alone for making a confirmed diagnosis. Firstly, a non-biased pathology analysis requires at least four to six endoscopic biopsy specimens to be taken from the duodenum of an individual patient [Bao et al. 2012]. This is necessary, as described in the Marsh-Oberhuber classification, the intestinal pathology and damage for CD varies in different individuals as per the disease stage. Also, improper sample preparation caused by poorly mounted samples or incorrect orientation can lead to false negative or positive results as endoscopic features are not sensitive and some are not specific [Bao et al. 2012].

Finally, to have a clear small bowel biopsy report, it is recommended that gluten be included in the diet to trigger histological relapse to validate CD. This is challenging as people who are already placed on a gluten free diet and are recovering, are hesitant to take the 6-8 weeks gluten challenge due to a fear of symptom exacerbation [Castillo et al. 2015]. Taken together, a diagnosis based solely on gastrointestinal damage is inadequate on its own particularly in patients with minimal intestinal damage [Hardy and Tye-Din 2016]. Thus, to increase the level of diagnostic precision as well as monitoring by coeliac sufferers, particularly for small children as well as patient with minimal intestinal damage, newer non-invasive, genetic and serological tests are required.

1.8.2 Genetic testing for CD

The HLA-DQ gene in the HLA complex on the 6p21 chromosome is the main genetic factor linked with CD. The strong link between CD and genetics is reflected in a high conformity rate of 75% in monozygotic twins [Greco et al. 2002]. While a majority of CD sufferers, about 95%, carry the DQ2 heterodimer, the others contain the HLA-DQ8 genotype [Howell et al.1986]. The HLA-DQ2 genotype is considered as an independent factor that influences the gut microbial composition particularly in infants expressing the genetic factors that contributes to CD development [Olivares et al. 2015].

HLA Class II molecules are heterodimeric molecules, composed of a 33-35 kDa α-chain and a 25-29 kDa β-chain. The C-terminal domains bind the CD4 T cells and are composed of α2 and β2 that contain hydrophobic membrane spanning sequences. Following synthesis, the class II molecules are free to bind antigenic peptides [Rioux and Abbas 2005].

Deamidated gliadin peptides are presented to mucosal CD4+T cells by HLA-DQ2 and DQ8 molecules, thereby, playing a key role in development of CD. Isolation of gliadin-reactive T cells from the small intestinal mucosa was used to understand the link between CD and HLA-DQ [Lundin et al. 1993]. When gluten was added to these activated T cells in the presence of HLA-DQ heterodimer, gluten was identified by the T cells. This helped to demonstrate the T cell-HLA-DQ association of CD.

The DQ association in DQ2 and DQ8-related CD, showed different mechanisms in CD progression. An increase in DQ2-mediation of CD was noticed following the deamidation of gliadin by the enzyme tissue transglutaminase (tTG). In a fine mapping study conducted to study the peptide-binding motif for HLA-DQ2, it was demonstrated that HLA-DQ2 prefers hydrophobic and negatively charged amino acids at anchor positions P1 and P9, particularly at P4, P6 and/or P7 [Costantini et al. 2005].

In contrast, HLA-DQ8 binding prefers glutamate at P1 and P9 to generate a stable peptide-MHC complex [Henderson et al. 2007] with the DQ8-restricted gliadin peptides located in protease sensitive sites of gliadin. Further, research showed that the T cell receptor attached centrally above HLA-DQ8-alpha-I-gliadin, allowing all complementarity-determining region-beta (CDR beta) loops to interact with the gliadin peptide [Broughton et al. 2012].

Given the strong link of HLA-DQ complex with CD, HLA-DQ2/8 genotyping is a commonly used test for estimating the risk of development of CD. The limiting factor for the genotyping test is the low predictive value as well as the likelihood ratio for the disease prevalence that greatly influence the genomic risk predictability. This was illustrated in a study involving 463 participants, out of which 16 patients were HLA-DQ2 and/or –DQ8 positive and were confirmed to have CD based on the intestinal damage. However, 192 patients were genetically positive but did not show the intestinal damage and were confirmed without CD in follow up treatment. This false diagnosis can be accounted to the high prevalence of the HLA-DQ genes in the general population [Hadithi et al. 2007, Husby et al. 2012].

Furthermore, in some Asian countries, such as Japan, and it has been observed that the prevalence of the genotypes HLA-DQ2 and DQ8 remains very low (around 10-20%) [Hall and Crowe 2011]. Sole reliance on HLA-DQ2/8 genotyping may significantly under-diagnose CD in such populations, particularly when other chronic abdominal symptoms are expressed in patients [Fukunaga et al. 2017].

Genome wide association mapping has pointed to 70 candidate genes in 42 non-HLA loci that have been shown to be linked with CD [Dubois et al. 2010]. This association indicates that multiple immunogenetic pathways are involved in CD pathogenesis. Genomic studies using an additional ~200 CD-associated single-nucleotide polymorphisms have been demonstrated as more effective predictors of CD as compared to the existing HLA typing [Abraham et al. 2015].

Further research, however, is necessary to establish the cost effectiveness as well as the clinical relevance of genomic testing [Abraham et al. 2015].

Another important concept is the effect and influence of dose of HLA on the CD susceptibility. It has been shown that individuals homozygous for the disease-associated DQA1*05:01-DQB1*02:01 haplotype or individuals possessing DQA1*05:01-DQB1*02:01/DQA1*02:01-DQB1*02:02 genotype have the highest risk for developing CD [Ploski et al. 1993]. The diffrences in the DR3-DQ2 haplotypes indicates that some other factors may be independently influencing the extent of risk for CD [Noble et al. 2006].

1.9 Detection of antibodies useful in the diagnosis of CD

Based on the underlying immune mechanisms of CD induction described above together with the resulting production of antibodies against gliadin as well as auto-antibodies (refer Figure 3), a variety of diagnostic tests have been developed. These auto-antibodies bear the typical characteristics of a conventional immune response to a foreign antigen, including, a high level of specificity, class-switching from IgM to IgG as well as other sub classes, affinity maturation i.e. auto-antibodies released later in the disease react more strongly with the target antigen as well as mutation of antibody genes with time [Miller et al. 1990]. Antibodies that have been studied thus far for their potential use as a diagnostic biomarker for screening large populations are listed below.

1.9.1 Anti-Gliadin Antibody (Anti-AGA)

Anti-gliadin antibodies are released following the binding of the B cell receptor to gliadin peptides that are presented by the HLA-DQ molecules. The first diagnostic tests developed using α-gliadin as the antigen were ELISA-based and were used to distinguish between adults with CD and those without [O'Farrelly et al. 1983]. The ELISA based test showed encouraging results for children under the age of 2 years, showing a sensitivity value of 100% for both IgA and IgG AGA in children under the age of 2 years (see Table 5), while sensitivity values dropped down to children above the age of 2, showing a sensitivity value of 64% and specificity value of 54% for IgA and IgG AGA antibodies, respectively [Savilahati et al. 1983]. The difference in the sensitivity values may be explained by the significant AGA titre difference in the CD affected patients below the age of 2 and the negative control. In fact, the titre values of anti-gliadin specific antibodies remained significantly higher even after placing the coeliac affected patients on GFD. In another study conducted on children, the IgG AGA showed a specificity of 90%, whereas the IgA AGA had a specificity of 65%. Based on these results, IgG AGA was therefore proposed as a marker for CD detection in children [Tucker et al. 1988].
Further studies detected IgG and IgA AGA based antibodies using mainly an ELISA method. These studies anticipated that AGA screening could be used as a basis for selecting children to undergo duodenal biopsy to confirm for CD. These studies, however, remained inconclusive as the predictive efficiency for these tests varied between 79 and 98% (see Table 5). The intra-test variability can be ascribed to several factors, including varying ratios of coeliac to control patients studied, the use of alternative techniques such as immunofluorescence and ELISA, different ELISA protocols being followed that lead to significant inter-laboratory variation as well as disparity in the cut off points used to determine the threshold for positive samples in the AGA assay in different laboratories.

In a later study, AGA IgG was quantified using an alternative method, based on a microfluidic immunosensor consisting of a modified Plexiglas device that is coupled with an electrochemical detector [Pereira et al. 2010]. The AGA IgG quantification was conducted based on the application of a heterogenous, non-competitive ELISA. Briefly, AGA IgG antibodies in human serum samples were allowed to react with gliadin protein that was immobilised on the surface of an immunosensor acting as a substrate. The immunosensor consisted of a Plexiglas device coupled to a gold electrode, with a central channel containing 3-aminopropyl-modified pore glass (AP-CPG). Alkaline phosphatase (AP) enzyme labelled secondary antibodies specific to human IgG were used to convert the p-aminophenyl phosphate (p-APP) to p-aminophenol (p-AP). This electrochemical back oxidation of p-aminophenol created a signal on the gold electrode. The amount of IgG antibodies to gliadin protein in the samples was, therefore, directly proportional to the product of the enzymatic reaction. However, as the quantification of IgG antibodies is a multi-step procedure, it requires careful handling, optimisation and higher cost, which has greatly limited the commercial potential of that device.

Table 5. Some of the reported Anti-Gliadin antibody (AGA) testing for screening CD

Study	AGA Test Method	Sensitivity %	Specificity %
O' Farrelly et al. 1983	ELISA	82% (IgA)	87% (IgA)
Savilhati et al. 1983	ELISA	100% (> 2 yrs.)	-
		60% (< 2 yrs.)	-
Tucker et al. 1988	ELISA	86% (IgA + IgG)	90% (IgA + IgG)
Bodé et al. 1993	DIG-ELISA (DIG: Diffusion in gel)	100% (IgA + IgG)	97% (IgA + IgG)

Lerner et al. 1994	ELISA	88% (IgG)	92% (IgG)
Chartrand et al. 1997	ELISA	93% (IgA + IgG)	71% (IgA + IgG)
Lagerquvist et al. 2008	ELISA	97.2% (IgA)	83.2% (IgA)

1.9.2 Anti-Endomysial Antibodies (Anti-EMA)

Anti-endomysial autoantibodies are specific to the smooth muscle endomysium of the gastrointestinal tract. The anti-EMA testing methods were developed in the mid-1980's and the predictive efficiency was proposed to be a significant improvement over the AGA test. Similar to the AGA test, the Anti-EMA auto-antibodies were shown to be induced by exposure to α-gliadin and have been found to mainly consist of IgA class antibodies [Ladinser et al. 1994, Picarelli 1999]. IgA and IgG-EMA detection is performed by indirect immunofluorescence (IFA) using sections of monkey esophagus or human umbilical cord as the substrate, followed by the individual reading of each sample using fluorescent microscopy. Briefly, patient sera were screened at a dilution of 1:10 in PBS, pH 7.6 and polyclonal fluorescein isothiocyanate (FITC)-labelled heavy chain specific rabbit human IgG and IgA are used as secondary antibodies Although, EMA testing has shown even higher sensitivity and specificity values as compared to AGA testing [Rostami et al. 1994], the major problems of the assay are its higher cost, limited capacity for automation as well as the need for experienced personnel for analysis [Leffler and Schuppan 2010].

1.9.3 Anti-Transglutaminase Antibodies (Anti-tTG)

An increase in anti-tTG titer in CD patients as compared to control patients was observed by Bruce et al. [1985] that led to the development of tissue transglutaminase based diagnostic assays. In these assays, patients showing very high titers of anti-tTG, were considered as confirmed CD positives and therefore these cases were exempted from small intestine biopsy [Hill and Holmes 2008, Vivas et al. 2009, Tortara et al. 2014]. This was supported in a recent study on 242 children in Sweden, where it was concluded that the detection of IgA/IgG anti-tTG remains the most accurate pre-biopsy test for children with a risk of developing CD [Dahlbom et al. 2016].

The initial tests were based on the determination of the titer of anti-tTG antibody by ELISA, the enzyme preparation was isolated from guinea pig liver and it gave excellent initial results (Table 6). However, follow-up studies showed lowered sensitivity values probably due to hepatic impurities affecting the process of guinea pig tTG preparation. This problem was overcome by developing an ELISA test using human recombinant tTG (h-tTG) as antigen and has since then been widely adopted for use in clinical laboratories [Sblattero et al. 2000] (Table 6).

Table 6. Some of the reported Anti-Transglutaminase antibody (anti-tTG) testing results for screening CD.

Study	Antigen used for tTG ELISA	Sensitivity % / Specificity %
Dieterich et al. 1998	Guinea pig transglutaminase	98.1% / 94.7%
Lock et al. 1999	Guinea pig transglutaminase	85% / 97%

Sblattero et al. 2000	Guinea pig transglutaminase	84% / 98%
Sblattero et al.2000	Recombinant human transglutaminase	91.5% / 99%
Lewis and Scott [2010]	Recombinant human transglutaminase	93% / 96.5%
Dahlbom et al. 2010	Recombinant human transglutaminase	96% / 99.5%

1.9.4 Anti-Deamidated Gliadin Peptide (Anti-DGP) antibodies

The enzyme tissue transglutaminase causes the selective deamination of gliadin peptides. Some of these deamidated gliadin peptides, particularly, containing the sequence QPEQPFP, have been used as an antigen. This peptide sequence was identified from the T lymphocytes of individuals that are genetically predisposed to CD. PEQ has been recognised as the core epitope in the sequence [Volta et al. 2008]. An ELISA test with synthetic deamidated gliadin peptides as antigen has been shown to have high specificity values, however, the sensitivity was variable particularly for children as shown in Table 7.

Existing diagnostic tests were compared with the DGP ELISA test to determine the most suitable test for diagnosis and follow-up of CD patients [Dahle et al. 2010]. In a study of 128 untreated CD patients and 134 controls, anti-DGP was shown to have higher specificity as well as higher diagnostic accuracy, although IgA anti-tTG showed the best sensitivity. In a later study it was concluded that DGP based tests showed improved specificity as they could be used to differentiate between adult patients with CD suffering from liver ailments as well as other gastrointestinal based disorders [Barbato et al. 2011]. Another advantage of the DGP based test

is the availability of an IgG based test has been particularly useful for individuals who are IgA deficient. In other studies, it has been shown that high titers of anti-DGP corresponded to severe intestinal damage and IgG-DGP can be used as a diagnostic marker for small children [Amarri et al. 2013, Schwertz et al. 2004].

Table 7. Some of the reported Anti-Deamidated gliadin peptide antibody (Anti-DGP) testing for screening CD.

Study	Population studied	Sensitivity %	Specificity %
Schwetrz et al. 2004	Children and adults	90.4% (IgA anti-DGP)	90.8% (IgA anti-DGP)
Agardh [2007]	Children	91% (IgA anti-DGP) 95% (IgG anti-DGP)	91% (IgA anti-DGP) 86% (IgG anti-DGP)
Ankelo et al. 2007	Children and adults	93.0% (IgA anti-DGP) 75% (IgG anti-DGP)	90.0% (IgA anti-DGP) 98% (IgG anti-DGP)
Rashtak et al. 2008	Children and adults	75% (IgA anti-DGP) 65.2% (IgG anti-DGP)	95.2% (IgA anti-DGP) 98% (IgG anti-DGP)
Basso et al. 2008	Children	80.7% (IgA anti-DGP) 80.0% (IgG anti-DGP)	93.0% (IgA anti-DGP) 96.0% (IgG anti-DGP)

Sugai et al. 2010	Adults (high-risk group)	98.4% (IgA anti-DGP) 95.2% (IgG anti-DGP)	92.7% (IgA anti-DGP) 100% (IgG anti-DGP)

1.9.5 Anti-Synapsin and Anti-Ganglioside antibodies

Although the gluten-dependent auto-antibodies namely, anti-gliadin and anti-transglutaminase are the main auto-antibodies studied, some other auto-antibodies have also been shown to be related with CD. Of interest, are the anti-ganglioside and anti-synapsin auto-antibodies; an understanding of the release of these auto-antibodies is particularly important to fully comprehend the neurological manifestations observed in patients with CD.

IgG antibodies to gangliosides have been observed in adult CD patients with neurological manifestations [Volta et al. 2004]. The gangliosides are sialic acid containing glycolipids consisting of a polar head group comprising glucose, galactose, N-acetyl glucosamine, sialic acid molecules and a ceramide tail. These are abundant in the nerve cell membrane where molecular mimicry between ganglioside and *Camplyobacter jejuni* lipo-oligosaccharide, a gram-negative bacterium has been implicated for causing the Guillain-Barre' syndrome [Yuki et al. 2004]. To understand the origin of anti-ganglioside antibodies in CD patients, Alaedini and Latov [2006], proposed haptenisation of gliadin with intestinal monosialotetrahexosylganglioside (GM1) caused by the adhesion of gliadin protein to

ganglioside located on the intestinal epithelial cells, as a possible trigger for release of anti-ganglioside antibodies.

Changes in gut microbiota may influence CD progression as has been demonstrated by *in-vitro* studies. It has been shown that the addition of *Bifidobacterium*, *E. coli* or *Shigella* can influence cytokine production after gliadin stimulation. *E. coli* and *Shigella* have also been shown to increase the translocation of gliadin peptide in intestinal loops [Cinova et al. 2011]. These changes in gut microbiota may play a key role in CD progression particularly affecting the epithelial barrier or aggravating the gliadin-specific immune response [Elena et al. 2015] and in turn leading to the release of neuronal antibodies.

In addition, immune cross-reactivity has been suggested between anti-gliadin antibody and synapsin 1, a phosphoprotein present in neurons of the central and peripheral nervous system. This is mainly attributed to the similarity in amino acid residues particularly the presence of high repeats of proline and glutamine residues [Alaedini et al. 2007]. It is hypothesised that as synapsin 1 is associated with synaptic vesicles, anti-gliadin antibodies and synapsin 1, cross-reactivity may trigger the release of neurotransmitter leading to extra-intestinal manifestations. This has been further supported by the presence of synapsin-1 in non-neuronal cells such as liver epithelial cells [Bustos et al. 2001].

1.10 Diagnosis based on Gluten-specific T cells

Detection of T cells in blood specific for immunodominant gluten-derived epitopes has been proposed as a diagnostic tool for CD patients [Anderson et al. 2005, Brottveit et al. 2011]. A new method of diagnosis for CD based on the detection of T cells in blood specific for immunodominant gluten-derived epitopes has been introduced [Goletti et al. 2005, Ruhwald et al. 2007]. Previously, assays to measure antigen-specific T cells, such as ELISA and ELISPOT

to detect IFN-γ or IFN-γ-inducible protein 10 released in whole blood or peripheral blood mononuclear cells (PBMC), had been applied for diagnosing *Myobacterium tuberculosis* infection [Lalvani et al. 2008].

Polyclonal gliadin-specific T cells *in vivo* were generated following the consumption of gluten containing food items for 3 days, and blood collection was carried out on day 6 to isolate the PBMC [Anderson et al. 2000]. Antigen-specific $CD4^+$ cells could be directly collected and measured using functional assays such as IFN-γ ELISpot, IFN-γ/IP-10 ELISA or tetramers, after the *in vivo* memory T cell population expansion. The obtained results have proven to be valuable in interpreting epitope hierarchies and phenotypes of the circulating $CD4^+$ T cells in CD patients [Tye-Din et al. 2010].

Another diagnostic assay based on the whole blood cytokine release assay has also been evaluated for diagnosis for CD [Ontiveros et al. 2014]. The sample cohort consisted of blood samples collected from donors confirmed to have CD before and after gluten challenge, non-CD donors on GFD as a control group, as well as CD sufferers not placed on GFD. The blood samples were incubated with antigenic proteins and peptides, following which, plasma IFN-γ and IFN-γ IP 10 were measured by ELISA and correlated with IFN-γ ELISpot.

While the T cell assays could not differentiate between CD patients on GFD and controls prior to gluten challenge, gluten eating CD patients carrying the HLA-DQ 2.5^+ genotype showed detectable T-cell responses. These studies showed that while whole blood IFN-γ ELISA and the ELISpot were both 85% sensitive and 100% specific for HLA-DQ 2.5^+ CD patients, whole blood IP-10 ELISA was 94% sensitive and 100% specific showing similar effectiveness in disease diagnosis. Though the cytokine assays are specific, their prospects as a method for mass screening are hindered, since in order to maintain T cell functionality, an immediate transfer of a blood sample to centralised facility is required or else false negative results may be obtained and that adds to the test costs [Lehmann and Zang 2012].

1.11 Saliva tests for CD

Saliva is a clear, slight acidic mucoserous, fluid composed of more than 99% water. It plays a crucial role in maintaining oral health and homeostasis. The rate of saliva secretion is controlled by the autonomic nervous system, with the average amount of saliva ranging between 500 and 700 mL per day, the average volume in the mouth being 1.1 mL. At rest, the salivary secretion is controlled by the submandibular and sublingual glands with secretion rates ranging from 0.25 to 0.35 mL/min. Sensory, electrical or mechanical stimuli can raise the secretion rate to up to 1.5 mL/min [Nauntofte et al. 2003]. IgA remains the largest immunological component and other major immunologic contents of saliva include IgG, and IgM. The plasma cells in the connective tissue produce secretory IgA and the duct cells of major and minor salivary glands help in its translocation.

The total mean protein concentration in normal saliva as determined by Lowry et al. [1951] is 1660 µg/mL (range 1000-3200 µg/mL). The concentration of albumin was determined by radioimmunoassay and was found to have a concentration of 59.7 µg/mL (range 37-92 µg/mL). Immunoglobulins were found to constitute around 10% of the total protein, as determined by solid phase radioimmunoassay. The most prominent immunoglobulin was IgA representing 87% of the salivary immunoglobulins with a mean concentration of 137 µg/mL (range 50-480). The mean concentration of IgG was found to be 16.0 µg/mL (range 7.2-37) and that of IgM was 4.08 µg/mL (range 1.7-7.8) [Gronbald 1982]. Protein biomarkers found in saliva are already in use to detect different diseases such as cancer [Salazer et al. 2014], Sjogren's syndrome [Baldini et al. 2011], bacterial infections such as tuberculosis [Jacobs et al. 2016], and viral infections including Influenza virus [Sueki et al. 2016].

Saliva has a high potential for use as a diagnostic fluid since it can be collected non-invasively. It is similar to blood as both these bio fluids and their molecular components share similarities

(Slavin 1998). Saliva based technologies have been developed by many researchers to detect the transition between health and disease. Whole saliva has been used to detect antibodies towards specific HIV viral protein epitopes [Scully 1997] as well as for diagnosis of viral hepatitis variants using ELISA with high sensitivity and specificity.

Saliva has been useful for diagnosing ovarian cancer as it was shown to contain the glycoprotein cancer antigen CA 125, a biomarker for ovarian cancer. Follow-up studies have indicated that salivary CA 125 is a more useful method for diagnosis as compared to serum analysis [Chen et al. 1990]. Another study by Navarro et al. [1997] showed that the biomarker related to breast cancer, epidermal growth factor (EGF), is higher in the saliva of women with primary breast cancer or those showing a recurrence of breast cancer as compared to women without disease. These studies demonstrate the potential of saliva to be a useful diagnostic fluid for monitoring as well as diagnosing a number of diseases.

1.11.1 Salivary Anti-gliadin antibodies for diagnosing CD

As the mouth forms an integral part of the gastrointestinal tract and any immune changes that occur in the intestine will be reflected in the saliva, it was hypothesised that CD-based antibodies can be detected. Testing for gliadin induced auto-antibodies in saliva at a young age has great potential as a non-invasive approach to help in the diagnosis of CD. Hakeem et al. [1992] first showed a significantly higher concentration of salivary AGA in patients with CD as compared to those recovering on a diet free from gluten. They proposed the use of salivary IgA AGA as a marker for detecting CD using the ELISA test. In a later study, people suffering from CD have indeed been shown to have raised levels of AGA, EMA and anti-tTG auto antibodies in their saliva [Lenander-Lumikari et al. 2000].

Competitive ELISA for human salivary IgA detection was developed by Wang et al. [2010]. The linear working range of the saliva based ELISA is from 0.1 to 100 μg/mL with a limit of detection being 0.05 μg/mL. In another study, by Tonutti et al. [2009], the diagnostic efficacy of the ELISA test using synthetic gliadin peptides to test saliva was evaluated and found to be highly specific (99.2%). This study also confirmed that the AGA test may have a diagnostic role in cases where there is a valid suspicion of CD, but anti-tTG or the EMA test are negative. In another study, salivary anti-tTG antibodies were detected using a fluid-phase radioimmunoassay (RIA) format [Bonamico et al. 2011]. The test involved the incubation of ^{35}S-methionine tTG with saliva samples diluted in buffer, anti-human IgA-agarose from goat was then added to separate the free and bound antibody labelled products. Using this method salivary IgA antibody to tTG was detected with a test sensitivity of 94.5%. This pilot study illustrated the usefulness and ease of a diagnostic method based on saliva collection and its suitability for potential use in young children.

Recently, a similar concept was applied to develop an electrochemical immunoassay using magnetic beads coated with tTG that reacted with anti-tTG IgA present in saliva [Adornetto et al. 2015]. An anti-human IgA conjugated with alkaline phosphatase (AP) enzyme was used as label, and a strip of eight magnetized screen–printed electrodes as the electrochemical transducer. The use of magnetised beads as a matrix in the test method is an improvement from the existing methods and bypasses problems intrinsic to RIA. Based on a blind study of 66 saliva samples, the test sensitivity was 95% and specificity 96%.

In spite of the fact that these studies show very high values of sensitivity and specificity for diagnosis for CD, the potential application of these test methods to a population screening strategy is limited. This is because the concentration of CD associated antibodies is very low in saliva as compared to serum. Another obstacle is increased concentrations of salivary glycoproteins, such as mucins and salivary agglutinins [Actis et al. 2005], leading to an increase

in protein aggregation that causes an increase in false positive results. Also, diagnosis based on the detection of salivary tTG antibody could give a high rate of false positives as described above due to high tTG titers found in people with other health problems such as liver disease, rheumatoid arthritis and inflammatory bowel disease (IBD).

1.12 The challenges in the development of a commercial kit for diagnosing CD

Serological antibodies against tTG and DGP have been used to develop a number of commercial kits such as Inova®, Quanta Lite®, Celikey®, Euroimmun® and these are being used for the screening and diagnosis of CD. Many unaware CD sufferers have been identified using these tests. In addition, the selection of candidates for intestinal biopsy has been aided by these serological methods. The ELISA based assays are a step ahead in the development of an observer-independent objective test for diagnosis for CD. In addition, the availability of serological tests has enabled large-scale screening of the general population that has proven to be useful to identify individuals with 'silent' CD.

One of the most recent diagnostic tests is a lateral flow assay to detect anti-DGP in CD patients commercially available as the SimtomaX® blood drop system developed by Augurix diagnostics [Benkebil et al. 2013]. The device principle is an antigen direct sandwich assay using synthetic DGP conjugated to a carrier protein. The test takes a total of 10-15 minutes and shows a sensitivity of 93.1% and a specificity of 95.0%. However, in a study on children, this point-of-care DGP based test was found suitable for diagnosing CD in a selected, high risk category paediatric population. Furthermore, the test specificity gets lowered as non-specific binding occurs in children suffering from other autoimmune conditions, such as Type 1 diabetes [Bienvenu et al. 2012]. The high costs of the kit as well as other shortcomings have had a negative effect on the commercial success of this point-of-care test.

In another study, serological screening using tTG and DGP was conducted to examine the prevalence rate of CD in patients with IBD. Elevated concentrations of tTG and DGP antibodies in serum were observed in all 172 patients with inflammatory bowel disease (IBD) as compared to 190 controls. However, no true positive for CD was noted as none of the patients were found to be HLA positive or could be biopsy defined. This study highlights the limitation of the existing serological tests in correctly diagnosing patients with IBD for CD arising, mainly due to the overlapping clinical symptoms and dysregulation of the immune system [Watanabe et al. 2014].

One of the explanations for the problems encountered using commercial kits is that most validation studies were based on a pre-selected population with a high CD prevalence rate comprised mainly of a group of biopsy confirmed subjects. Furthermore, the composition of the control group consists mainly of subjects who have normal intestinal histology and excludes patients with milder histological abnormalities or those with IgA deficiency [Lewis and Scott 2010, Dahlbom 2010]. Variabilities in the characteristics of recruited patients such as their age, their family histories or association with autoimmune diseases can also lead to a selection bias that may influence in the outcome of small scale test kit results versus commercial kits used on a large scale in a clinical setting.

Recently, the European Society for Paediatric Gastroenterology, Hepatology, and Nutrition (ESPGHAN) developed guidelines for the diagnosis of CD in children with a requirement for 4 components: 1. A demonstration of coeliac symptoms; 2. An ELISA test for anti-tTG; 3. An IFA test for anti-EMA; and 4. Testing positive for the HLA-DQ2 genotype (Figure 7). These guidelines do not apply to children with features outside the stated limitations. However, given the high prevalence of HLA-DQ2/8 genes in the Western population and very low prevalence in some Asian populations, genetic testing is not definitive for diagnosis for CD [Hadithi et al. 2007, Husby et al. 2012, Fukunaga et al. 2017]. Furthermore, significant differences exist

between the serological tests; for example, in assay methodology and interpretation some commercial kits use logarithmic scales, while others use linear scales for reporting the results. An inter-observer variability must also be considered by clinicians when assessing results of EMA immunofluorescence.

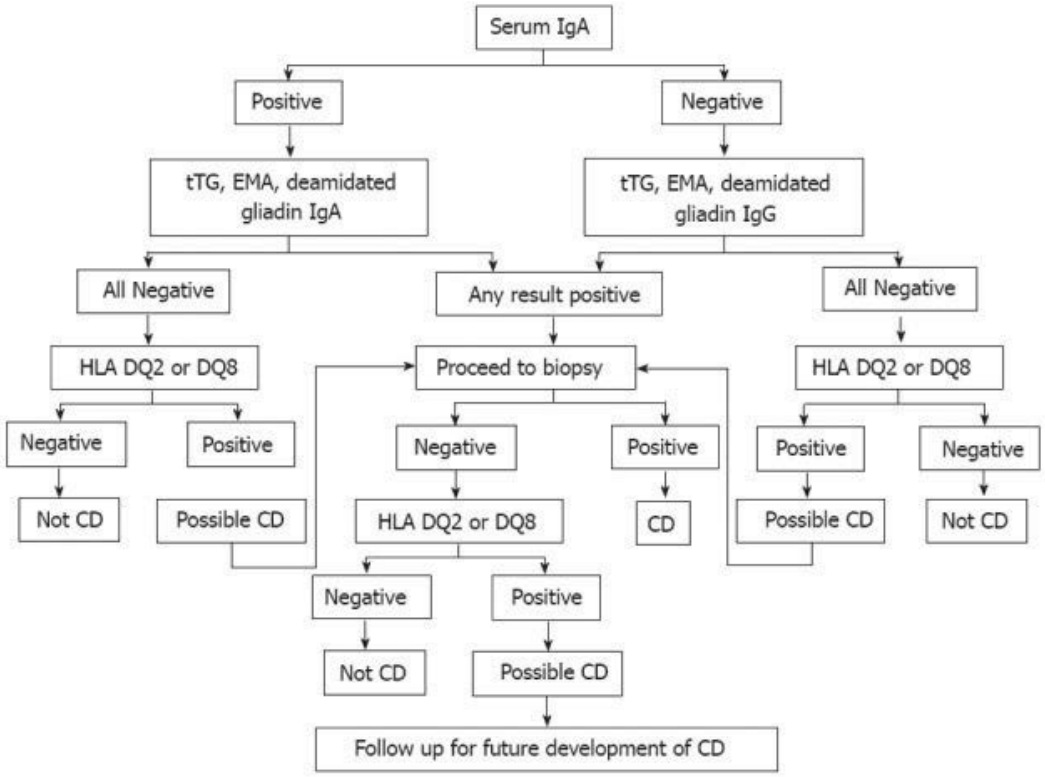

Figure 7: CD diagnostic algorithm (adapted from Mayo Medical Laboratories, Mayo Foundation for Medical Education and Research).

1.13 Outlook for the future development of new diagnostic tools for CD

Current point-of-care methods for identifying CD have been regarded as insufficient on their own to enable an accurate diagnosis without the need for intestinal biopsy. This is particularly

true for early stage 1 and 2 CD that could benefit from a gluten free diet, but the sensitivity of the existing tests is not sufficient to differentiate from CD.

Currently, several new approaches for diagnosis for CD to improve risk stratification in the general public (such as genome-wide association studies based on single nucleotide polymorphisms) are being developed. In addition, cytokine assays, IFN-γ ELISA, and IP-10 release assays for the detection of rare gluten-specific T cells are being adapted for the clinical diagnosis of CD. In fact, the characterisation of these T cell epitopes has helped in the development of a novel therapeutic vaccine, Nexvax2 that can induce tolerance in CD sufferers. The peptide vaccine has entered the Phase 2 clinical trials. It employs three different peptides (gliadin, hordein and secalin) and targets the T-cell epitopes in CD patients carrying the genotype HLA DQ 2.5^{+} to ultimately reprogram gluten-specific T cells [Wungjiranirun et al. 2016].

Novel technologies that can be applied to CD diagnostics open up new opportunities in the development of point-of-care platforms for use in low-resource laboratory settings as well as for home-based detection. Optical biosensors such as surface plasmon resonance (SPR) biosensors are particularly useful in detecting and quantifying target compounds with high sensitivity. Recently, SPR biosensors have been used in a competitive immunoassay to detect digested gluten peptides in urine [Soler et al. 2016]. In another study, quantified gluten immunogenic peptides (GIP) in stool using ELISA has been shown to help in the clinical management of CD sufferers [Comino et al. 2016].

There are examples of successful diagnostic approaches using microfluidics and nanotechnology, which include the detection of glucose levels in diabetic patients, hormone levels in pregnancy or ovulation, as well as illicit drug tests. Combining paper and nitrocellulose-based microfluidics with colorimetric and nanoparticle-based detection has been applied for the diagnosis of diseases, such as HIV [Rohrman et al. 2012], malaria [Fu et al.

2012] and tuberculosis [Veigas et al. 2012]. These approaches illustrate the feasibility of developing a point-of-care device for diagnosing CD. Indeed, the development of a microfluidics-based device for diagnosis for CD is likely to be the best approach to develop a useful and effective tool for mass screenings. Such a device would be simple, low-cost, light weight, portable with enough capability to be used for fully quantified and multiplexed assays.

1.14 CD Treatment and Management

To date, the most reliable treatment for CD remains total and lifelong avoidance of gluten ingestion. This necessitates continuous education as well as awareness of patients and their families by dieticians and doctors. Support groups and awareness centers play an instrumental role of dispersing information as well as providing support. In relation to this, the National Food Authority has re-defined the term 'gluten-free'. Earlier, <0.02% gluten concentration was considered as gluten free but now, gluten free now means absolute absence of gluten, as such <0.02% is currently labelled as 'low-gluten'. Another important consideration is that products labelled as 'wheat free' may not necessarily be gluten-free. The wheat free products may contain gluten as it is found in some other grains such as rye, barley, triticale, spelt and semolina [Fasano and Catassi 2001].

As the understanding of CD pathogenesis along with the associated risks improves, early diagnosis becomes more crucial. This is also because of the establishment of a direct link between times of gluten exposure to the disease progression. Based on the epidemiological studies, it is hypothesised that if CD develops early with typical gastrointestinal symptoms, early diagnosis and prescription to a gluten free diet could be life-saving. If, on the other hand, symptoms are atypical or completely absent, diagnosis becomes delayed and difficult. In such cases, continued exposure to gluten would only increase the risk of complications.

CHAPTER II

Background on the nanoparticles

2.1 Gold Nanoparticles

The term nanoparticles refer to particles with diameters in the size range of 1-200 nm [National Nanotechnology Initiative]. The colloidal gold nanoparticles (AuNPs) show vibrant colours produced by their interaction with visible light. There are different methods for generating the metal nanoparticles. The two main strategies are bottom up or top down method. The common top down techniques include photolithography and electron beam lithography. The bottom up techniques include templating, chemical, electrochemical, thermal and photochemical techniques [Jin et al. 2001]. These techniques make use of a capping agent such as a surfactant that prevents the aggregation of the nanoparticles [Shimoni and Valenzuela 2017]. The shape and size of the nanoparticles is also dependent on the reduction technique, time and the capping material used. Nanoparticles of different shapes such as spheres, rods, cubes, wires, tubes, triangular prisms and tetrahedral nanoparticles and sizes have been generated using various reduction techniques. In addition to their small size, the nanoparticles show high surface to volume ratios.

The most common chemical method for generating spherical gold nanoparticles is the citrate reduction method. The gold nanoparticles can be produced by reduction of chloroauric acid ($H[AuCl_4]$) using a reducing agent such as citrate [Turkevich et al. 1951]. The factors controlling the size distribution are the ratio of gold to citrate, the order of addition of reagents and temperature. Citrate also acts a capping agent by stabilising the AuNP through electrostatic interactions between the metal surface and lone pair of electrons on oxygen.

2.2 Properties of gold nanoparticles

AuNPs possess useful physical and chemical properties that make them an excellent platform for the development of novel sensors. AuNP synthesis is relatively straightforward and the nanoparticles once synthesised, remain stable for long time periods. This can be due to their two main structural components: the metal core and the surface coating. While the core determines the physical characteristics of the nanoparticle, the surface coating of the nanoparticle acts as a barrier between the nanoparticle core and the environment. The surface coating plays a vital role in protecting and stabilising the core integrity as well as in determining the chemical behaviour of the nanoparticle. As a result, AuNPs show high stability and biological compatibility with controllable shapes along with size dispersion [Sanvicens and Marco 2008, El-Sayed 2001].

There are three principle properties that make the gold nanoparticles valuable. Firstly, the particles are resistant to oxidation in room temperature, this helps in the adsorption of molecules on the gold surface using either gold-sulphur bond or electrostatic interactions. Secondly, AuNPs show surface plasmon resonance in the visible range of the spectrum. Finally, a high surface-to-volume ratio helps in the functionalisation of the nanoparticles with a wide range of ligands for detection of molecules as well as biological targets [Daniel and Astruc 2004]. These novel properties of gold nanoparticles have led to their growing use in the field of medical biotechnology.

2.3 Optical properties of gold nanoparticles for sensing applications

The AuNPs show unique optical property, localised surface plasmon resonance (LSPR), which is defined as “the collective oscillation of the nanostructure’s conduction band electrons in

resonance with the incident electromagnetic field'' [Jensen et al. 2000]. The origin of this phenomenon was first described by Mie in 1908, who solved Maxwell's electromagnetic equation for interaction of electromagnetic field with homogenous spherical small sized particles [Mie 1908]. The LSPR spectrum is strongly dependent on the size, shape and dielectric constant of the nanoparticle. For AuNPs, resonance is achieved at visible wavelength that contributes to the intense colour [Mock et al. 2003].

Surface plasmons are longitudinal waves and their dispersion relation is given by Equation 1:

$$k_{SP} = \frac{\omega}{c}\left[\frac{\varepsilon_m \varepsilon_d}{\varepsilon_m + \varepsilon_d}\right]^{1/2}$$

Where k_{SP} is the propagation constant of the surface plasmons, ω is the angular frequency, c is the speed of light in vacuum, and ε_m and ε_d are the dielectric constants of the metal and dielectric, respectively.

The origin of surface plasmon resonance is due to the free d electrons in gold that can travel freely through the material. Due to a small mean free path of gold ~ 50 nm, all interactions take place at the metal surface. Free-electrons in the metal begin to oscillate when light is in resonance creating a standing oscillation with the electron density in the particle being polarized to one surface. This resonance condition is known as the surface plasmon resonance and is located at the surface [Willets et al. 2007].

SPR arises when the frequency of the emerging electromagnetic wave propagates at the metal-dielectric interface and shows resonance with the oscillating surface conduction electrons in the metal [Homola et al. 1999]. With a change in shape or size of the nanoparticle, the surface geometry changes, that in turn, changes the electron field density. A similar shift in the surface plasmon absorption maximum takes place following the adsorption of a molecule on the metal surface [Eustis and El-Sayed 2006].

2.4 SPR-based biosensors

A typical biosensor is comprised of a bioreceptor, an interface to generate a signal following a specific biological event and a sensor that acts as a transducer or a detector. A SPR based biosensor is comprised of a SPR sensor and suitable surface functionalisation that acts as the biorecognition element. SPR based biosensors are advantageous as the bioreceptor and the detector are connected that helps in generating a compact, small-sized portable and low-cost device. Further SPR based biosensors can be categorised as sensors with angular wavelength intensity, or phase modulation based on the characteristics of the optical wave interaction with the surface plasmons that are being measured [Lee 2008].

SPR biosensors, based on wavelength modification, employ a polychromatic wavelength and the resonance wavelength corresponding to the surface plasmon excitation. The intensity and phase shift of the interacting optical wave at fixed wavelength and angle of incidence is examined in SPR sensors with intensity and phase modulation, respectively. The sensitivity for the SPR sensor is defined as the "ratio of the change of the sensor output dY (wavelength of resonance) to the change of the refractive index of the sensed medium dn," described in Equation 2 as, $S = dY/dn$.

Sensor resolution is defined as the "smallest change in refractive index of the sensed medium that produces a noticeable change in the sensor output". Therefore, the limit of detection of SPR sensors is dependent on the sensor resolution.

2.5 Gold nanoparticles as SPR biosensors

One of the most commonly used platforms for SPR biosensors use AuNP as sensors. The immobilisation of bioreceptors is based on the attachment of sulphur-containing ligands as the

gold-sulphur bonds is easily formed and allows direct attachment of the receptors to the gold layers. The bioreceptors can be either physically coated or chemically attached to the AuNP surface [Wijaya et al. 2011].

While the AuNPs absorb and scatter light intensely at their surface plasmon resonance [Jain et al. 2006], SPR frequency is sensitive to the inter-particle distance between the nanoparticles. Inter-particle plasmon coupling results in significant red-shift (~525 nm to ~650 nm) and broadening of the spectrum leading to the formation of a new absorption band at longer wavelengths when AuNPs aggregate. This aggregation of AuNPs is caused by the increase in electric dipole-dipole interaction as well as overlapping of plasmons of neighbouring particles. Therefore, when the inter-particle distance is substantially greater than the average particle diameter, the AuNPs appear red. Aggregation of the nanoparticles, however, results in a decrease in the inter-particle distance to less than average particle diameter, turning the colour of the aggregates to blue (Figure 8).

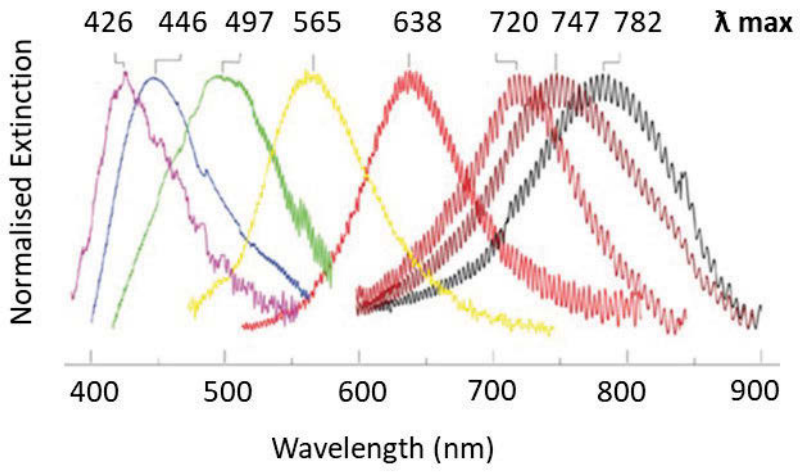

Figure 8: Representation of surface plasmon resonance for gold nanoparticles. *Isolated gold nanospheres absorb blue light because of inter-band electronic transitions in the gold. As red light is not absorbed, the AuNP suspension appears red. When the gold nanoparticles aggregate, their peak plasmon resonance shifts* [adapted from Haes et al. 2001].

For spherical nanoparticles, a surface plasmon resonance in the mid-visible region of the spectrum (520 to 550 nm), green light, corresponds to the surface plasmon band in the nanometre scale for noble metal nanoparticles. This absorption originates from the collective oscillation of the valence electrons due to resonant excitation by the incident photons [Bohren and Huffman 1998]. Further, it has been demonstrated that heating of the particles following the absorption of light, leads to a highly localised increase in temperature. This phenomenon has been further exploited in the proposed photo-thermal therapeutic uses of gold nanoparticles [Pissuwan et al. 2006]. Inter-particle surface coupling is a consequence of the presence of nanoparticles, (d>3.5 nm), to each other. AuNP aggregation leads to a significant red-to-blue shift and broadening of the surface plasmon resonance band that can be readily observed as colour change by the naked eye at nanomolar concentrations [Su et al. 2003].

2.6 Protein adsorption to nanoparticle surface

'Protein corona' or protein adsorption onto nanoparticles (AuNPs) depends on the size [Lundqvist et al. 2008, Deng et al. 2011], charge [Huang et al. 2013, Feliu et al. 2012], incubation time, temperature [Lesniak et al. 2010, Mahmoudi et al. 2013], the colloidal stability of AuNPs [Gebauer et al. 2012], as well as on the types of proteins [Tenzer et al. 2011]. Physiochemically, protein adsorption onto nanoparticles has been described to resemble ligand binding [del Pino et al. 2014].

The equivalence principle of nanoparticle-protein interaction

Proteins have been shown to adsorb as well as desorb to the surface of AuNPs and have been shown to displace other proteins or ligand shell around the AuNPs. This binding is based on the law of mass action that is used to express the fraction of AuNPs saturated with proteins. It

depends on the concentration of free proteins and free AuNPs as well as the concentration at which half of the AuNPs are saturated.

In a state of equilibrium, the AuNPs are loaded on average with N proteins, N_{max} being the maximum number of proteins that each AuNP can bind to. Upon reaching a state of saturation, no additional proteins can bind to the AuNPs. This increases the fraction of unbound protein that is described in Equation 3, using Dissociation Equilibrium constant (K_D)

$$K_D = c(NP)\, c^n(P)/c(P_nNP)$$

Where c(NP), c^n (P) and c (P_nNP) represent the concentrations of free nanoparticles, unbound proteins and protein-nanoparticle complexes, respectively. Also, $K'_D = K_D^{1/n}$ where K'_D is used to describe the concentration at which half of the AuNPs are saturated with proteins.

Initially at low protein concentration, K'_D value is low so that a higher fraction of proteins can bind to the AuNP surface. The protein also displays higher binding probability to the AuNP surface. At equilibrium, the total protein concentration reaches around K'_D, wherein a significant amount of proteins are already bound. Due to the unavailability of a free binding site on the AuNP surface, only a few additional proteins can further bind to the AuNPs after which an equivalence point is reached. Once the AuNPs are saturated, additional proteins cannot bind. These excess unbound proteins may then aggregate, disrupting the colloidal stability of the AuNPs.

Another important factor is the multifunctional nature of the binding interactions of the proteins to the nanoparticles (NP), which may affect the cooperative nature of the protein-NP complex formation. The binding association constant K for proteins onto AuNPs has been shown to increase progressively with nanoparticle diameter in the range between 5 and 60 nm. A higher protein packing density on the surface of larger nanoparticles leads to a corresponding increase in K. Whereas, a less efficient polymer surface packing is observed in larger nanoparticles because of the increased interactions by the unfolded protein conformations. This also

emphasises the importance of the conformational state of the coated proteins, particularly in understanding the nature of protein layers that form on the nanoparticles as well as the variation of K with nanoparticle size [Silvia et al. 2009].

In real bodily fluids, such as serum and saliva, the total protein concentration can be as large as 35% by volume and there can be several proteins present. Subsequently, there is increased competition between these proteins in their adsorption on the nanoparticles dispersed within this complex biological environment. Initially, the two major proteins present in the plasma (human serum albumin and fibrinogen) generally dominate the interaction with nanoparticles due to their wide availability, but over time, these are displaced by proteins with higher affinity, a lower abundance and slower adsorption kinetics. The inter-protein competition and displacement that can result in the coating of non-specific proteins onto the AuNP surface is known as the Vroman effect [Jung et al. 2003]. This non-specific protein binding may result in a decreased sensitivity of the AuNPs, particularly when used for testing biological markers in serum. The problem can be overcome by adding BSA protein to AuNPs that would block the free binding sites thereby reducing non-specific protein adsorption.

The cooperativity of the protein-nanoparticle binding process is quantified by the Hill coefficient (n). Proteins such as human serum albumin, histone, fibrinogen, and globulin, have anti-cooperative binding ($n<1$), which indicates that the association energy per particle will progressively decrease with continued protein adsorption. Insulin, however, presents an inverse trend and has $n>1$. The tendency of a decreased cooperativity of protein upon binding to larger nanoparticles demonstrates changes in the physical-chemical properties of the nanoparticle upon continued protein adsorption. These results help to understand that for protein adsorption on the negatively charged citrate-coated gold nanoparticle surface, there should be a reduction in the electrostatic binding energy that reduces the relative magnitudes of the enthalpy and entropies of protein binding [Lynch et al. 2007]. This would enable rationalisation of the anti-

cooperativity of the protein adsorption to the nanoparticle. If on the other hand, the nanoparticles induce the proteins to organise at their boundaries, one can expect an enhancement of the cooperativity of the nanoparticle-protein binding transition.

2.7 Colorimetric sensing using gold nanoparticles

Gold nanospheres have higher surface-to-volume ratios, which helps in their functionalisation as well use as bio-probes. Biomolecules, such as DNA/RNA oligonucleotides, can be easily attached to the AuNP surface through polymers such as polyethylene glycol (PEG) [Sperling and Parak 2010, Verma and Stellaci 2010]. This binding is facilitated by the presence of negative electronic shielding that provides a Coulomb force that can bind different molecules [Link and El-Sayed 2003]. AuNPs can be conjugated to biomolecules due to their high affinity for amines, thiols and phosphines. The biosensor technologies based on the aggregation of AuNPs have been used to detect metal ions as well as to probe biomolecular interactions.

2.7.1 Detection of metal ions

AuNPs have been used for colorimetric detection of alkali metals such as Na^+ in urine following formation of a sandwich complex between functionalised AuNP, chelating ligands and Na^+ [Lin et al. 2005]. Detection of heavy metal ions such as Pb^{2+}, Cd^{2+} and Hg^{2+} is vital as these metal ions pose many health hazards. A colorimetric sensor using AuNPs functionalised with chelating agents was developed to detect Pb^{2+} [Chai et al. 2010]. The detection of Pb^{2+} was based on the disruption of the AuNP aggregate formed following the hydrogen bonding between carboxylic acid residues in methanol/water solvent system. Pb^{2+} disrupts this hydrogen-bonded network of AuNP causing electrostatic repulsion between the AuNPs,

causing a blue-to-red colour change indicating Pb^{2+} presence. This system has shown high sensitivity for other metal ions such as Cd^{2+} and Cu^{2+} as well [Wang et al. 2013].

DNA functionalised AuNPs have also been used for the detection of Hg^{2+}. Mirkin et al. [1997] reported a highly selective, colorimetric polynucleotide-based detection method using mercaptoalkyl-oligonucleotide modified AuNPs. For the detection, two different thiolated-DNA sequences (designated as probe 1 and probe 2) were used for the functionalisation of the AuNPs. On mixing, probe 1 and probe 2 formed aggregates of AuNP with lower melting temperature (Tm) because of the T-T mismatches in the base sequence. Addition of Hg^{2+} resulted in the formation of an enlarged polymeric network comprising of T- Hg^{2+}-T. Following aggregate formation, an increase in Tm as well as changes in the absorbance spectra arising from the formation of extended polymeric nanoparticle aggregates were observed. A high sensitivity of the method was demonstrated, as little as 10 fmol of an analyte oligonucleotide could be detected by using the phenomena of aggregation of gold nanoparticles. Later, thymine-functionalised AuNPs were used for the colorimetric detection of Hg^{2+} ions. Similarly, anionic species such as fluoride ions in water have been detected using AuNPs coated with thio-glucose groups. Fluoride ions in a narrow concentration range (20-40 mM) can be detected by this method [Watanabe et al. 2005].

2.7.2 Detection of proteins

A number of diseases including cancer, have been linked with the presence of certain proteins that are useful as biomarkers and enable diagnosis of these diseases. Additionally, functionalised AuNPs have been used successfully for colorimetric sensing of proteins. One of the examples includes the detection of carbohydrate binding proteins using carbohydrate functionalised AuNPs [Otsuka et al. 2001]. Quantitative detection of lectin was carried out

using β-D-lactopyranoside (Lac)-functionalised AuNPs wherein the degree of colloidal aggregation was found to be proportional to the protein concentration. This method was found to be sensitive to detect 1 ppm of lectin concentration [Duncan et al. 2003]. In another study, sialic acid functionalised AuNPs have been applied to detect JC virus like particles (VLPs) using sialic acid recognition [Niikura et al. 2009].

Aptamers, which can be oligonucleotide single-stranded DNA or RNA (ssDNA or ssRNA) or peptide molecules with a domain that can bind to specific target molecules with high specificity and affinity have also been used to act as linkers. The structural and chemical properties of aptamers enable them to recognise molecules just like antibodies. Zhang et al. [2013] used aptamers to create an extensive network of nanoparticles adsorbed with DNA. These can then be used to detect molecules such as adenosine and cocaine. The addition of such compounds led to disassembly of the network in a colorimetric based disassembly process.

AuNPs functionalised with platelet-derived growth factors (PDGFs)-specific aptamers have been used as probes to detect PDGFs at nanomolar concentrations [Huang et al. 2005]. Furthermore, the aptamer-AuNP-PDGF scaffold was used to detect PDGF receptors through a competitive binding assay [Huang et al. 2007]. An AuNP based test to determine the level of anti-protein A in aqueous and serum solutions was reported by Thanh and Rosenzweig [2002]. The technique shows a sensitivity limit of 2 μg/mL for anti-protein in serum samples, the result is comparable to ELISA. Colorimetric detection of proteases, such as thermolysin have been carried out using dithiol-functionalised peptides [Laromaine et al. 2007]. This was achieved by using a self-assembled peptide-functionalised nanoparticle network that was activated by thermolysin derived from *B. Thermoproteolyticus rokko*. This developed assay presented a simple, highly sensitive and an efficient method to detect the presence of proteases.

Huang [2007] developed an AuNP-based immunochromatographic assay for the detection of the bacterium, *Staphylococcus aureus*. Detection of protein A, which is present in the cell

membrane of *S. aureus* strains, was carried out using AuNPs embedded on an immunochromatographic strip functionalised with anti-protein A antibodies. While the time for detection was less than 10 minutes, the sensitivity limit for the device to detect protein A was down to a concentration of 25 ng/mL. A similar immunochromatographic test strip for the detection of porcine reproductive and respiratory syndrome virus (PRRSV) was reported by Zhou et al. [2009]. The detection for the PRRSV is based on the aggregation of AuNPs resulting from the capture of the antibodies by the functionalised AuNPs, leading to the formation of a reddish-purple band. An immunogold based chromatographic test for the detection of melamine residues in raw milk, milk products as well as in animal feed was developed by Xiao et al. [2011]. The test is useful for quick, on-site determination of melamine residues in a large number of samples.

AuNP based immunosensors have been used to develop a pregnancy test based on the detection of the pregnancy test marker, namely, human chorionic gonadotrophin hormone (β-hCG), a hormone released by pregnant women. The test consists of AuNPs functionalised with antigen β-hCG (Mab II) sprayed on a conjugation pad for specific binding with the target monoclonal antibody. This monoclonal antibody was immobilised on the test line (T zone) of the nitrocellulose membrane to capture the immune complex formed using the AuNPs. In the presence of β-hCG, the AuNPs aggregated on the test line and a red colour indicates positive for the test [2014]. These immunogold tests help to demonstrate the wide application of the gold protein conjugates and their interactions with antibodies that can prove beneficial in developing new assays.

2.8 Aims and Project Objectives

In order to develop a coeliac diagnostic assay based on the properties of the gold nanoparticles combined with the specificity of the antibodies from serum as well as saliva; the following aims have been addressed in this work:

1. To develop methods for the binding and adsorption of proteins such as gliadin and their related peptides on the surface of gold nanoparticles.

2. To detect and measure the concentrations of antibodies to be used as biomarkers in serum and saliva.

3. To test and validate the developed test on real patient serum samples.

CHAPTER III

Materials and Methods

3.1 Reagents

20 nm citrate stabilised gold nanoparticles (AuNPs), bovine serum albumin (BSA), Gliadin, anti-gliadin antibody (AGA) from rabbit, and IgG antibody from whole normal rabbit serum, 4-(2-hydroxyethyl)-1-piperazineethanesulfonic acid (HEPES), Phosphate-Buffered Saline (PBS) were all obtained from Sigma-Aldrich (Australia).

Isopropyl alcohol was obtained from Nalgene® and ammonium sulphate was obtained from Ajax Chemicals. Poly (ethylene glycol) [*N*-(2-maleimidoethyl) carbamoyl] methyl ether 2-(biotinylamino) ethane (i.e. Biotin-PEG_{11}-Maleimide) and NeutrAvidin were all obtained from Thermo Fisher Scientific Australia.

3.1.1 Peptide sequence

The peptide sequence (QLQPFPQPQLPYPQPQC) was synthesised from ChinaPeptides Co., Ltd. (China). The synthetic crude peptides were purified by reversed-phase liquid chromatography to give a satisfactory peptide sequence (~90% homogeneity by analytical HPLC) with the correct amino acid sequences and mass spectra. The peptide contained residues 57-72 of α-gliadin and was designated as follows: Peptide: QLQPFPQPQLPYPQPQC.

3.1.2 Clinical samples for assay validation

Anonymised patient samples were provided by Dr Jason Tye-Din from the Walter and Eliza Hall Institute of Medical Research (WEHI Institute, Melbourne Parkville, Australia). They were collected with informed consent and approval of Melbourne Health and WEHI Human Research Ethic Committees (2003.009 and 03/04) respectively. Ethical approval was also obtained from the University of Technology Sydney Research Ethics committee (UTS HREC ETH16-0841) before testing the clinical samples.

Samples were collected from patients with active CD (pre-treatment), treated CD (on a gluten free diet) and controls without CD. All cases of CD were medically diagnosed and based on typical small intestinal histology in conjunction with positive CD serology.

The cohort consisted of some samples that were found to be haemolytic and had been stored for > 5 years, these samples were removed to maintain assay homogeneity. In the clinical study thirty human serum samples were analysed in a blinded assessment. No prior knowledge of the CD status or any other clinical condition of any of the patient samples was known while testing.

3.2 Alpha-gliadin derived from *Triticum aestivum*

Alpha (α)-type gliadin with an average molecular weight of 31 kDa, was used in this study. It is the most common form of gliadin found in nature and represents 15-30% of the total proteins in wheat grain [Wang et al. 2007]. Additionally, α-gliadins have been shown to induce small intestine inflammation in patients suffering from CD [Anderson et al. 2000]. The term “gliadin” as used in this study includes “α-gliadin”.

A study conducted by Dohlman and colleagues [1993] to examine the structural properties of autoantigens showed that the human specific autoantigens were often found to have a highly

charged surface with repetitive elements as compared with other protein sequences in GenBank. The ability of gliadin protein to trigger CD can be also understood from its structural features. The protein contains a unique structural domain; the repetitive domain, that contains an elevated content of amino acids glutamine and proline that are arranged in a repetitive pattern. In addition, gliadin also contains six cysteine residues that form three intramolecular bonds resulting in a globular structure.

In this study, the whole hydrophobic gliadin protein as well as a peptide sequence derived from gliadin were coated on the surface of the 20 nm AuNP surface. To coat gliadin, first, gliadin was solubilised in a three-step protocol, following which AuNPs were added drop-wise to obtain gliadin coated AuNPs. I developed protocols for binding of the hydrophobic gliadin protein and the peptide on the surface of the AuNPs. The peptide sequence derived from gliadin was coated to the AuNPs by using the highly specific biotin-NeutrAvidin interactions and use of a Biotin-$(PEG)_{11}$-Maleimide linker.

I then developed the serological assay, in a simple, single antibody step diagnostic test. Finally, I used this diagnostic assay on thirty patient serum samples in a blinded assessment and compared the results with the previously run serological and pathological tests on these patients using both the gliadin and peptide-coated nanoparticles.

3.3 Coating of gliadin on the AuNP surface

In the present study, 20 nm AuNP citrate stabilised nanoparticles were used. The citrate layer provides long term stability to the AuNP and is weakly associated to the nanoparticle surface. This citrate layer can be easily displaced by a range of molecules including proteins. Adsorption of gliadin on the surface of AuNPs followed by displacement of the citrate layer

involved non-covalent processes based on the ionic interactions between the negatively charged nanoparticle and the positively charged amino acids in the protein. Some interactions also occurred due to co-valent binding between the AuNP and the conducting electrons of nitrogen and sulphur atoms present in the protein [Tsai et al. 2011].

3.4 Coating of the peptide sequence to AuNP using Avidin-Biotin interaction

AuNP biofunctionalisation using a low-molecular bio-functional linker is a widely adopted method for coating biomolecules. The linker molecule contains an anchor group for binding to the AuNP and a functional group that enables covalent interaction with the peptide sequence.

The functionality of the linker is based on the use of avidin-biotin interactions that have been extensively applied in the development of immunoassays [Kendall et al. 1982]. Avidin (67 kDa) including Streptavidin and NeutrAvidin, are tetrameric proteins that can bind to biotin, a co-factor that plays a role in multiple eukaryotic biological processes. The avidin-protein interaction is the strongest known non-covalent interaction ($K_D = 10^{-15}$ M) between a protein and ligand. Apart from the high binding affinity, the symmetry of the biotin-binding pockets, placed in pairs at opposite faces of the protein helps in protein-ligand interaction (Figure 9).

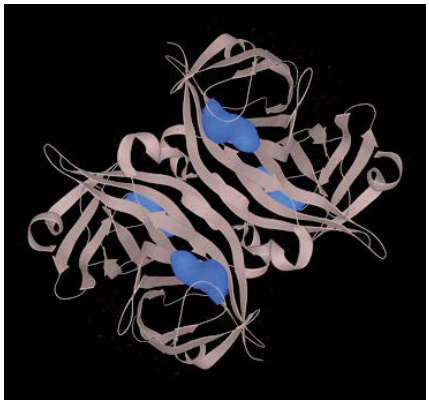

Figure 9: Representation of Avidin-Biotin interactions (PMID: 2911722). *Biotin is shown in cyan. The tetrameric Neutravidin is represented by flat arrows and ribbon protein structure.*

As endogenous biotin can reduce specificity in the immunoassays [Sastry et al. 1998], therefore, a maleimide-activated, sulfhydryl-reactive biotinyl linker ($C_{41}H_{71}N_5O_{16}S$) was used to coat peptide sequence to the AuNP. This biotinylating linker contains an 11-unit Polyethylene Glycol (PEG) spacer arm that improves water solubility as well as prevents aggregation. The biotinylated and PEGylated peptide showed high affinity to the avidin coated AuNPs. Once formed, it remained stable allowing addition of more biotinylated peptide per AuNP without any related loss to specificity.

3.5 Calculation of the molar extinction coefficient of gliadin, BSA and peptide

The molar extinction coefficient, also known as the molar absorption coefficient of a particular protein is the absorbance of the protein at the ultraviolet wavelength at 280 nm. Absorbance of a protein at 280 nm is related to its amino acids that contain aromatic rings, for example, amino acids tryptophan (Trp, W), tyrosine (Tyr, Y) and to a lesser extent amino acid cysteine (Cys, C). The molar extinction coefficient of a particular protein can be calculated from its

protein sequence. The calculation is performed based on the weighted sum of the 280 nm molar absorption coefficients of these three constituent amino acids denoted as W, Y and C, as described in the following Equation 4 [Gill et al. 1989 and Pace et al. 1995]:

$$\varepsilon = (nW \times 5500) + (nY \times 1490) + (nC \times 125)$$

where n is the number of each residue and the stated values are the amino acid absorption at 280 nm.

The ProtParam tool (ExPasy Bioinformatics Resource Portal) was used to compute the molar extinction coefficient of gliadin and BSA. Gliadin was specified as a Swiss-Prot accession number (PO2863). The computation was carried out on the complete sequence of gliadin composed of 286 amino acids. BSA is specified as a Swiss-Prot accession number (PO2769). The extinction coefficient was calculated on the complete sequence composed of 607 amino acids. The peptide sequence of 17 amino acids (QLQPFPQPQLPYPQPQC) was used for the analysis. Table 8 describes the molar absorption coefficient for both the proteins as well as the peptide.

Table 8: Calculated molar absorption coefficients of gliadin, BSA protein and peptide.

Protein/Peptide	Molecular Weight	Extinction Coefficient
Gliadin	31 kDa	19285 $M^{-1}cm^{-1}$
BSA	66.5 kDa	47790 $M^{-1}cm^{-1}$
QLQPFPQPQLPYPQPQC	2 kDa	1490 $M^{-1}cm^{-1}$

3.6 Titration procedure to find amount of protein needed to saturate and stabilise the colloidal gold

The concentration of BSA, gliadin and the peptide sequence that saturates the AuNP surface was determined by carrying out a titration. The pH of the colloidal gold was first, adjusted to match the isoelectric point (pI) of the proteins, *i.e*. 4.6 for BSA, 7.65 for gliadin and 5.21 for the peptide sequence. Between 0 to 10 mg/mL of gliadin, BSA and peptide added in 100 µL of 20 nm AuNPs while vortexing. The AuNP-protein conjugate was incubated for 2-3 minutes at room temperature. The colour change was observed to determine the protein concentration at which the AuNP surface is saturated and no aggregation of AuNPs has occurred.

3.7 Gliadin solubilisation in solvents

Solubility of gliadin was first tested using a variety of solvents including non-polar, polar aprotic and polar protic solvents. The solvents tested included, acetone (polar aprotic), chloroform (non-polar), dimethylsulphoxide (DMSO; polar aprotic), dimethylformamide (DMF; polar aprotic) and methanol (polar protic). 1 mg of gliadin (in powdered form) was dissolved in these solvents by adding and stirring. Solubility was determined by visual inspection and it was observed that in all the polar aprotic solvents tested, no solubility was obtained.

Solubility of gliadin was also tested using different solvent combinations. The various solvent combinations tested included; a polar aprotic solvent (acetone) and a non-polar solvent (chloroform), polar protic solvent (methanol) and a non-polar solvent (dichloromethane (DCM)) and two polar protic solvents (isopropanol and ethanol). It was observed that only partial solubility of gliadin could be achieved in these solvents. It was further observed during

validation that 70% ethanol caused flocculation of the AuNPs leading to a decrease in the ability of AuNPs to coat gliadin. The use of 70% ethanol was therefore discontinued.

Subsequently, to achieve high solubilisation of gliadin by unfolding the globular structure of the protein a three-step protocol comprising; (i) use of a surfactant (ii) the use of a polar protic solvent and (iii) a heating step was devised as shown below in Figure 10.

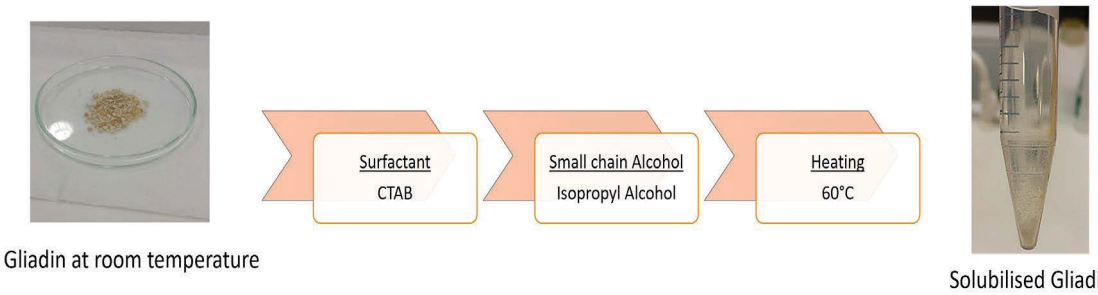

Figure 10: Three step protocol for solubilisation of gliadin using a surfactant, small chain alcohol and heating.

3.8 Validation of the gliadin protein solubilisation protocol

Step (i) Surfactant and polar protic solvent

In step (i) of the protein solubilisation protocol, the use of a surfactant was tested to determine if dissolving the gliadin protein by decreasing the surface tension between the protein and water would improve gliadin solubilisation. Surfactants have previously been used in the DNA extraction as well as protein isolation from plant tissues such as wheat. A number of surfactants such as Tween 20, Tween 40 and Tween 60 were also tested, the results obtained using these surfactants showed aggregation that had possibly occurred due to the formation of large

micelles. The use of these surfactants was therefore discontinued in the study. On the other hand, surfactants such as CTAB (cetyltrimethylammonium bromide), have been shown to help in the disruption of the plant cell membrane that enables release of the cellular constituents as well as to separate the proteins from the DNA [Rogers and Bendich 1989].

Given the structure of gliadin, an anionic surfactant, such as sodium dodecyl sulphate (SDS) and a cationic surfactant such as CTAB were chosen as possible surfactants that could interact with the plant derived protein (gliadin) by forming smaller micelles and help in solubilisation of the protein.

To compare the colloidal stability of gliadin in these two different surfactants, two samples were prepared. Firstly, 1 mg of gliadin was dissolved in 500 µL of 10 mM CTAB in water and 500 µL of isopropyl alcohol (IPA). Secondly, 1 mg of gliadin was dissolved in 500 µL of 10 mM SDS in water and 500 µL of IPA. The final gliadin concentration for each sample was 1 mg/mL.

It was observed that at the same concentration (10 mM), while SDS caused protein aggregation, CTAB formed small micelles by forming electrostatic and hydrophobic interactions with gliadin and helped in solubilising the protein. In particular, size distribution by volume for gliadin indicated the formation of small micelles (between 90 nm and 417 nm) when dissolved in CTAB, whereas in the presence of SDS, large micelles (between 90 nm and 750 nm) were formed that resulted in protein aggregation. From this, it was determined that a cationic surfactant, CTAB, was particularly useful in the solubilisation of gliadin.

Step (ii) Polar protic solvent

In step (ii) of the solubilisation protocol, it was determined if a polar protic solvent such as IPA could be used. This was based on the theory that IPA could act as a diluent for gliadin by

entering the interfacial area of the protein, pulling apart the surfactant molecules and in the process, improve gliadin solubilisation.

1 mg of gliadin was added to 500 µL of 10 mM CTAB in water and 500 µL of IPA. As shown in Table 9, it was found that IPA with surfactant CTAB, does improve the solubility of gliadin.

Table 9: Average protein concentration (mg/mL) of gliadin in samples with and without the addition of IPA

Sample	Average Protein Concentration (mg/mL)
Gliadin/CTAB/IPA/60°C	0.73
Gliadin/CTAB/60°C	0.57

Step (iii) Heating

In step (iii) of the solubilisation protocol, it was investigated if the effect of heating helps in the solubilisation of 1 mg/ml of gliadin in a mixture comprising the surfactant CTAB and the polar aprotic solvent IPA. Heating was performed at a temperature range of 20°C to 80°C for 5 minutes. The protein concentration was measured after the heating step using the NanoDrop. Results are provided in Figure 11.

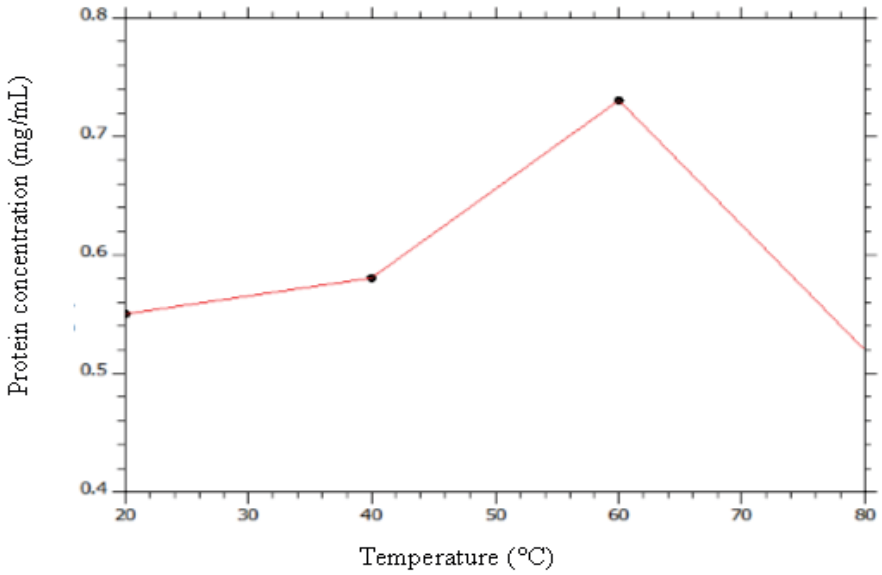

Figure 11: Average protein concentration (mg/mL) of gliadin at different temperatures (20°C to 80°C)

As shown in Figure 11, it was found that the gliadin concentration reached a maximum at 60°C, indicating an increase in protein solubilisation. The increase in protein concentration at 60°C may be caused by a linear decrease in hydrogen bonds and electrostatic bonds within the gliadin protein. When the temperature was increased above 60°C, a decrease in protein concentration was observed. This decrease in protein concentration may be caused by the protein undergoing denaturation, which may involve a helix-coil transition. This may also result in exposure of the immunogenic epitopes of gliadin that are responsible for triggering CD.

3.9 Preparation of the AuNPs coated with gliadin protein

5 mg of gliadin was dissolved in 2.5 mL of 10mM aqueous CTAB in a 15 mL Falcon™ tube. The tube was then heated for 5 minutes at 60°C and vortexed for 10 minutes. 2.5 mL of IPA

was added to the tube and vortexed again for 10 minutes to completely dissolve gliadin. The dissolved gliadin was then filtered using a Ministart® non-pyrogenic filter unit with a pore size of 0.2 µm.

600 µL of 20 nm AuNPs was added dropwise to a Falcon Centrifuge tube containing 2.8 mL of the filtered flow-through of solubilised gliadin followed by quick vortex. The dispersion was mixed for 60 minutes with a repeated vortexing every 10 minutes followed by centrifugation at 4500×g for 30 minutes. The supernatant was discarded, and the pellet was re-dissolved in 150 µL of MilliQ water. The 20 nm AuNPs coated with gliadin were stored at 4°C for up to 4 weeks. Figure 12 represents the preparation of AuNPs coated with gliadin protein.

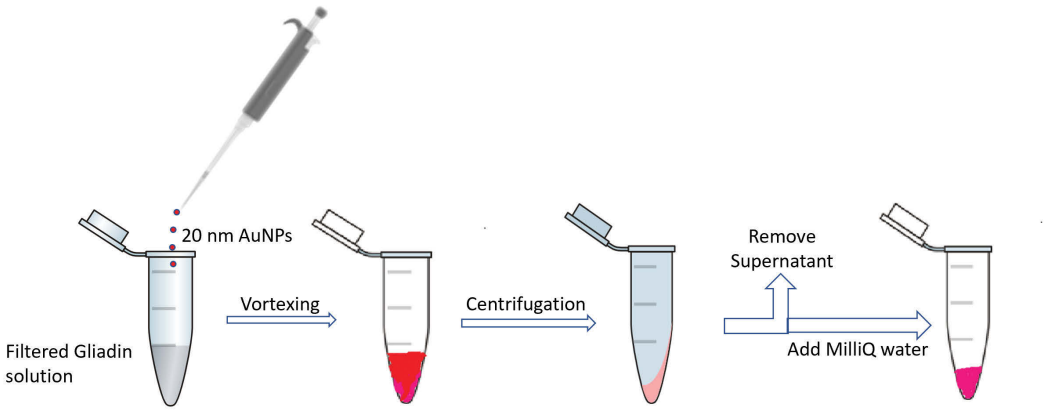

Figure 12: Schematic representation of the surface modification of AuNPs with gliadin

3.9.1 Determination of the optimal conditions to coat gliadin on the surface of gold nanoparticles (AuNPs)

Incubation period of gliadin with AuNP

The optimal time period for incubating solubilised gliadin with AuNPs was determined. It was found that 30 minutes resulted in poor coating of gliadin on the surface of the 20 nm AuNPs. Poor adsorption was characterised by poor pellet formation following centrifugation. While, incubation at 90 minutes resulted in AuNP aggregation that was observed as a colour change from red to purple in some tubes. It was determined that 60 minutes of incubation at room temperature was the preferred incubation period for gliadin adsorption to AuNPs.

Solvent for re-dispersal of gliadin-AuNP pellet

The effect of re-dispersing the gliadin-AuNP pellet in MilliQ water, HEPES buffer and PBS buffer was studied using dynamic light scattering (DLS). In each experiment, three different samples were prepared, and readings were taken in triplicate. Aggregation of the AuNPs in solution resulted in an increase in diameter of the AuNPs that was indicated by a peak shift to the right on the DLS.

A variation in the peaks was observed for the three different samples of gliadin-AuNP pellet when HEPES or PBS buffer was used for pellet dispersal. In all the samples, the peak shifted towards the right indicating an increase in the size of gliadin-AuNPs, representing likely aggregation.

On the other hand, peaks for the gliadin-AuNP pellet re-dispersed with MilliQ water remained constant for three different samples. This indicated no relative change in the size of the particles and most importantly, indicated no aggregation amongst the gliadin-AuNPs. Subsequently, MilliQ water was used for gliadin-AuNP pellet dispersal.

Ratio of AuNP to gliadin

The suitable ratios of AuNPs to gliadin to be used in the adsorption step were also determined. Experiments were conducted using 20 nm AuNPs coated with gliadin at different volume titrations for AuNPs and solubilised gliadin. Results were based on the data obtained using DLS and UV-vis absorbance spectrophotometer (Table 10).

Table 10: Range of AuNP: gliadin ratios

Volume of AuNP	Volume of solubilised gliadin	AuNP: Gliadin ratio
600 µL	2800 µL	(1:4.6)
600 µL	2000 µL	(1:3.3)
300 µL	1000 µL	(1:3.3)
100 µL	500 µL	(1:5)
150 µL	600 µL	(1:4)

Based on the titrations it was determined that a ratio of 20 nm AuNP to solubilised gliadin of 1:4.6 achieved a particularly beneficial extent of adsorption *i.e.* 600 µL of 20 nm AuNPs were added dropwise to 2800 µL of solubilised gliadin.

3.10 Preparation of the AuNPs coated with Bovine Serum Albumin (B.S.A)

500 µL of 10 mg/mL BSA dissolved in 10mM HEPES was added to 50 µL of 20 nm AuNPs while vortexing. The tube was incubated for 30 minutes at room temperature with repeated vortexing. The solution was centrifuged for 30 minutes at 4500×g, supernatant discarded, and the pellet was re-suspended in 500 µL HEPES buffer. The process was repeated twice after

which the pellet was re-suspended in 500 µL HEPES buffer followed by centrifugation at 4500×g for 30 minutes using an Eppendorf® Microcentrifuge. The BSA coated AuNPs were stored at 4°C. Figure 13 represents the preparation of AuNPs coated with BSA.

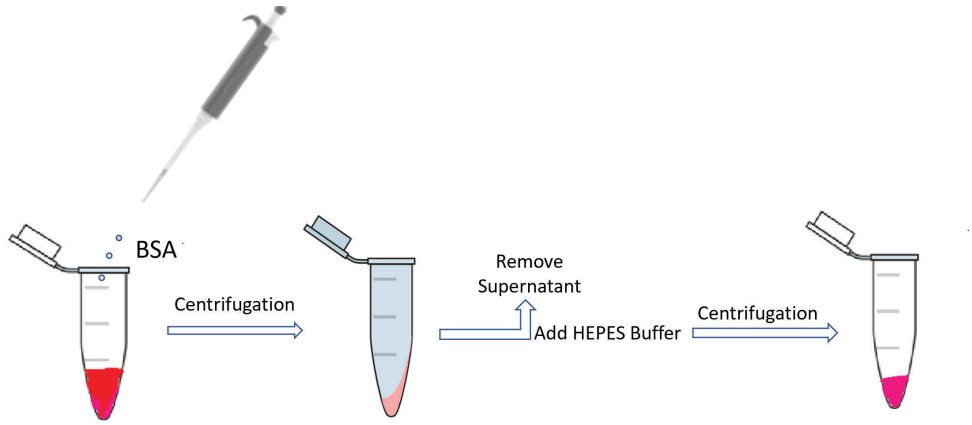

Figure 13: Schematic representation of the preparation of AuNPs coated with BSA.

3.11 Preparation of AuNPs coated with peptide sequence

The peptide (QLQPFPQPQLPYPQPQC) was coated to the surface of the AuNPs in two stages: first, coating with NeutrAvidin followed by a second step of binding of the peptide through a biotin-$(PEG)_{11}$-Maleimide linker molecule.

Preparation of the AuNPs coated with NeutrAvidin

300 µL of 20 nm AuNP were added dropwise to 200 µL of NeutrAvidin dissolved in 10mM HEPES (1 mg/mL) while vortexing. The tube was incubated for 60 minutes at room temperature with repeated vortexing. The solution was centrifuged for 30 minutes at 4500×g, supernatant discarded, and the pellet was re-suspended in 200 µL MilliQ water. The process was repeated twice after which the pellet was re-suspended in 200 µL HEPES buffer followed by centrifugation at 4500×g for 30 minutes using an Eppendorf® Microcentrifuge. The

NeutrAvidin coated AuNPs were stored at 4°C. Figure 14 represents the preparation of AuNPs coated with NeutrAvidin.

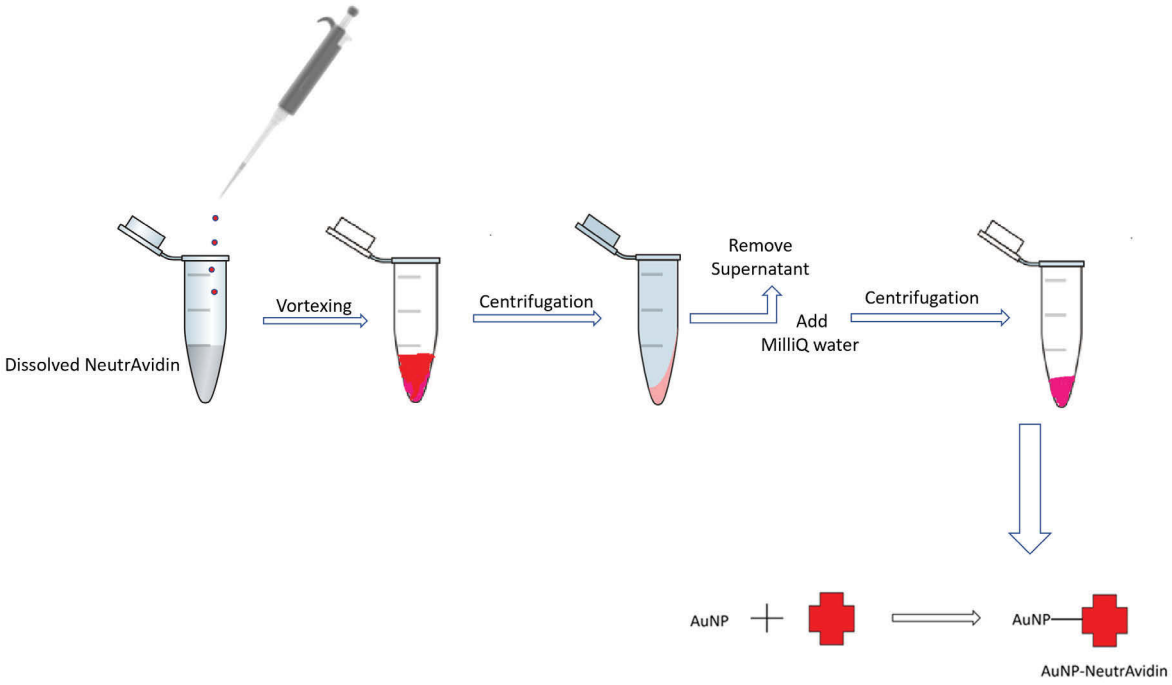

Figure 14: Schematic representation of the preparation of AuNPs coated with NeutrAvidin.

Binding of Peptide to linker molecule

300 µL of 0.5 mg/mL (2.5x 10^{-4} M) peptide (QLQPFPQPQLPYPQPQC) dissolved in MilliQ water was added dropwise to 700 µL of 0.5 mg/mL (5.4 x 10^{-4} M) Poly (ethylene glycol) [*N*-(2-maleimidoethyl) carbamoyl] methyl ether 2-(biotinylamino) ethane (i.e. Biotin-PEG-Maleimide) dissolved in MilliQ water, (M_n 5,400, MW 921 Da) having maleimide at the Ω-end and biotin at the α-end. This solution was left overnight at room temperature. Reaction between maleimide and cysteine is highly efficient with high yield [Baldwin and Kiick 2011]. No further separation steps between product and reagents have been done as excess of reagents would be removed in the steps following the addition of nanoparticles. Figure 15 shows the preparation of the peptide-linker molecule.

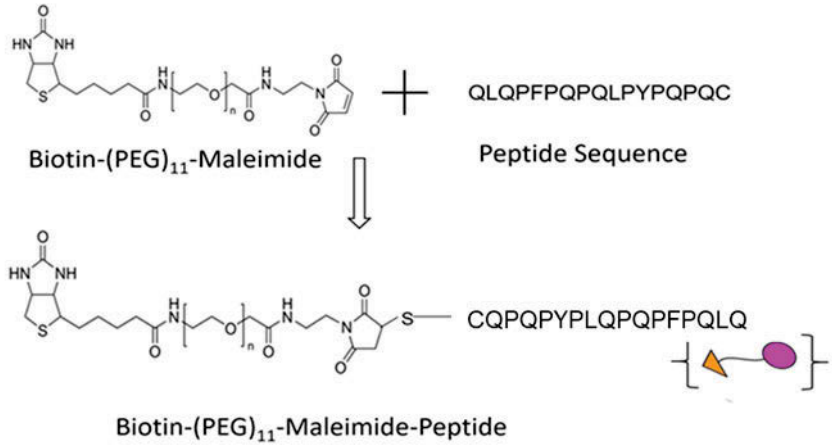

Figure 15: The preparation of the Biotin-$(PEG)_{11}$-Maleimide-peptide molecule.

Preparation of the AuNPs coated with peptide using linker

The NeutrAvidin coated AuNPs were centrifuged at 4500×g for 30 minutes using an Eppendorf® Microcentrifuge, supernatant discarded, the pellet was re-suspended in 100 µL of the peptide-linker solution. The tube was incubated for 60 minutes at room temperature with repeated vortexing. The solution was centrifuged for 5 minutes at 4500×g, supernatant was discarded, and the pellet was re-suspended in 100 µL of MilliQ water. The peptide coated AuNPs were stored at 4°C for up to 4 weeks. Figure 16 shows the preparation of the AuNPs coated with the peptide using linker molecule.

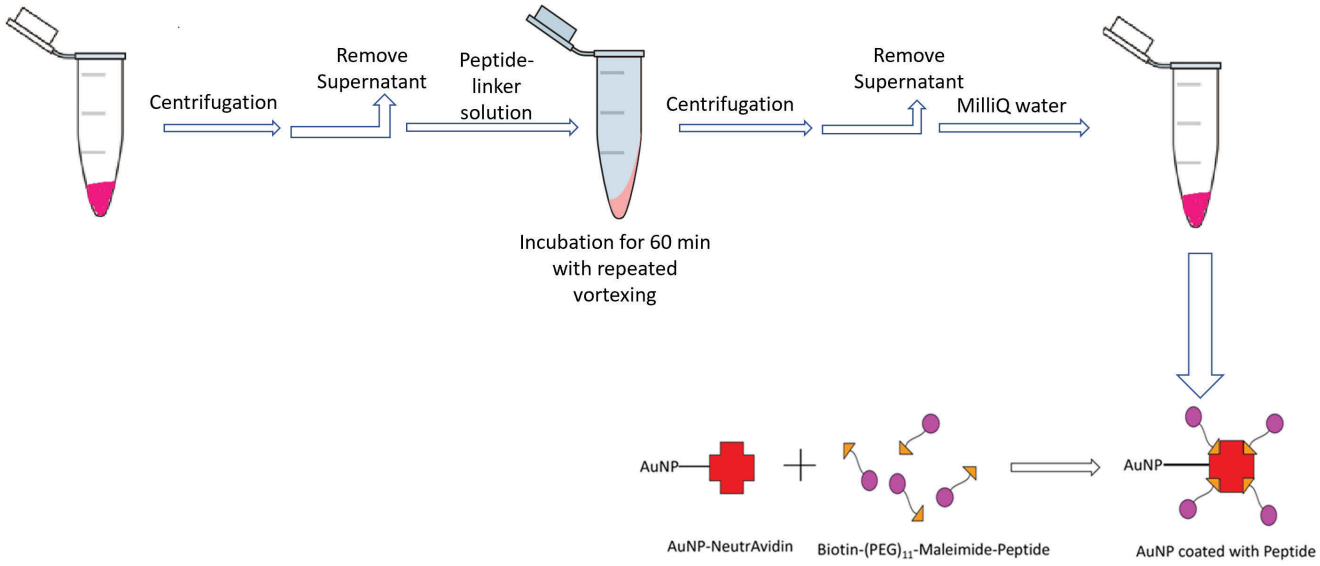

Figure 16: Schematic showing the preparation of the AuNPs coated with the peptide using linker molecule.

3.12 Characterisation of the protein and peptide coated AuNPs

Nano drop (ND-1000 Nanodrop Technologies, Inc.) was performed on the AuNPs coated with proteins and peptide to check for concentration and purity of the coated protein and peptide on the AuNPs. The Nanodrop ND 1000 Spectrophotometer measures the absorbance of a protein/peptide sample. The software uses the Beer-Lambert to describe absorbance as shown in Equation 5; A = €cl where '€' is the extinction coefficient of the specific protein and 'l' is the path length of 10 mm at A 280. In a typical measurement, 2 µL of the protein/peptide sample was pipetted onto the measuring pedestal and the concentration of the sample based on the spectral measurement was determined by the Nanodrop ND software directly.

Size measurements using Dynamic Light Scattering

The hydrodynamic diameter of the colloidal gold nanoparticles was measured with the help of dynamic light scattering (DLS) (Malvern technologies, Inc.), which is based on Brownian motion, and measures the intensity fluctuations of the light diffused by nanoparticles in medium. One of the main advantages of the DLS technique is that samples can be analysed quickly and in solution.

As DLS is based on the light scattering from the AuNPs, to separate the light scattered from the free proteins and the AuNPs, the nanoparticles used in this study were significantly larger in size (20 nm) than the proteins (~ 8 nm). This enabled convenient measurement of the increase in hydrodynamic radii following the protein corona formation and determination of protein-nanoparticle complexes.

DLS uses a monochromatic laser to illuminate the colloidal AuNP solution while a photon detector records the scattering intensity with time. The detection limit of DLS is dependent on the scattering light intensity that is related to the power of the incident light, the type of detector and the detection angle [Berne et al. 1976]. As the larger nanoparticles scatter light more strongly than smaller nanoparticles [Jain et al. 2006, Huhn et al. 2013], AuNPs coated with protein show strong light-scattering intensity allowing DLS to sensitively detect protein adsorption. The result is represented as a distribution of sizes resulting due to the natural conformational variations in the large number of atoms involved.

DLS measurements were carried out at 25°C in disposable cuvettes using a sample volume of 500 µL, prior to starting analysis, the samples were equilibrated for 4 min. The instrument was equipped with a 633 nm laser; measurements were detected using a 173° back scattering detector. Each measurement consisted of 3 runs over 2 minutes each and each sample was measured in triplicate and the mean value reported.

Transmission Electron Microscopy

Transmission electron microscopy (TEM) is a powerful tool to investigate the size, dispersion and shape of nanoparticles. TEM imaging has significantly higher resolution as compared to light since electrons are used to illuminate the sample. Briefly, the electron beam is focussed on the specimen and the condenser aperture controls the convergence angle of the beam. The specimen chamber is placed below the condenser and is one of the most critical parts of the microscope. The specimen rod holds the specimen on a support grid between the pole pieces of the objective lens. The first intermediate image and diffraction pattern of the specimen is obtained using the objective lens. The diameter of the objective aperture controls the resolution as it manages the angular range of scattered electrons that travel down the column. The first projector lens in the image mode is focussed on the image plane of the objective, the remaining projector lenses strengthen the magnification of the final image on the screen. The charged coupled device (CCD) array camera is used for capturing the image. The output is combined with Image J, an image processing public domain software from National Institute of Health (NIH).

The image contrast in TEM originates due to the scattering of the incident beam by the specimen. For biological specimens and non-crystalline materials like polymers, the image contrast, is mainly dependent on the mass-thickness contrast mechanism that arises from incoherent Rutherford scattering of electrons. The cross section for Rutherford scatter is dependent on the atomic number (Z) and the thickness, t, of the specimen. Therefore, with an increase in the specimen thickness, there is more electron scatter and these regions appear darker as compared to the low-mass regions with the same thickness. The TEM variables that influence the mass-thickness contrast for a specimen are the kV and the objective aperture size. A larger aperture would allow more scattered electrons that would lower the contrast between the scattering and non-scattering regions, a lower kV would cause more electron scattering

outside a given aperture leading to an increase in contrast but lowered intensity [Williams and Carter 1996].

While, negative stain is useful to visualise macro-bio-molecules such as DNA [Oliver 1973], these methods were found to be incompatible with protein-films bound on colloidal surfaces. This is mainly because protein films are thicker, have an amorphous substructure and are not clearly resolved by negative staining. TEM can however, be effectively used to resolve globular proteins such as gliadin as well as a peptide on the surface of colloidal gold nanoparticles. The visualisation of gliadin does not require any staining or labelling and is based on the scattering absorption contrast created by the coated protein film on the AuNP surface. Though this contrast is weak, it can be clearly detected against the background signal of the specimen support film. In the case of gliadin, when AuNPs are coated with an optimised amount of the protein, it is visible as a monolayer with a sharp border and constant thickness on the gold nanoparticle surface. In comparison, AuNPs coated with an excess of gliadin, show multilayers of the protein characterised by regions with a smeared border alongside regions with a sharp defined border [Jürgen's et al. 1999].

In this study, high-resolution transmission electron microscopy (TEM) images were recorded with a FEI Tecnai TEM 200V fitted with a Gatan (Pleasantville, CA) CCD camera. Samples were prepared by placing 2 μL of AuNP coated with the protein gliadin as well as the peptide onto a carbon-coated TEM grid grid (300 mesh, Agar Scientific, UK) and the film allowed to air dry for 15 minutes.

UV-Vis spectral measurements

UV-Vis absorbance spectroscopy was used to characterise the proteins coated on AuNP surface. The absorption spectrum is determined both by the chemical structure as well as the environment i.e. the solvent polarity. All measurements were performed in MilliQ water as the solvent. While 20 nm AuNPs show a strong absorbance at 525 nm, protein as well as peptide showed a strong absorbance in the ~ 200 nm range (Figure 17).

Following the coating of the protein/peptide on the AuNP, an increase in the wavelength or red shift was observed. This shift was caused by the aggregation of the AuNPs following the interaction with the AGA and this helps to determine the assay specificity.

UV-Vis measurements were carried out using a Cary Series UV-Vis spectrophotometer (Agilent Technologies) using a standard 1 cm path-length quartz cuvette. Spectra were obtained from 200 nm to 800 nm. MilliQ water was used as the blank.

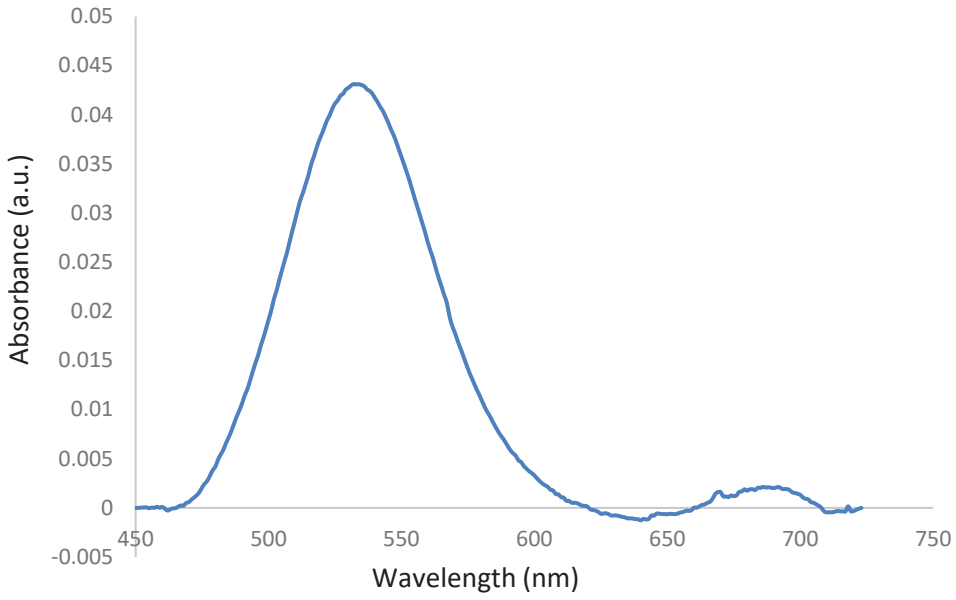

Figure 17: UV-Vis spectra of 20 nm gold nanoparticles at 525 nm.

3.13 Antibody Titration

Anti-Gliadin antibody (AGA) raised in rabbit against gliadin as the immunogen was used to interact with the AuNPs coated with gliadin. A series of dilutions with concentrations 2 µg/mL, 4 µg/mL, 6 µg/mL, 8 µg/mL and 10 µg/mL were prepared in 10mM HEPES buffer to determine the optimum antibody titer. The optimum antibody titer is defined as 'the highest dilution of an antiserum that results in maximum specific staining with the least amount of background under specific test conditions'. IgG from rabbit serum was used as a control antibody and added to AuNPs coated with gliadin/peptide sequence in concentrations ranging from 2 µg/mL to 10 µg/mL. MilliQ water was added to the tubes to make the final volume in each Eppendorf tube to be 225 µL.

The highest dilution was determined by the absolute amount of specific antibodies present. The number of moles of AuNPs, gliadin, peptide, avidin and Maleimide-PEG_{11}-Biotin and AGA as calculated can be found in the following tables (Table 11, 12 and 13).

Table 11. No. of moles of gold nanoparticles used in the analysis.

Gold Nanoparticles	
Title	**Measurement**
Size of Gold Nanoparticle	20 nm
Total number of particles /mL	7.00×10^{11}
Mass of one particle	8.08×10^{-17}g
Total mass of gold per mL	5.66×10^{-5}g

Total moles of gold per 1000 mL	2.87×10^{-4}
Amount of gold nanoparticles used for binding	600 μL
Number of moles of gold nanoparticles in 0.6 mL	1.722×10^{-4} mol

Table 12. No. of moles of Gliadin, peptide, Maleimide-PEG_{11}-Biotin and NeutrAvidin used in the analysis.

Gliadin	
Title	**Measurement**
Molecular weight of gliadin	31 kDa
No. of moles in 1 mg of gliadin	32.26×10^{-9} mol
Peptide	
Molecular weight of peptide	2 kDa
No. of moles in 1 mg of peptide	5×10^{-4} mol
Maleimide-PEG_{11}-Biotin	
Molecular weight of Maleimide-PEG_{11}-Biotin	921 Da
No. of moles in 1 mg of peptide	10.8×10^{-6} mol

NeutrAvidin	
Molecular weight of Avidin	67 kDa
No. of moles in 1 mg of Avidin	1.4×10^{-5} mol

Table 13. **No. of moles of Anti-Gliadin antibody used in the analysis.**

Anti-Gliadin Antibody	
Title	**Measurement**
Molecular weight of IgG	150 kDa
No. of moles in 1 mg of antibody	6.67×10^{-9} mol
Given concentration of antibody	10 mg/mL
Threshold dilution of antibody in saliva/serum	2 µg/mL
2 µg/mL of antibody contains	1.334×10^{-10} mol

3.14 Antigen-Antibody Interactions

Antibody molecules are Y shaped consisting of two variable regions (Fab) and the stem, a constant region (Fc) [Janeway et al. 2001]. The antibody molecules are flexible at the hinge region and some flexibility is also found at the junction between the variable (V) and constant (C) domains that allows the bending and rotation of the V and C domains. The major antigen-antibody interactions include electrostatic forces, hydrogen bonds, Van der Waal's forces and hydrophobic interactions.

The dimensions of the Fab fragment are 40 Å by 50 Å by 80 Å and consist of two globular regions of approximately equal size. The axis of rotation between the VH and VL domains varies from 165^0C to180^0C. The VH-VL interface has a large contact surface in the range of 1400-1900 Å (Davies et al. 1986), wherein the antibody combining site is an irregular and rather flat surface with protuberances and depressions formed by the amino acid side chains of the complementary determining region's (CDRs) of VH and VL [Amit et al. 1986].

In comparison, the size of the AuNP particle is 20 nm and with gliadin not being a very large molecule with a molecular weight of 31 kDa. The protein is globular and therefore tends to have an overall compact structure of spherical shape with polar or hydrophilic amino acids on the surface and hydrophobic amino acids directed towards the core (Figure 18). This arrangement is considered as energetically favourable as it reduces contact with water by placing hydrophobic residues in the core and the surface polar residues can interact with water. The protein structure is maintained by noncovalent forces such as electrostatic interactions, van der Waals forces and hydrogen bonding. In addition, disulphide bridges, a type of covalent bond between the sulphur atoms of the cysteine amino acids also play an important role in stabilising the gliadin protein.

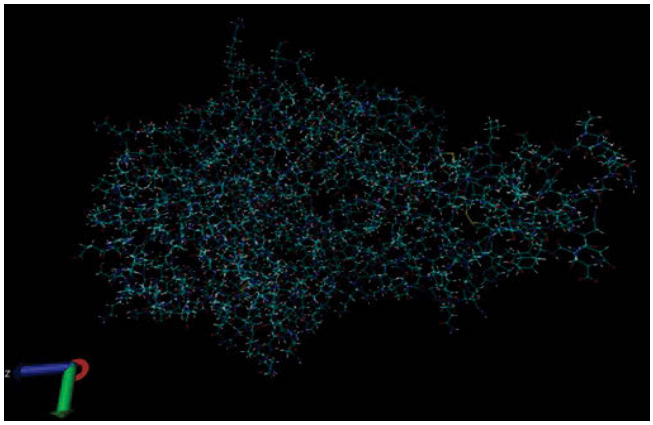

Figure 18: 3-D structure of the hydrophobic and globular protein gliadin.

The secondary structure of the protein is presented below using Ribbons (https://sgce.cbse.uab.edu/ribbons/), a UNIX program that generates the protein secondary structure. The secondary structure elements are comprised of solid spirals and arrows representing α-helices and β-strands respectively. Hydrophobic amino acid residues of the α-helix tend to face the inside while the hydrophilic amino acids face outside. The commonly found amino acids in α- helix are alanine, glutamine, leucine and methionine.

Amino acid residues like proline, glutamic acid and tyrosine prefer the β-strands. The β conformation is pleated; with the main backbone a zigzag and side chains placed on the opposite sides of the sheet. The β-strands are stabilised by hydrogen bonds between the amino acids of the alternating strands. The strands buried at the core of the protein are nearly all hydrophobic residues while the β-strands near the surface of the protein have alternating hydrophilic and hydrophobic residues. The β-strands can either run in the same direction to form a parallel sheet or can run in the reverse direction to form the anti-parallel sheet or it can be a mixture of both. The secondary structure of gliadin is presented below in Figure 19.

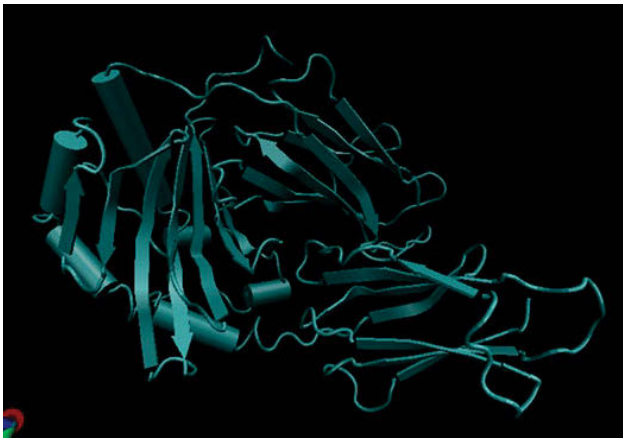

Figure 19: Secondary structure of hydrophobic and globular protein gliadin. *The solid spirals represent the α-helices and the arrows represent the β-strands respectively.*

The structural comparison indicated that interactions between the antigen bound to the AuNP and the antibody are dimensionally feasible. The dimensional representation of interactions of AuNP coated to the globular whole protein, gliadin, with the IgG antibody are represented in the Figure 20 below.

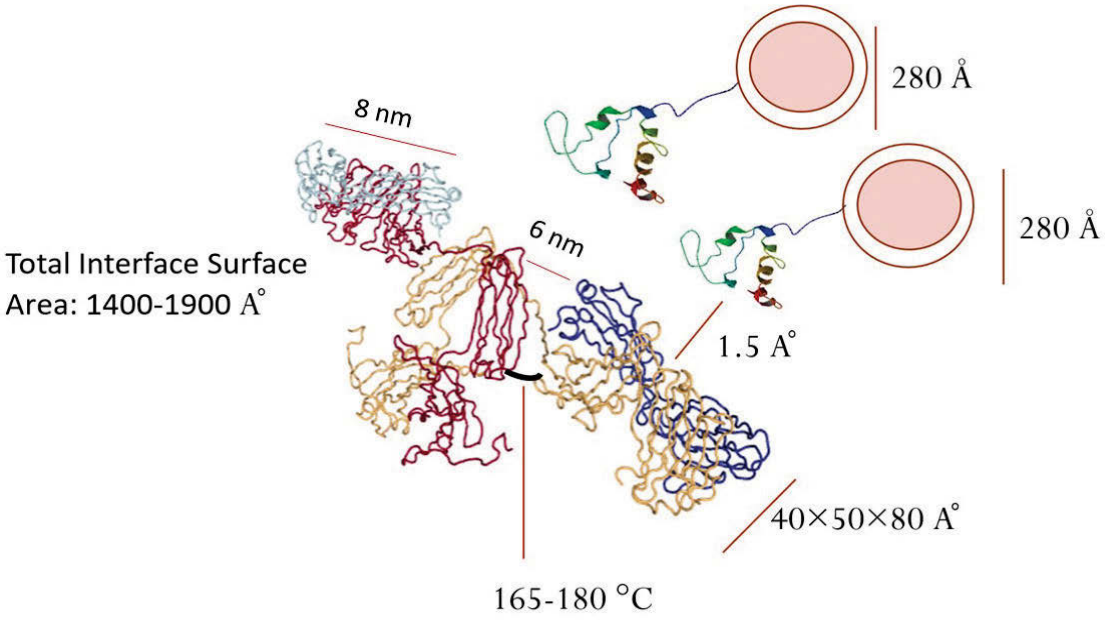

Figure 20: Dimensional representation of interactions of AuNP coated with gliadin and IgG antibody.

3.15 Antibody Specificity

An antibody (Ab) molecule is specific to the antigenic determinant to which it binds, the specificity is further related to the affinity and avidity of the antibody. Antibody affinity is associated with the preciseness of a stereochemical fit of an antibody combining site to its complementary antigen determinant. Mathematically, affinity is expressed by an association constant (K, 1/mol) that can be calculated at equilibrium conditions between the bound and unbound antigen (Ag) when in a reversible interaction with a homogenous antigen binding site.

Avidity on the other hand, is a functional term that defines the efficiency of antibodies in a test. The multiple interacting components are assumed to follow the law of mass action defined by the formula: Ab + Ag $\rightleftharpoons$ Ab-Ag and can be expressed by an association constant K_a.

It is however, commonly observed that some antigenic determinants are shared between molecules- this is particularly seen in similar molecules of related species. In such a scenario, some antibodies that are induced in response to one antigen may combine with another antigen as well and then they are said to be cross-reacting.

3.16 Hypothesis of the study

In the immunoassay developed in this study, the Anti-gliadin antibody (AGA) from rabbit was added at different concentrations to determine the specificity of the reaction between gliadin coated AuNPs and AGA. The IgG from normal rabbit serum was used as a control antibody and added to AuNPs coated with gliadin at similar concentrations to determine the effect of a non-specific antibody on the gliadin coated AuNPs.

The hypothesis of the study is that in the presence of the specific antibody i.e. Anti-gliadin antibody, there would be an increase in the gliadin coated nanoparticle to nanoparticle

interactions that would lead to an aggregation of gliadin coated AuNPs as well as the formation of a precipitate. This would result in a decrease as well as a shift in absorbance maxima values based on the UV-Vis spectrophotometer.

On the other hand, in the presence of a non-specific antibody (IgG) there would be no increased nanoparticle-nanoparticle interactions with the colloidal AuNPs remaining as a suspension. In addition, there would be no decrease or shift in the absorbance maximum as observed by the UV-Vis spectrophotometer. The hypothesis is represented in Figures 21, 22 below.

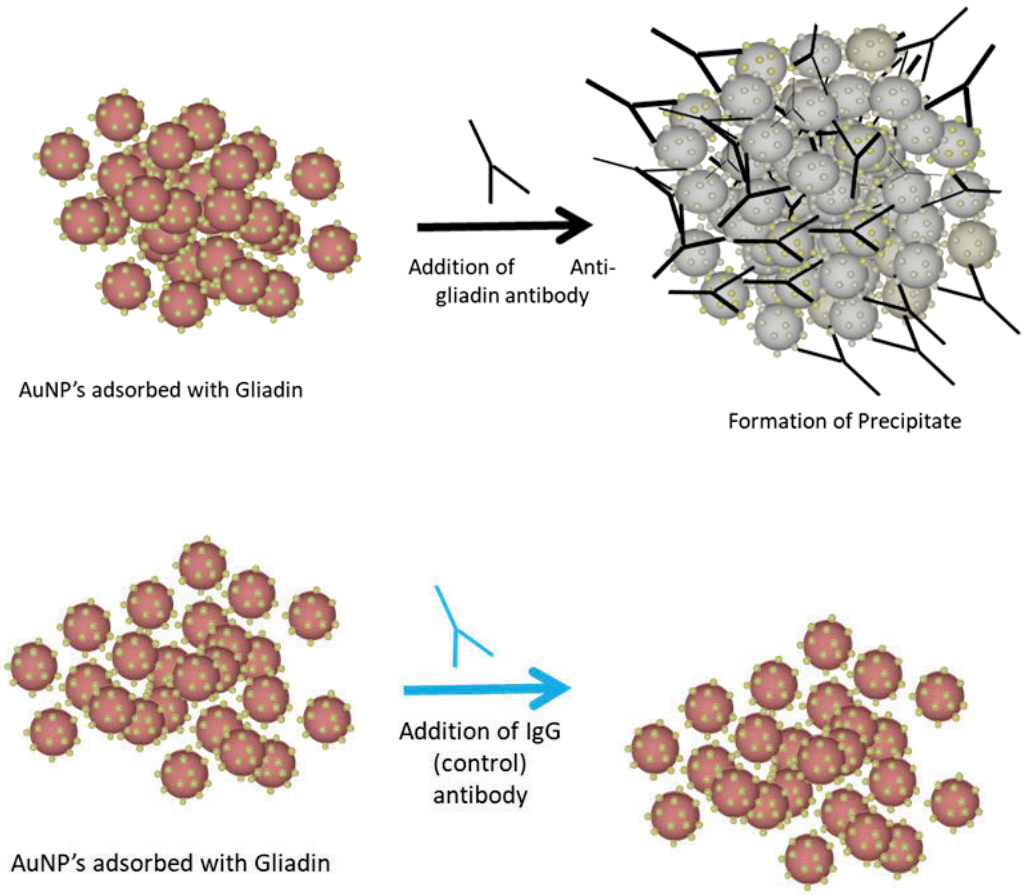

Figure 21: Representation of specificity of Antigen-Antibody interactions. *A) Interactions of AuNP coated with gliadin with Anti-gliadin antibody B) Interaction of AuNP coated with gliadin with IgG (control) antibody.*

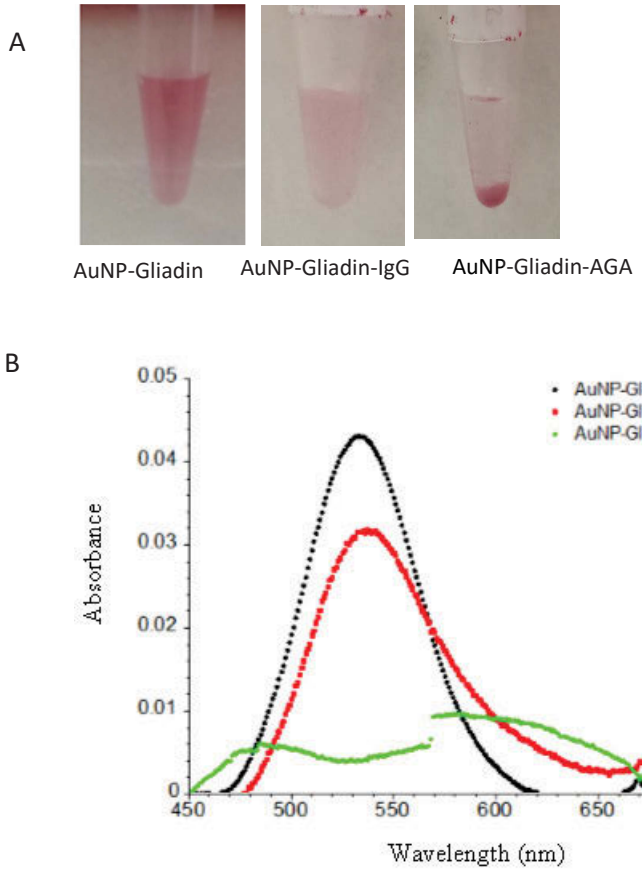

Figure 22: Representation of specificity of Antigen-Antibody interactions hypothesis

A) Formation of precipitate following the interactions of AuNP coated with gliadin with Anti-gliadin antibody whereas on addition of control antibody the solution remains a suspension

B) UV-Vis spectra showing the interaction of AuNP coated with gliadin with IgG (control) antibody.

3.17 Analysis of the interaction of gliadin-AuNP with anti-gliadin antibody and non-specific IgG antibody

The immunoassay used to assess the activity of AuNPs coated with gliadin with the antibodies is outlined below. Assay steps were performed at room temperature. Briefly, 150 µL of AuNPs

coated with gliadin were added to 1.5 mL low protein binding Eppendorf® tubes. 1 µl of 20% BSA dissolved in MilliQ water was used as the blocking agent and was added to 150 µL of 20 nm AuNPs coated with gliadin. AGA (1 mg/mL) from rabbit was added to each of the tubes corresponding to concentrations ranging from 2 µg/mL to 10 µg/mL (i.e. 1 µL to 5 µL). IgG from normal rabbit serum (1 mg/mL) was used as a control antibody and added to 150 µL of AuNPs coated with gliadin in concentrations ranging from 2 µg/mL to 10 µg/mL (1 µL to 5 µL). MilliQ water was added to the tubes to bring the final volume in each Eppendorf®tube up to 225 µL. The UV-Vis absorption spectra of solutions containing gliadin coated gold nanoparticles and AGA at increasing dilutions (2 µg/mL, 4 µg/mL, 6 µg/mL, 8 µg/mL and 10 µg/mL) were studied using UV-Vis spectrophotometer. Readings were taken in triplicate and a student's t-test was used to determine the p value.

In another control experiment, 200 µL of AuNPs coated with BSA were added to 1.5 mL low protein binding Eppendorf® tubes. Anti-gliadin antibody from rabbit was added to each of the tubes in concentrations ranging from 2 µg/mL to 10 µg/mL to compare the specificity of the reaction between BSA coated AuNPs with the gliadin coated AuNPs.

3.18 Analysis of the interaction of AuNPs coated with peptide with anti-gliadin antibody and non-specific IgG antibody

The immunoassay used to assess the activity of AuNPs coated with peptide with the antibodies is outlined below. Assay steps were performed at room temperature. Briefly, 150 µL of AuNPs coated with peptide were added to 1.5 mL low protein binding Eppendorf® tubes. AGA (1 mg/mL) from rabbit was added to each of the tubes corresponding to concentrations ranging from 2 µg/mL to 20 µg/mL (i.e. 1 µL to 10 µL) to determine the specificity of the reaction between peptide coated AuNPs and AGA.

IgG from normal rabbit serum (1 mg/mL) was used as a control antibody and added to 150 µL of AuNPs coated with peptide in concentrations ranging from 2 µg/mL to 20 µg/mL (i.e. 1 µL to 10 µL). MilliQ water was added to the tubes to bring the final volume in each Eppendorf tube up to 225 µL. The UV-Vis absorption spectra of solutions containing peptide coated gold nanoparticles and AGA at increasing dilutions (2 µg/mL, 4 µg/mL, 6 µg/mL, 8 µg/mL, 10 µg/mL, 12 µg/mL, 14 µg/mL, 16 µg/mL, 18 µg/mL and 20 µg/mL) were studied using a Cary Series UV-Vis spectrophotometer. Readings were taken in triplicate and a student's t-test was used to determine the p value.

3.19 Analysis of the interaction of gliadin-AuNPs with anti-gliadin antibodies in human saliva

Human saliva samples spiked with anti-gliadin antibodies at various dilutions comparable to that seen in patients with CD were prepared. Approximately 300 µL of normal human saliva was spiked with anti-gliadin antibody at various dilutions comparable to that seen in patients with CD and was added to 200 µL 20 nm AuNPs coated with gliadin, gently mixed and was allowed to incubate for 30 minutes. 500 µL of the sample was used for UV-Vis analysis. At least three independent experiments were conducted for each assay.

3.20 Analysis of the interaction of gliadin-AuNPs with anti-gliadin antibodies in human serum

The general immunoassay format used to assess the activity of AuNPs coated with gliadin with anti-gliadin antibodies is outlined below. Assay steps were performed at room temperature.

Normal human serum was diluted to 1:10, 1:20 and 1:50 using 10 mM HEPES buffer. 75 µL of serum from each of the dilutions was spiked with AGA at various dilutions comparable to that seen in patients with CD.

To prevent non-specific binding, 1 µl of 20% BSA dissolved in MilliQ water and was added to 150 µL of 20 nm AuNPs coated with gliadin. The tubes were incubated for 30 minutes at room temperature. 75 µL of normal serum spiked with AGA at increasing dilutions of 2 µg/mL, 4 µg/mL, 6 µg/mL, 8 µg/mL and 10 µg/mL was then added to 20 nm AuNPs coated with gliadin. The tubes were then incubated for 30 minutes at room temperature.

3.21 Analysis of the interaction of peptide-AuNPs with anti-gliadin antibodies in human serum

Normal human serum was diluted to 1:20 using 10 mM HEPES buffer. 75 µL of serum from the dilution was spiked with AGA at various dilutions comparable to that seen in patients with CD.

To prevent non-specific binding, 1 µl of 20% BSA dissolved in MilliQ water was added to 150 µL of 20 nm AuNPs coated with peptide. The tubes were incubated for 30 minutes at room temperature. 75 µL of normal serum spiked with AGA at increasing dilutions of 2 µg/mL, 4 µg/mL, 6 µg/mL, 8 µg/mL and 10 µg/mL, 12 µg/mL, 14 µg/mL, 16 µg/mL, 18 µg/mL and 20 µg/mL was then added to AuNPs coated with peptide. The tubes were then incubated for 30 minutes at room temperature.

3.22 Analysis for Anti-gliadin antibody in clinical human serum

Anonymised patient samples were collected with active CD (pre-treatment), treated CD (on a gluten free diet) as well as controls without CD. All cases of CD were medically diagnosed and based on typical small intestinal histology in conjunction with positive CD serology. No prior knowledge on the CD status was known while testing.

Prior to testing, each human serum sample was diluted to 1:10, 1:20 and 1:50 using 10 mM HEPES buffer. 1 µl of 20% BSA dissolved in MilliQ water was added to 20 nm AuNPs coated with gliadin or 20 nm AuNPs coated with peptide to prevent non-specific binding. 75 µL of serum from each of the dilutions was then added to 20 nm AuNPs coated with gliadin or 20 nm AuNPs coated with peptide. The tubes were incubated for 15 minutes at room temperature before the absorbance was measured using a UV-Vis spectrophotometer. Following testing, the whole serum clinical samples were then concentrated, desalted and tested again as outlined below.

3.23 Concentration of immunoglobulins in clinical human serum

Whole serum clinical samples obtained for the validation study were thawed at room temperature. 200 µL of each serum sample was pipetted out to a low-protein binding 1.5 mL Eppendorf® tube and centrifuged at 6000 rpm for 15 minutes. The supernatant was removed, and the serum samples were diluted by adding 200 µL of 10mM PBS. An equal volume of saturated ammonium sulphate solution was added slowly to achieve a 33% saturated (v/v) final concentration with continuous stirring of the tubes. The tubes were kept at 4°C for 30 minutes and then centrifuged again at 5000 rpm for 15 minutes. The supernatant was removed, and the

pellet was re-suspended by adding 200 µL of 10mM PBS. The concentrated serum solution was stored at - 20°C till further use (Figure 23).

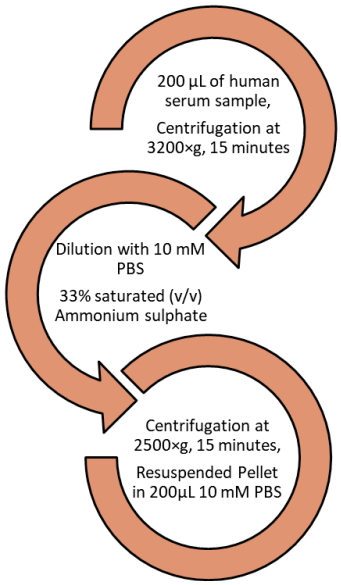

Figure 23: Schematic showing the concentration of immunoglobulins using saturated ammonium sulphate solution

3.24 Desalting of concentrated immunoglobulins

Zeba^{TM} Spin desalting columns (Thermo Scientific^{TM}) were used for the desalting of the immunoglobulins from the concentrated serum solution according to the manufacturer's instructions. Briefly, each desalting column was prepared by centrifuging the column at 2000 rpm for 1 minute to remove the storage solution. The column was then washed three times with 300 µL of 10mM HEPES Buffer which was used as the equilibration buffer for column preparation. 100 µL of the concentrated immunoglobulins from whole human serum were then passed through the column by centrifuging at 2000 rpm for 2 minutes. The flow-through was collected, the final concentration of the total immunoglobulins was measured using the NanoDrop and stored at -20°C till further use.

3.25 Analysis for Anti-gliadin antibody in concentrated clinical human serum

1 µl of 20% BSA dissolved in MilliQ water was added to 20 nm AuNPs coated with gliadin or 20 nm AuNPs coated with peptide to prevent non-specific binding. 75 µL of serum from each of the dilutions was then added to 20 nm AuNPs coated with gliadin or 20 nm AuNPs coated with peptide. The tubes were incubated for 15 minutes at room temperature before the absorbance was measured using a UV-Vis spectrophotometer.

3.26 Composition of the patient sample cohort assessed for assay validation

Active CD sufferers

Active CD is characterised by the typical malabsorption symptoms with diarrhea, weight loss, growth failure, fatigue, abdominal pain and severe intestinal damage affecting the small intestine. Histology shows continuous lesions and total villous atrophy as well as an increase in the intraepithelial lymphocytes (IELs). It is also associated with an adaptive T-cell mediated response (to gluten) determined by the presence of specific AGA, EMA, tTG and DGP antibodies. In these cases, particularly, antibodies to tissue transglutaminase are usually evident. Table 14 shows the histology and serology levels of active coeliac sufferers in the clinical sample cohort analysed in this study.

Table 14. Serology levels of active coeliac sufferers in the clinical sample cohort based on the histology and tTG (Tissue transglutaminase), DGP (Deamidated gliadin peptides) results are indicated as IgA or IgG levels followed by normal reference ranges in brackets.

Volunteer	Histology	tTG-IgA	DGP-IgG
n.1	CD	1 (<4)	3 (<20)
n.3	CD	>100 (<4)	33 (<20)
n.5	CD	>100 (<4)	>100 (<20)
n.6	CD	217 (<5)	>150 (<20)
n.7	CD	13 (0-6)	23 (0-6)
n.8	CD	>100 (<5)	>100 (<20)
n.9	CD	11 (0-6)	1.4 (0-6)
n.10	CD	9 (<4)	97 (<20)
n.14	CD	47 (<5)	86 (<5)
n.15	CD	74 (0-20)	-
n.16	CD	145 (0-20)	-
n.17	CD	57 (<4)	93 (<20)
n.18	CD	149 (<20)	63 (<20)
n.19	CD	>100 (<4)	>100 (<20)
n.22	CD	180 (0-6)	21 (0-6)
n.23	CD	20 (0-6)	8.1 (0-6)

Sub-clinical CD

In sub-clinical forms, such as undiagnosed or potential coeliac sufferers, the gastrointestinal presentation can be mild or even absent, the diagnosis depends on the extra-intestinal symptoms. The atypical CD usually present limited or no intestinal symptoms. Extra-intestinal features usually dominate and these include changes such as iron deficiency anaemia, osteopenia related fracture, peripheral neuropathy, infertility, abnormal liver diagnosis, or skin rashes characterised as dermatitis herpetiformis. Continued evaluation may reveal histological changes caused as a result of untreated CD, as well as positive serological results.

Undiagnosed coeliac sufferers

Undiagnosed CD is usually defined by the presence of a pre-disposing gene, such as, HLA-DQ2 and/or HLA-DQ8, but may have normal intestinal architecture with an increased number of intraepithelial lymphocytes. The undiagnosed coeliac sufferer's present positive CD serology in patients with patchy/ irregular mucosal lesions that then develops with typical atrophy of small intestine mucosa if left untreated. Table 15 shows the histology and serology levels of undiagnosed coeliac sufferers in the clinical sample cohort analysed in this study.

Table 15. Serology levels of undiagnosed coeliac sufferers in the clinical sample cohort based on histology and tTG (Tissue transglutaminase), DGP (Deamidated gliadin peptides) results are indicated as IgA or IgG levels followed by normal reference ranges in brackets.

Volunteer	Histology	tTG-IgA	DGP-IgG
n.24	Mucosal lesions	5 (<20)	17 (<20)
n.25	Mucosal lesions	28 (0-6)	22 (0-6)

n.26	Mucosal lesions	4.8 (0-6)	22 (0-6)

Potential coeliac sufferers

Potential CD refers to people with a normal small intestinal mucosa but are at increased risk of developing CD as indicated by positive CD serology. These include first-degree relatives of CD sufferers that are HLA-DQ2/8 positive. The histology in these cases is characterised by a normal villous architecture along with a demonstration of pathological symptoms such as increased $\gamma\delta^+$ intraepithelial lymphocytes (IELs) that can lead to mucosal inflammation, as well as the presence of gliadin specific antibodies, usually at low titres (<1:40).

An increased number of aberrant IELs are considered as a prognostic marker to differentiate between type I and type II refractory CD forms. Aberrant IELs show the presence of cytoplasmic CD3 expression but no expression of CD4 and CD8 T-cell markers. Increased IELs may be used to support or exclude diagnosis for CD and may be used for a follow-up as well as. Table 16 shows the histology and serology levels of potential coeliac sufferers in the clinical sample cohort analysed in this study.

Table 16. Serology levels of potential coeliac sufferers in the clinical sample cohort based on histology and tTG (Tissue transglutaminase), DGP (Deamidated gliadin peptides) results are indicated as IgA or IgG levels followed by normal reference ranges in brackets.

Volunteer	Histology	tTG-IgA	DGP-IgG
n.27	Increased $\gamma\delta^+$ IELs	12 (0-6)	18 (0-6)
n.28	Increased $\gamma\delta^+$ IELs	11 (0-6)	13 (0-6)

n.29	Increased $\gamma\delta^+$ IELs	<5 (<5)	<20 (<20)
n.30	Increased $\gamma\delta^+$ IELs	<5 (<5)	22 (<20)

CD and Type 1 Diabetes

For patients with Type 1 Diabetes (T1DM), the prevalence of CD in T1DM is reported to vary considerably, due to the common genetic background as well as the multiple environmental and immunological factors. In addition, most T1DM patients, particularly diabetic children, have an undiagnosed form of the disease characterised by the absence of both gastrointestinal and extra-intestinal signs and are often regarded as asymptomatic. Table 17 shows the histology and serology levels of coeliac sufferers with T1DM in the clinical sample cohort analysed in this study.

Table 17. Serology levels of coeliac sufferers with Type 1 Diabetes in the clinical sample cohort based on histology and tTG (Tissue transglutaminase), DGP (Deamidated gliadin peptides) results are indicated as IgA or IgG levels followed by normal reference ranges in brackets.

Volunteer	Histology	tTG-IgA	DGP-IgG
n.4	CD	121 (<20)	-

Treated Coeliac Sufferers

The only effective treatment available for CD sufferers is a strict, life-long gluten free diet (GFD). The United States Food and Drug Administration has set the limit of (August 2011) of < 20 ppm gluten (equivalent to 10 ppm gliadin) for gluten-free foods. In addition, the total consumption of gluten-free products must also be monitored carefully as it may exceed the tolerable limit of each coeliac individual. Cross-contamination in food products is another cause of concern as the presence of hidden gliadin in contaminated food products poses risk for coeliac consumers. It has been reasoned that continued long term, regular ingestion of small amounts of gliadin may cause positive tTG and characteristic small bowel biopsy. Table 18 shows the histology and serology levels of coeliac sufferers on a gluten free diet in the clinical sample cohort analysed in this study.

Table 18. Serology levels of treated coeliac sufferers in the clinical sample cohort based on histology and tTG (Tissue transglutaminase), DGP (Deamidated gliadin peptides) results are indicated as IgA or IgG levels followed by normal reference ranges in brackets.

Volunteer	Histology	tTG-IgA	DGP-IgG
n.11[ɪ]	CD	18.2 (0<20)	3 (0.20)
n.12[ɪɪ]	CD	16 (0-20)	7 (<20)

[ɪ] Following GFD > 8 weeks, [ɪɪ] Following GFD < 2 weeks

Non-Coeliac Samples

The cohort included four samples identified as negative for CD based on biopsy. Table 19 shows the histology and serology levels of non-coeliac sufferers in the clinical sample cohort analysed in this study.

Table 19. Serology levels of treated coeliac sufferers in the clinical sample cohort based on histology and tTG (Tissue transglutaminase), DGP (Deamidated gliadin peptides) results are indicated as IgA or IgG levels followed by normal reference ranges in brackets.

Volunteer	Histology	tTG-IgA	DGP-IgG
n.2	Non-CD	0.1 (0-6)	0.2 (0-6)
n.13	Non-CD	4 (0-20)	-
n.20	Non-CD	3.8 (<6)	37 (<6)
n.21	Non-CD	<5 (<5)	<20 (<20)

3.27 Determination of Immunoassay sensitivity

Sensitivity analysis (SA) helps to determine the robustness of the assay by examining the effect of changes by varying the concentrations of AGA and the control antibody (IgG from rabbit serum) on the AuNP coated with gliadin or with peptide. A colorimetric response curve was plotted to represent the sensitivity values obtained for the different dilution values for both the AGA and the control antibody.

For AuNP coated with gliadin, the assay sensitivity was calculated as described by Equation 6, Colorimetric Response = $I_{max\ at\ 532\ nm}$/ $I_{at\ 550}$ nm i.e. spectral absorbance value obtained at 532 nm which is the wavelength where AuNP coated with gliadin show maximum absorbance by

itself (no antibodies are added) divided by the absorbance at 550 nm where a shift in absorbance is observed following the interaction of AGA with the gliadin coated AuNPs.

An increase in the colorimetric response was observed, reaching a maximum value when anti-gliadin antibody is added at a concentration of 8 µg/mL to the AuNP coated with gliadin. The curve begins to drop when the anti-gliadin antibody concentration reaches 10 µg/mL. For the control antibody, the response curve is constant with only a slight increase at the control antibody dilution of 6 µg/mL. The near constant colorimetric response curve obtained for the control antibody as compared to the response curve obtained for anti-gliadin antibody helped to demonstrate the specificity of the assay (Figure 24).

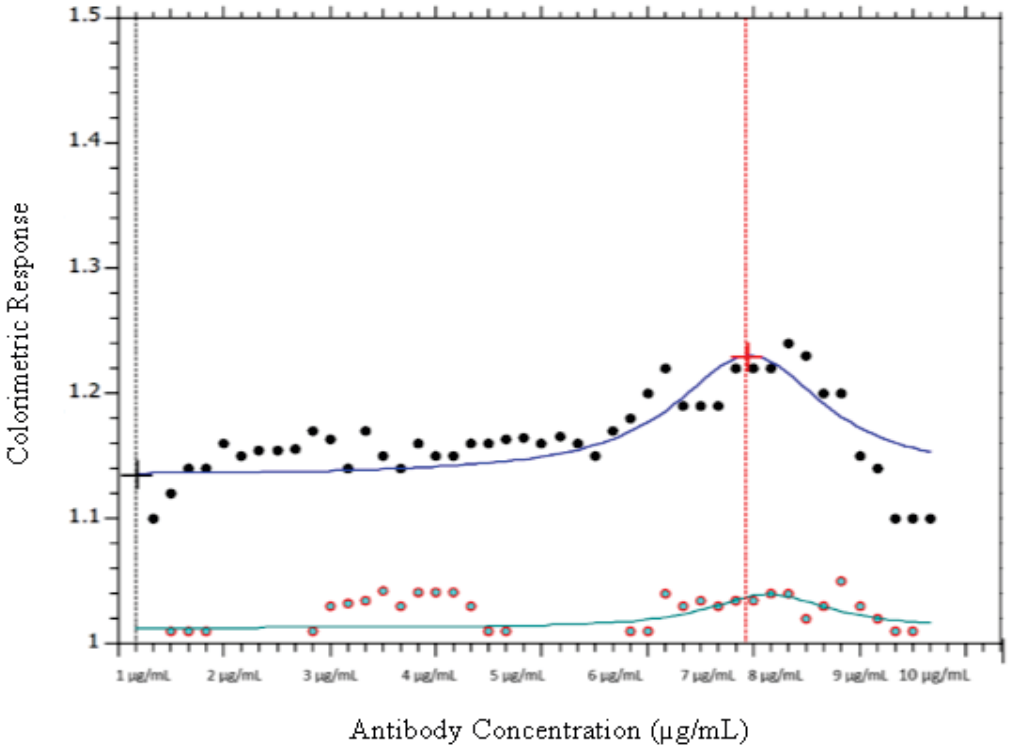

Figure 24: Colorimetric response curve plotted in AuNPs coated with gliadin. *Anti-gliadin antibody and the control antibody (IgG from rabbit serum) were added at dilutions 2 µg/mL, 4 µg/mL, 6 µg/mL, 8 µg/mL and 10 µg/mL.*

A similar colorimetric response was plotted for the peptide coated AuNPs, as described by Equation 7, Colorimetric Response = $I_{max\ at\ 527\ nm}$/ $I_{at\ 550\ nm}$ i.e. spectral absorbance value obtained at 527 nm which is the wavelength where AuNP coated with peptide sequence show maximum absorbance by itself (no antibodies are added) divided by the absorbance at 550 nm where a shift in absorbance is observed following the interaction of the AGA to the peptide coated AuNP.

3.27.1 Colorimetric Response calculation for clinical sample analysis

While testing the clinical sample serum which is a complex fluid, the presence of several proteins and factors can affect the interaction of the AuNPs coated with gliadin/peptide with the AGA. To account for these variables, the assay sensitivity in serum was calculated as described by Equation 8, Colorimetric Response = $I_{max\ at\ 580\ nm}$/ $I_{at\ 532\ nm}$ i.e. absorbance value obtained at 580 nm, the wavelength where a shift in absorbance is observed following the interaction of the antibody to the AuNP coated with gliadin in serum divided by the maximum absorbance value of AuNP coated with gliadin in serum.

Similarly, a colorimetric response for peptide coated AuNPs is determined by Equation 9, Colorimetric Response = $I_{max\ at\ 580\ nm}$/ $I_{at\ 527\ nm}$ i.e. absorbance value obtained at 580 nm, the wavelength where a shift in absorbance is observed following the interaction of the antibody with the AuNP coated with peptide in serum divided by the maximum absorbance value of AuNP coated with peptide in serum.

3.28 Statistical Analysis

The UV-vis absorbance readings of gliadin or peptide coated AuNPs following interactions with AGA and IgG from rabbit serum (control antibody) were taken in triplicate and were used to calculate the percentage absorbance. The students t-test was used to compare the sets of quantitative data that were collected independently of one another to calculate the p value and determine statistical significance.

CHAPTER IV

Novel diagnostic assay for coeliac disease using gliadin coated gold nanoparticles

4.1 Background

CD is an immune mediated disorder affecting the small intestine in genetically predisposed individuals. As discussed in chapter 1, in spite of the great progress made in research on CD, there is still an urgent need for a valid serological or point-of-care test, for early diagnosis of the disease. In this chapter, I present a novel diagnostic test for CD based on the coating of gold nanoparticles with gliadin, the highly antigenic protein that induces CD.

I first developed a protocol for binding of the hydrophobic gliadin protein on the surface of the gold nanoparticles. I then developed the serological assay, in a simple, single step diagnostic test. Finally, I used this diagnostic assay on 30 patient serum samples in a blinded assessment and compared the results with the previously run serological and pathological tests on these patients. The characterisation techniques demonstrated the binding of the hydrophobic gliadin on the surface of the gold nanoparticles. The developed assay was tested on real patient samples and the data showed that this test had an overall accuracy of over 96%. The results indicate that the potential of gold nanoparticles coated with gliadin in detection of CD sufferers.

This work is a part of the International patent PCT/AU2018/050125 that has been published with International Publication No. WO 2018/148801. This chapter is written in the form of a paper that has been submitted to a journal and is under review.

4.2 Introduction

The field of biodiagnostics has experienced an explosive growth over the last decade [Kumar et al. 2015]. Portable diagnostic kits are highly sought after as they offer a relatively fast, easy and simple technology to detect a large number of biomarkers. Despite these advancements, there are still disorders that would greatly benefit from developing a lab based or point-of-care diagnostic test. One such disorder is CD.

CD is a chronic immune mediated disease that effects the small intestine induced by the consumption of gluten, a protein found in wheat and other cereal grains [Ludvigsson et al. 2013]. Epidemiological studies have shown that there is a worldwide distribution of CD with a high proportion of CD sufferers going undiagnosed [Marsh et al. 2015]. Early diagnosis is important in order to prevent the progression of CD that can often lead to serious complications.

Symptoms of CD vary greatly in different individuals, and include anaemia, anorexia, weight loss, abdominal pain, diarrhea, chronic fatigue, constipation, joint pain as well as an increased level of liver enzymes [Tonutti and Bizzaro 2014]. Due to the wide variability in symptoms and similarity to other gastrointestinal disorders such as Crohn's disease and Inflammatory Bowel Disease (IBD), it has proven difficult to correctly diagnose CD at an early stage by a medical practitioner.

The first step for diagnosis for CD in clinical practice is serologic testing for gliadin-induced autoantibodies; the two key ones are anti-gliadin antibody (AGA) or tissue anti-transglutaminase (tTG) antibody. The most reliable method for diagnosing CD, however, is gastrointestinal endoscopy. This method relies on acquiring a tissue sample for mucosal biopsy that is used to visualise varying degrees of intestinal damage, from mild abnormalities to completely flat mucosa [Ludvigsson et al. 2013, Oberhuber et al. 1999]. In addition, genetic testing for individuals with a high probability of developing CD, i.e. those showing the

presence of the main susceptibility genes HLA-DQ2 (specifically HLA-DQ2.5 and HLA-DQ2.2) and HLA-DQ8, is also used in combination with the other serological approaches for diagnosis [Tye-Din et al. 2015]. Typically, CD patients present higher serum titers of AGA and anti-tTG antibodies that are detectable using a lab-based, enzyme-linked immunosorbent assay (ELISA) test [Dahlbom et al. 2016, Benkebil et al. 2013]. In non-CD patients, these two types of antibodies are generally undetectable in serum.

Over the years, tTG antibodies showed higher specificity and sensitivity values as compared to AGA tests, which led to the abandoning of whole gliadin protein specific AGA as the biomarker for diagnosing CD. More recently, ELISA tests using human recombinant tTG (h-tTG) or deamidated gliadin peptide (DGP) as the antigen source have further improved the sensitivity of CD using the patient's blood serum. However, increased tTG antibody titers are also associated with Type 1 diabetes as well as some liver disorders, and this can generate an unacceptable number of false positive results.

A number of commercial kits based on the serological testing of antibodies against tTG and DGP have been introduced and used for large-scale screening of the general population. However, the existing point-of-care methods for identifying CD are unable to provide the required diagnostic accuracy and might be affected by the higher variability in the characteristics of patients such as their age, family history or other clinical associations such as autoimmune diseases [Kaur et al. 2017].

Over the last decade, nanoparticle-based technology has been applied to the early detection of multiple diseases such as HIV [Laderman et al. 2008], other pathogenic infections [Lindhardt et al. 2009, Rong-Hwa et al. 2010], pregnancy testing in humans [Su et al. 2014], detection of GLUT 1 in diabetic rats [Alkaladi et al. 2014] and many other applications [Biagini et al. 2006, Tippkötter et al. 2009, Li et al. 2009]. This technology has proven to be highly sensitive and

accurate, and easy to perform. Nanotechnology-based approaches have been employed to deliver a point-of-care test for CD detection, involving coating of DGP on a carrier protein as the antigen and using colloidal gold anti-human antibodies as the signal detector to identify anti-DGP antibodies in serum samples. Although it is a plausible approach, the test was found to be less specific than expected, which limited its potential as a population screening tool [Bienvenu et al. 2012].

In this study, I present data which demonstrates accurate detection of anti-gliadin antibodies using gold nanoparticles (AuNPs) coated with the hydrophobic whole gliadin protein. I have developed a promising new test by establishment of a stable suspension (without any significant level of aggregation) of gliadin coated AuNPs, enabling me to perform the test as a single step assay. Use of nanoparticles was essential to achieve a test with high sensitivity and specificity levels when using serum samples to detect AGA; as it is hypothesised that the curvature of AuNPs might have increased the exposure of hidden epitopes in gliadin.

The diagnostic method was tested on 30 patient serum samples and found that the assay achieved a very high level of accuracy (>96%) in distinguishing CD from non-CD patients. This level of accuracy is in the range required for a serological test as both in the clinic or home one would expect to find only a relatively small proportion of people tested with CD. In addition, these results using a single step assay for detection of AGA eliminate multiple steps followed in existing serological tests that sometimes leads to user dependent error. One-step detection would be particularly useful in aiding the large-scale screening of the general population, particularly in the preselection of CD in small children, who may have undiagnosed/potential CD by parents or medical practitioners, which can be then confirmed by mucosal biopsy.

4.3 Materials and Methods

4.3.1 Reagents

20 nm citrate stabilised gold nanoparticles (AuNPs), gliadin, bovine serum albumin (BSA), anti-gliadin antibody from rabbit, and IgG antibody from whole normal rabbit serum, Cetyl Trimethylammonium Bromide (CTAB), 4-(2-hydroxyethyl)-1-piperazineethanesulfonic acid (HEPES), Phosphate-Buffered Saline (PBS) were all obtained from Sigma-Aldrich (Australia). Isopropyl alcohol (IPA) was obtained from Nalgene® and ammonium sulphate was obtained from Ajax Chemicals.

4.3.2 Preparation of the AuNPs coated with gliadin protein

5 mg of gliadin was dissolved in 2.5 mL of 10mM aqueous CTAB in a 15 mL Falcon^{TM} tube. The tube was then heated for 5 minutes at 60°C and vortexed for 10 minutes. 2.5 mL of IPA was added to the tube and vortexed again for 10 minutes to completely dissolve gliadin. The dissolved gliadin was then filtered using a Ministart® non-pyrogenic filter unit with a pore size of 0.2 µm.

600 µL of 20 nm AuNPs was added dropwise to the Falcon Centrifuge tube containing 2.8 mL of the filtered flow-through of solubilised gliadin followed by quick vortex. The dispersion was mixed for 60 minutes with a repeated vortexing every 10 minutes followed by centrifugation at 4500×g for 30 minutes. The supernatant was discarded, and the pellet was re-dissolved in 150 µL of MilliQ water. The 20 nm AuNPs coated with gliadin were stored at 4°C for up to 4 weeks.

4.3.3 Preparation of the AuNPs coated with BSA

500 µL of 10 mg/mL BSA dissolved in 10mM HEPES was added to 50 µL of 20 nm AuNPs while vortexing. The tube was incubated for 30 minutes at room temperature with repeated vortexing. The solution was centrifuged for 30 minutes at 4500×g, supernatant discarded, and the pellet was re-suspended in 500 µL MilliQ water. The process was repeated twice after which the pellet was re-suspended in 500 µL HEPES buffer followed by centrifugation at 4500×g for 30 minutes using an Eppendorf® Microcentrifuge. The BSA coated AuNPs were stored at 4°C.

4.3.4 Determination of the concentration of gliadin and BSA coated AuNPs

Nanodrop (ND-1000 Nanodrop Technologies, Inc.) was performed on the AuNPs coated with gliadin and BSA to check for concentration and purity. As gliadin was dissolved in a cationic surfactant (CTAB) followed by a polar aprotic solvent (IPA) different controls were used to determine the background absorbance's due to the use of these solvents. Molar extinction coefficient was calculated by the ProtParam tool (ExPasy Bioinformatics Resource Portal) presented in Table 8 (refer chapter III).

Dynamic Light Scattering (DLS)

The nanoparticle hydrodynamic radius was measured using Zetasizer Nano (Malvern Technologies, Inc.). Measurements were carried out at 25°C in disposable cuvettes using a sample volume of 500 µL. Each sample was measured in triplicate and the mean value was calculated.

Transmission Electron Microscopy (TEM)

High-resolution transmission electron microscopy (TEM) micrographs were obtained using a FEI Tecnai TEM 200V fitted with a Gatan (Pleasantville, CA) CCD camera. Samples were prepared by placing 2 µL of AuNP coated with gliadin onto a carbon-coated TEM grid (Agar Scientific, UK) and the film allowed to air dry for 15 minutes.

UV-Vis Measurements

UV-Vis measurements were carried out using a Cary Series UV-Vis spectrophotometer (Agilent Technologies) using a standard 1 cm path-length quartz cuvette. Spectra were obtained from 200 nm to 800 nm. MilliQ water was used as the blank.

4.3.5 Assay for AGA

The immunoassay used to assess the activity of AuNPs coated with gliadin with the antibodies is outlined below. Assay steps were performed at room temperature. Briefly, 150 µL of AuNPs coated with gliadin were added to 1.5 mL low protein binding Eppendorf® tubes. 1 µl of 20% BSA dissolved in MilliQ water was used as the blocking agent and was added to 150 µL of 20 nm AuNPs coated with gliadin. AGA (1 mg/mL) from rabbit was added to each of the tubes corresponding to concentrations ranging from 2 µg/mL to 10 µg/mL (i.e. 1 µL to 5 µL). IgG from normal rabbit serum (1 mg/mL) was used as a control antibody and added to 150 µL of AuNPs coated with gliadin in concentrations ranging from 2 µg/mL to 10 µg/mL (1 µL to 5 µL). MilliQ water was added to the tubes to bring the final volume in each Eppendorf tube up to 225 µL. The UV-Vis absorption spectra of solutions containing gliadin coated gold nanoparticles and AGA at increasing dilutions (2 µg/mL, 4 µg/mL, 6 µg/mL, 8 µg/mL and 10

μg/mL) were studied using UV-Vis spectrophotometer. Readings were taken in triplicate and the student's t-test was used to determine the p value.

Assay for AGA in spiked human serum

Normal human serum was diluted to 1:10, 1:20 and 1:50 using 10 mM HEPES buffer. 75 μL of serum from each of the dilutions was spiked with AGA at various dilutions comparable to that seen in patients with CD.

To prevent non-specific binding, 1 μl of 20% BSA dissolved in MilliQ water and was added to 150 μL of 20 nm AuNPs coated with gliadin. The tubes were incubated for 30 minutes at room temperature. 75 μL of normal serum spiked with AGA at increasing dilutions of 2 μg/mL, 4 μg/mL, 6 μg/mL, 8 μg/mL and 10 μg/mL was then added to 20 nm AuNPs coated with gliadin. The tubes were then incubated for 30 minutes at room temperature.

Assay for AGA in clinical human serum

Anonymised patient samples were provided by Dr Jason Tye-Din from the Walter and Eliza Hall Institute of Medical Research (WEHI Institute, Melbourne Parkville, Australia). They were collected with informed consent and approval of Melbourne Health and WEHI Human Research Ethic Committees (2003.009 and 03/04) respectively. Ethical approval was also obtained from the University of Technology Sydney Research Ethics committee (UTS HREC ETH16-0841) before testing the clinical samples. The cohort consisted of some samples that were found to be haemolytic and had been stored for > 5 years, these samples were taken out to maintain assay homogeneity. In the clinical study 30 human serum samples were analysed in a blinded assessment. No prior knowledge on the CD status or any other clinical condition

of any of the patient samples was known while testing. Samples were collected from patients with active CD (pre-treatment), treated CD (on a gluten free diet) and controls without CD. The histological interpretation and the serology levels for each of the clinical sample tested using biopsy and the existing commercially available serology tests is presented in Tables 1 and 2. All cases of CD were medically diagnosed and based on typical small intestinal histology in conjunction with positive CD serology.

Prior to testing, each human serum sample was diluted to 1:10, 1:20 and 1:50 using 10 mM HEPES buffer. 1 µl of 20% BSA dissolved in MilliQ water was added to 20 nm AuNPs coated with gliadin to prevent non-specific binding. 75 µL of serum from each of the dilutions was then added to 20 nm AuNPs coated with gliadin. The tubes were incubated for 15 minutes at room temperature before the absorbance was measured using a UV-Vis spectrophotometer.

Concentration of Immunoglobulins in clinical human serum

200 µL of each human serum sample was centrifuged at 3200×g for 15 minutes. The supernatant was removed, and the serum samples were diluted with 200 µL of 10mM PBS. An equal volume of saturated ammonium sulphate solution was added slowly to achieve a 33% saturated (v/v) final concentration with continuous stirring of the tubes. Samples were kept at 4°C for 30 minutes and then centrifuged again at 2500×g for 15 minutes. The supernatant was removed, and the pellet was re-suspended by adding 200 µL of 10mM PBS. The concentrated serum solution was stored at -20°C till further use.

Zeba^{TM} Spin desalting columns (Thermo Scientific^{TM}) were used for the de salting of the immunoglobulins from the concentrated serum solution according to the manufacturer's instructions. The final concentration of the total immunoglobulins was measured using the NanoDrop and stored at -20°C until further use.

4.3.6 Colorimetric Response Curve

A colorimetric response curve was plotted to represent the sensitivity values obtained for the different dilution values for both the AGA and the control antibody (IgG from rabbit serum). The assay sensitivity was determined based on the colorimetric response values calculated as Colorimetric Response = $I_{\text{max at 532 nm}}$/ $I_{\text{550 nm}}$ i.e. spectral absorbance value obtained at 532 nm. 532 nm is the wavelength where AuNP coated with gliadin shows maximum absorbance by itself (no antibodies are added) divided by the absorbance at 550 nm where a shift in absorbance is observed following the interaction of the antibody with the AuNP coated with gliadin.

The assay sensitivity in spiked serum was calculated as Colorimetric Response = $I_{\text{max at 580 nm}}$/ $I_{\text{532 nm}}$ i.e. absorbance value obtained at 580 nm. This is the wavelength where a shift in absorbance is observed following the interaction of the antibody with the AuNP coated with gliadin in serum divided by the maximum absorbance value of AuNP coated with gliadin in serum.

4.4 Results and Discussion

Gliadin, which is found in wheat and other cereal grains, is the antigenic protein that induces CD. Gliadin epitopes are recognised by T cells that stimulate the formation of CD4, natural killer (NK)-like cells, as well as the release of pro-inflammatory cytokines such as IFN-γ thereby, activating the adaptive immune response [Abadie et al. 2011, Malamut et al. 2010].

Gliadin is a 32-35,000 molecular weight, mostly hydrophobic wheat protein that is only slightly soluble in aqueous solution. In order to use it to coat AuNPs and develop an assay for AGA, I needed to overcome the problem of aggregation of the coated nanoparticles. In previous studies using coated AuNPs, the vast majority of work used water-soluble molecules such as DNA/RNA [Elghanian et al. 1997, Lee et al. 2007, Wang et al. 2016], peptides [Sperling and Parak 2010, Slocik et al. 2011], growth factors [Huang et al. 2005] and albumins to coat the nanoparticles [Brewer et al. 2005]. Thus, a new method was developed in order to establish a stable colloidal suspension of gliadin coated AuNPs under physiological conditions.

I tested a variety of protic and aprotic solvents such as acetone, chloroform, di-chloromethanol, di-methylformamide and methanol where I observed only very partial solubility of the protein. Sufficient solubilisation of gliadin was finally achieved using the cationic surfactant CTAB and 70% isopropanol previously used in other studies to extract proteins from wheat [Watson and Thompson 1986].

The solubilisation of gliadin allowed us to adsorb the protein on the surface of AuNPs, which was monitored by UV-Vis measurements [Link and El-Sayed 1999]. A red shift was observed in the absorbance maximum from 525 nm to 532 nm, indicating that the protein was efficiently coated onto the AuNPs surface (Figure 25A). In addition, no measurable decrease of absorbance was observed at peak wavelength or an increase of absorbance at longer

wavelengths (600-700 nm) suggesting the colloidal dispersion of protein-coated AuNPs was stable and no strong AuNP-to-AuNP interactions or aggregation took place.

DLS was used to further confirm there was no aggregation, which had showed an increase in hydrodynamic diameter from 20 nm to 28 nm following coating with gliadin (Figure 25B). As the molar mass of the protein is directly proportional to its hydrodynamic radius in solution [Jans et al. 2009], an increase in the hydrodynamic radius indicates coating of gold nanoparticles with gliadin had occurred. A similar test using control AuNPs coated with BSA (molecular weight = 66 kDa) was carried out where an average particle diameter of 32 nm, correlating with the larger size of the protein was determined.

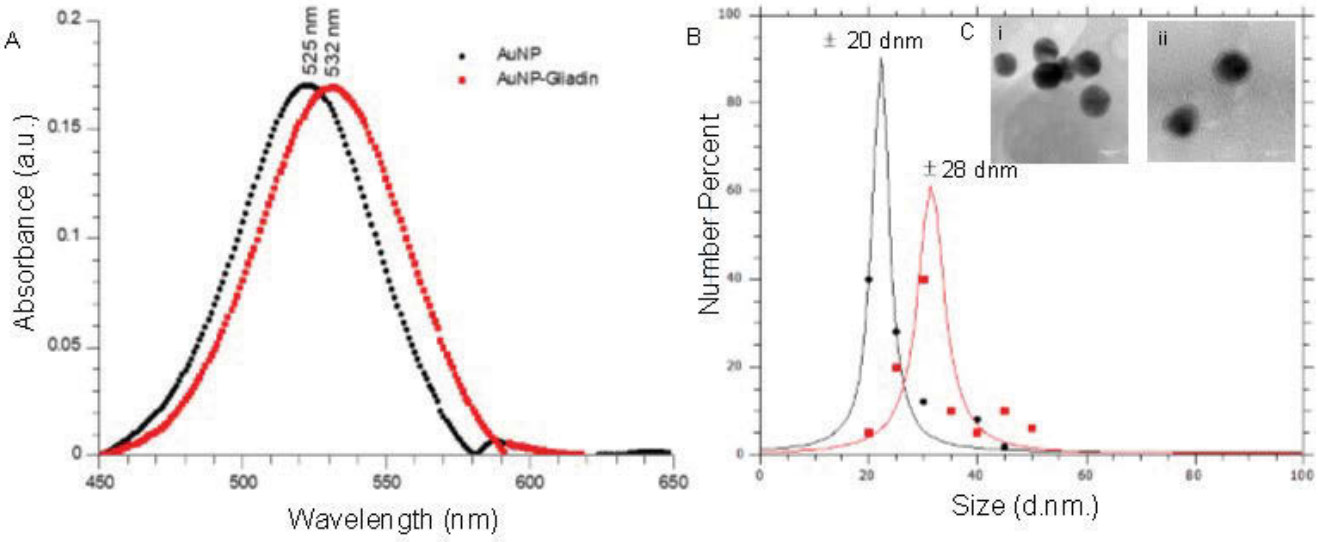

Figure 25: Characterisation of gliadin coated AuNPs *(A) Characterisation of AuNP coated with gliadin using a UV-Vis Spectrophotometer show a spectral red shift in wavelength from 525 nm (for 20 nm AuNP only) to 532 nm (for 20 nm AuNP coated with gliadin). (B) Characterisation of AuNP coated with gliadin using DLS, showing an increase in the hydrodynamic size of the uncoated vs coated particles from 20 nm to 28 nm respectively. (C) High resolution TEM images of (i) uncoated AuNPs, (ii) gliadin coated AuNPs showing a*

'halo' layer indicating coating of the gold with the protein had occurred. In contrast, the 'halo' effect was not observed on the surface of the un-coated AuNPs.

To directly observe gliadin coated on AuNPs, high-resolution TEM imaging was used. The presence of a thin layer of material (1-2 nm) (Figure 25C (ii)) surrounding the nanoparticles, which was not observed on the surface of the uncoated nanoparticles (seen in Figure 25 C (i)) [Jürgen's et al. 1999] confirmed the adsorption of protein.

4.4.1 Incubation of gliadin-coated AuNPs with AGA

To examine the ability of gliadin-coated AuNPs to detect AGA, serial dilutions of rabbit anti-gliadin IgG polyclonal antibody in a range that normally exists in human serum [O'Farrelly et al. 1983, Al-Bayaty et al. 1989] were tested. After 30 minutes incubation a significant reduction in colour as well as a decrease in the absorbance peak with a shift from 532 nm to 580 nm (Figure 26A) was observed. These results showed that in the presence of the AGA there is increased nanoparticle-to-nanoparticle interaction leading to aggregation and precipitation of the AuNPs.

As a control, normal rabbit serum IgG antibody with the gliadin coated AuNPs were tested. No significant change in colour or shift in the wavelength or size of the absorbance peak after taking the dilution factor into account was found (Figure 26 A, B). In addition, at all the tested concentrations, the absorbance was significantly lower using AGA as compared to normal IgG, reaching its minimum value in the range of 4-8 μg/mL ($p < 0.005$, Figure 26 B). These results demonstrate the specificity of the interaction between AuNP-gliadin to AGA and also demonstrate the sensitivity of the assay to detect AGA down to a concentration of 2 μg/mL.

Uncoated AuNPs and those coated with an irrelevant antigen, BSA, incubated with AGA as controls for specificity were also tested. The results did not show any significant change in absorbance or aggregation (Figure 27 and 28) confirming the specificity of the assay for whole gliadin.

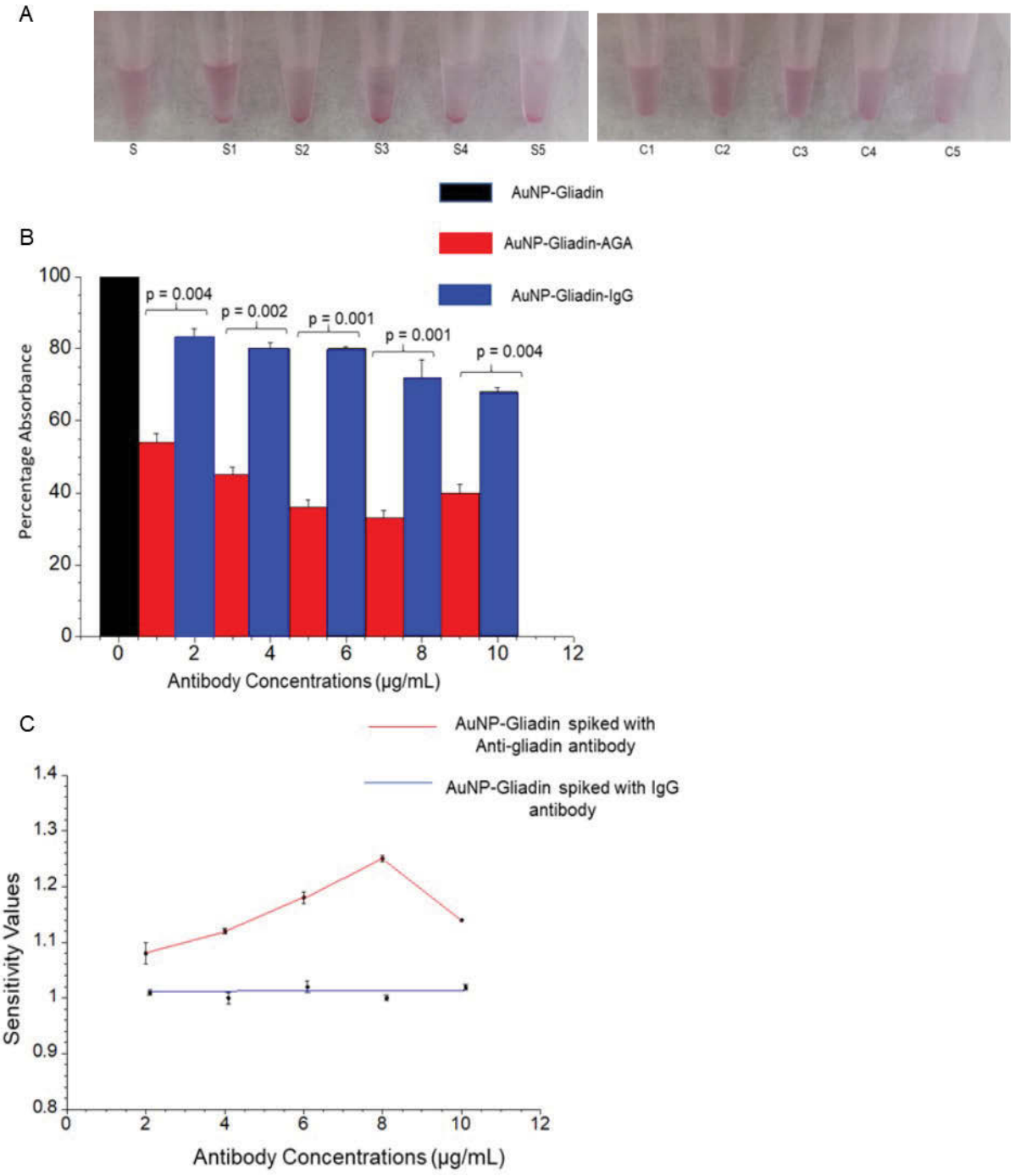

Figure 26: Testing gliadin-coated AuNPs with AGA *(A) Reduction in colour from red to translucent and lowered absorbance was observed in AuNP coated with gliadin (S) and incubated with AGA at various dilutions (S1) 2 µg/mL, (S2) 4 µg/mL, (S3) 6 µg/mL, (S4) 8 µg/mL and (S5) 10 µg/mL. No significant change in colour or shift in peak wavelength was observed in gliadin coated AuNP incubated with control rabbit IgG at all dilutions tested (C1) 2 µg/mL, (C2) 4 µg/mL, (C3) 6 µg/mL, (C4) 8 µg/mL and (C5) 10 µg/mL. Figure 27 (B) Representation of specificity based on UV-Vis absorbance spectra for the antibody interactions at equal concentrations of AGA and control antibody. Figure 27 (C) Colorimetric response curve plotted on AuNP coated with gliadin following the addition of AGA at different dilutions.*

To assess the specificity of the AGA toward gliadin coated AuNPs, a colorimetric response between our assays was calculated (Figure 26 C, Table 20). It was found that the response reaches a maximum value at a concentration of 8 µg/mL of AGA. The near constant colorimetric response curve obtained for the control antibody as compared to the response curve obtained for AGA further demonstrates the specificity of the assay.

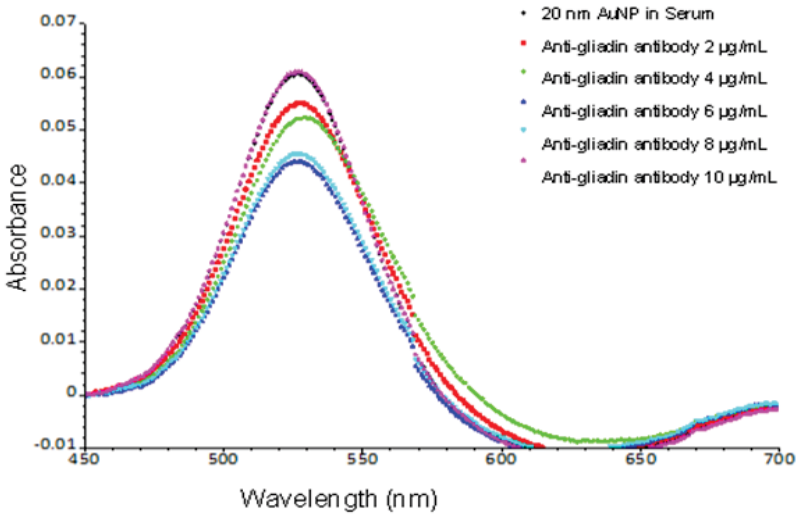

Figure 27: Incubation of uncoated AuNPs in serum with AGA at various dilutions.

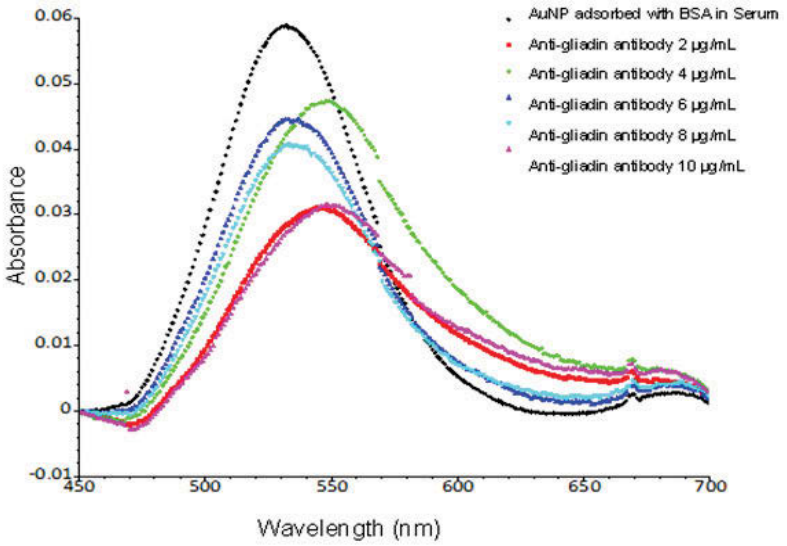

Figure 28: Incubation of BSA coated AuNPs in serum with AGA at various dilutions.

Table 20. Calculated p-value in AuNP coated with gliadin in the presence of AGA antibody and the control antibody (IgG from rabbit serum) at dilutions 2-10 µg/mL.

Sample	Percentage Absorbance	*t-test* p-values
AuNP coated with Gliadin	100	
Anti-gliadin antibody 2.0 µg/mL	54	0.004
Control antibody 2.0 µg/mL	83	
Anti-gliadin antibody 4.0 µg/mL	45	0.002
Control antibody 4.0 µg/mL	80	
Anti-gliadin antibody 6.0 µg/mL	36	0.001
Control antibody 6.0 µg/mL	80	

Anti-gliadin antibody 8.0 µg/mL	33	0.001
Control antibody 8.0 µg/mL	72	
Anti-gliadin antibody 10.0 µg/mL	40	0.004
Control antibody 10.0 µg/mL	68	

4.4.2 Testing AGA in spiked serum

Human serum is a complex fluid containing various proteins, peptides as well as nucleic acids. To reduce background binding, 1% BSA as a blocking agent was used, to lower the non-specific interaction with the gliadin coated AuNPs. Spiked human serum containing 2-10 µg/mL AGA was incubated with gliadin-coated AuNPs. The results showed an increase in aggregation and precipitation, which was easily detectable by eye (Figure 29). A reduction in the colour of the solution from red to translucent was observed as shown in Figure 29 B. This change was further supported by the observation of an increase in the colorimetric response that reached a maximum at 8 µg/mL of AGA (Figure 29 A, Figure 30 and Figure 31). In contrast, when normal rabbit IgG to the human serum was added, no precipitate formation or change in colour was observed. Normal serum itself did not show any change in absorbance with the response curve being constant and low at all IgG concentrations.

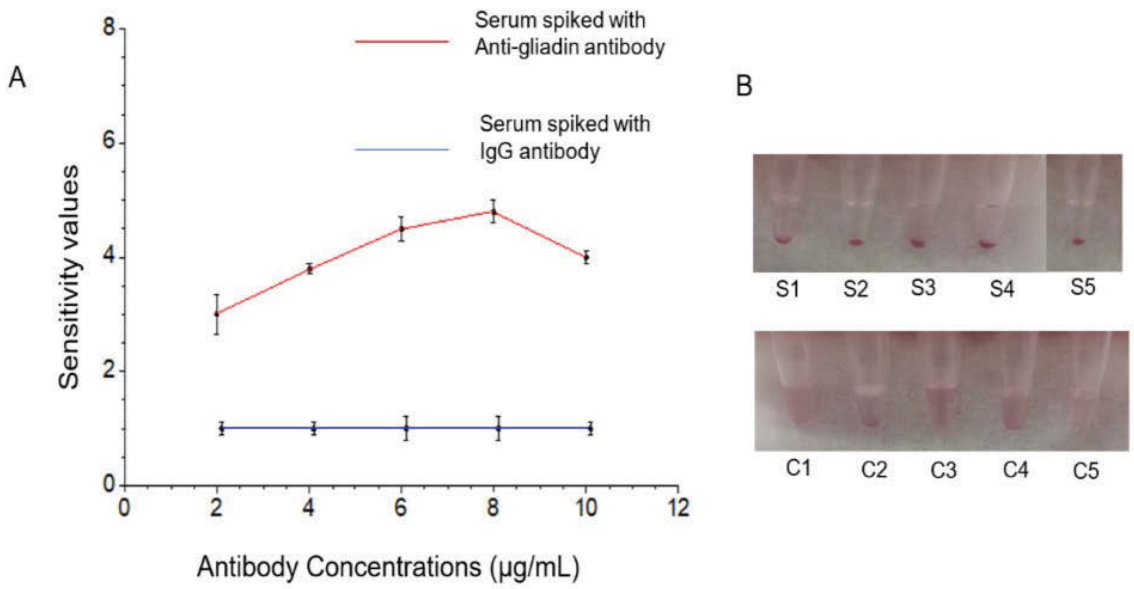

Figure 29: Detection of AGA in spiked human serum using gliadin-coated AuNPs. *(A) Colorimetric response curve of AuNP coated with gliadin in serum diluted 1:20 following the addition of AGA at different concentrations. (B) Reduction in colour from red to translucent as well as precipitate formation was observed in AuNP coated with gliadin in the presence of AGA and serum at different concentrations (S1-S5). No reduction in colour from red to translucent or precipitate formation was observed in AuNP coated with gliadin in the presence of control IgG and serum (C1-C5).*

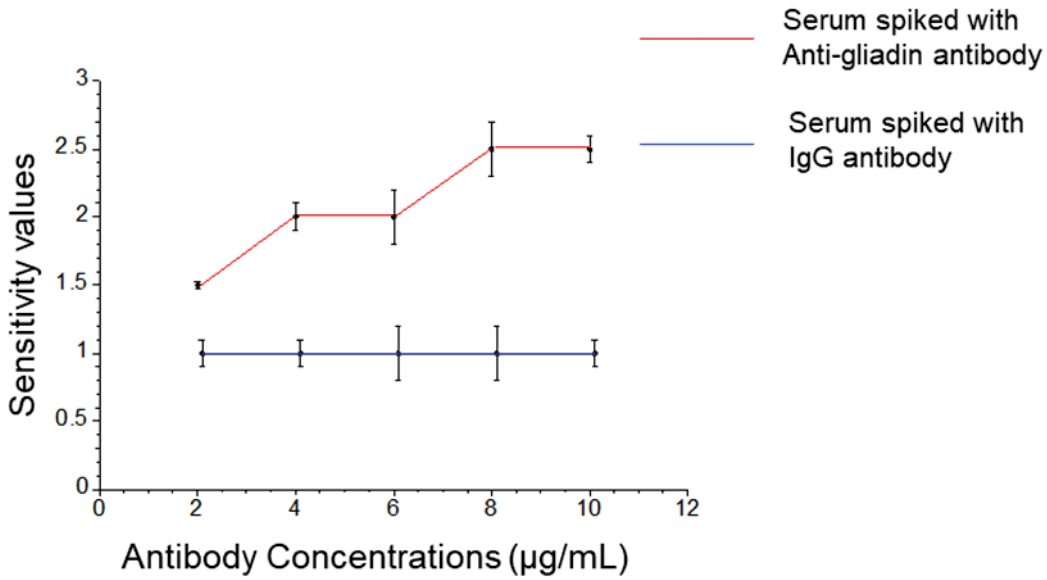

Figure 30: Colorimetric response curve plotted in AuNP coated with gliadin in 1:10 diluted serum following the addition of AGA antibody at dilutions 2 µg/mL, 4 µg/mL, 6 µg/mL, 8 µg/mL and 10 µg/mL.

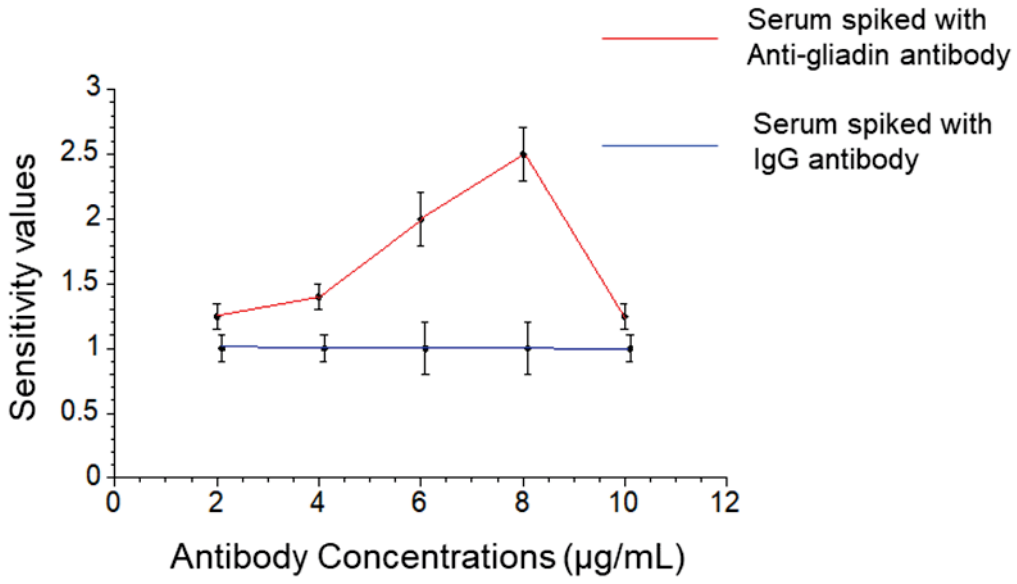

Figure 31: Colorimetric response curve plotted in AuNP coated with gliadin in 1:50 diluted serum following the addition of AGA at dilutions 2 µg/mL, 4 µg/mL, 6 µg/mL, 8 µg/mL and 10 µg/mL.

4.4.3 Anti-gliadin antibody binding to gliadin-AuNPs in saliva

UV–Vis spectrophotometry was used to confirm that the gliadin-AuNP were able to interact with anti-gliadin antibodies in saliva samples. A decrease in the absorption wavelength was observed when the gliadin coated AuNPs were added to saliva samples containing anti-gliadin antibodies. Normal saliva itself did not show any absorbance and behaved like water with zero absorbance value. These readings confirmed that the anti-gliadin antibodies can cause aggregation in the presence of saliva and their specificity is not affected by other constituents in saliva. A change in colour from red to translucent was also observed (Figure 32).

A

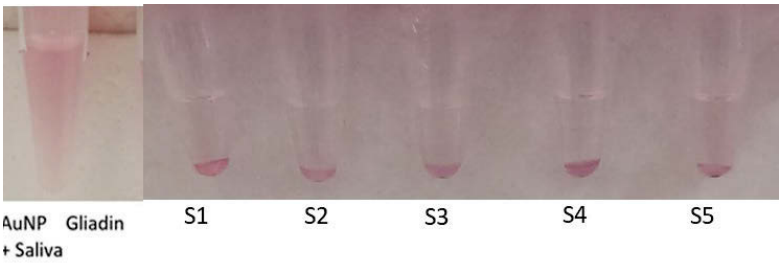

B

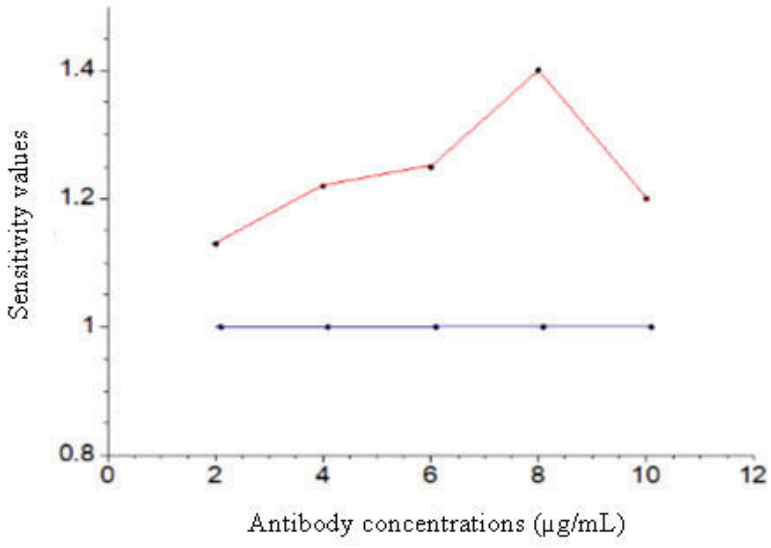

Figure 32: Testing gliadin-coated AuNPs with AGA in saliva

(A) Reduction in colour from red to translucent and lowered absorbance was observed in AuNP coated with gliadin (S) and incubated with AGA at various dilutions (S1) 2 µg/mL, (S2) 4 µg/mL, (S3) 6 µg/mL, (S4) 8 µg/mL and (S5) 10 µg/mL. (B) Colorimetric response curve plotted on AuNP coated with gliadin following the addition of AGA in saliva at different dilutions.

A colorimetric response curve was plotted to represent the sensitivity values obtained for the different dilution values. A linear increase in the colorimetric response was observed, reaching a maximum value when anti-gliadin antibody is added at a concentration of 8 µg/mL to 20 nm AuNPs coated with gliadin in the presence of saliva. The response curve begins to show a drop in the colorimetric response value when the anti-gliadin concentration is increased to 10 µg/mL. The antibody concentrations are similar to those normally observed in patients' with CD saliva [Lenander-Lumikari et al. 2000 and Tucker et al. 1988].

4.4.4 Testing clinical samples

To assess the clinical relevance of the developed method, I next used the gliadin coated AuNPs to test a selected set of human serum samples obtained from patients with CD or controls without CD. The goal of the study was to test the ability of the assay to distinguish between previously diagnosed CD patients from non-CD individuals.

The results for the 30 clinical samples were recorded after the visual examination of precipitate formation and the determination of a shift or change in absorbance values using a UV-Vis spectrophotometer. Based on the results observed by eye, the samples have been divided into three categories: clear precipitation, aggregation and colloidal suspension. Out of the thirty clinical samples tested, nineteen samples showed clear precipitation within 15 minutes and formed a pellet indicating they were positive for CD. Seven samples began to start showing the formation of aggregated particles (but no pellet) within 15 minutes and these were observed

for another 15 minutes for further confirmation as CD positive. In four samples, there was no precipitation or formation of aggregates within 15 minutes, and remained as a colloidal suspension, and were classified as negative for CD.

The assay sensitivity was determined based on the colorimetric response obtained for each serum sample and was calculated as Colorimetric Response = $I_{\text{max at 580 nm}}/ I_{532\text{ nm}}$. Using this method, the calculated colorimetric response for normal serum i.e. serum from non-CD patients is 1 and this acts as the cut-off value. Therefore, for the clinical samples, based on the spectral absorbance data, a value of ≤ 1 is indicated as negative for CD and a value above 1 is considered CD positive. Based on the observation and calculation of the colorimetric response curve, I have summarised the outcomes in Tables 21, 22 and Figure 33 along with the results reported using other serological methods, biopsy and histology.

Table 21. Comparison of the patient samples analysed using the AuNP-AGA test with the previously existing histology and serological* results

Volunteer	Histology	tTG-IgA	DGP-IgG	AuNP-AGA Test
n.1	CD	1 (<4)	3 (<20)	CD Positive
n.2	Non-CD	0.1 (0-6)	0.2 (0-6)	CD Negative
n.3	CD	>100 (<4)	33 (<20)	CD Positive
n.4	CD	121 (<20)		CD Positive
n.5	CD	>100 (<4)	>100 (<20)	CD Positive
n.6	CD	217 (<5)	>150 (<20)	CD Positive
n.7	CD	13 (0-6)	23 (0-6)	CD Positive
n.8	CD	>100 (<5)	>100 (<20)	CD Positive
n.9	CD	11 (0-6)	1.4 (0-6)	CD Positive
n.10	CD	9 (<4)	97 (<20)	CD Positive

n.11[ɪ]	CD	18.2 (0<20)	3 (0.20)	CD Negative
n.12[ɪɪ]	CD	16 (0-20)	7 (<20)	CD Positive
n.13	Non-CD	4 (0-20)		CD Negative
n.14	CD	47 (<5)	86 (<5)	CD Positive
n.15	CD	74 (0-20)		CD Positive
n.16	CD	145 (0-20)		CD Positive
n.17	CD	57 (<4)	93 (<20)	CD Positive
n.18	CD	149 (<20)	63 (<20)	CD Positive
n.19	CD	>100 (<4)	>100 (<20)	CD Positive
n.20[ɪɪɪ]	Non-CD	3.8 (<6)	37 (<6)	CD Positive
n.21	Non-CD	<5 (<5)	<20 (<20)	CD Negative
n.22	CD	180 (0-6)	21 (0-6)	CD Positive
n.23	CD	20 (0-6)	8.1 (0-6)	CD Positive

* Serology tTG (Tissue transglutaminase), DGP (Deamidated gliadin peptides) results are indicated as IgA or IgG levels with assay kits obtained from different manufacturers with different test results followed by normal reference ranges in brackets [ɪ] Following GFD > 8 weeks, [ɪɪ] Following GFD < 2 weeks, [ɪɪɪ] False positive based on histology and tTG antibody titre.

Table 22. Analysis of 7 samples with potential or undiagnosed CD using the AuNP-AGA test as compared with previously existing serology*. Cases are separated into those with histological observations of patchy /irregular mucosal lesions or those with mucosal inflammation resulting from an increase in $\gamma\delta^+$ IELs.

Volunteer	Histology	tTG-IgA	DGP-IgG	AuNP-AGA Test
n.24	Mucosal lesions	5 (<20)	17 (<20)	CD Positive
n.25	Mucosal lesions	28 (0-6)	22 (0-6)	CD Positive

n.26	Mucosal lesions	4.8 (0-6)	22 (0-6)	CD Positive
n.27	Increased $\gamma\delta^+$ IELs	12 (0-6)	18 (0-6)	CD Positive
n.28	Increased $\gamma\delta^+$ IELs	11 (0-6)	13 (0-6)	CD Positive
n.29	Increased $\gamma\delta^+$ IELs	<5 (<5)	<20 (<20)	CD Positive
n.30	Increased $\gamma\delta^+$ IELs	<5 (<5)	22 (<20)	CD Positive

* Serology tTG (Tissue transglutaminase), DGP (Deamidated gliadin peptides) results are indicated as IgA or IgG levels obtained from different manufacturers followed by normal reference ranges in brackets, IELs (Intraepithelial lymphocytes).

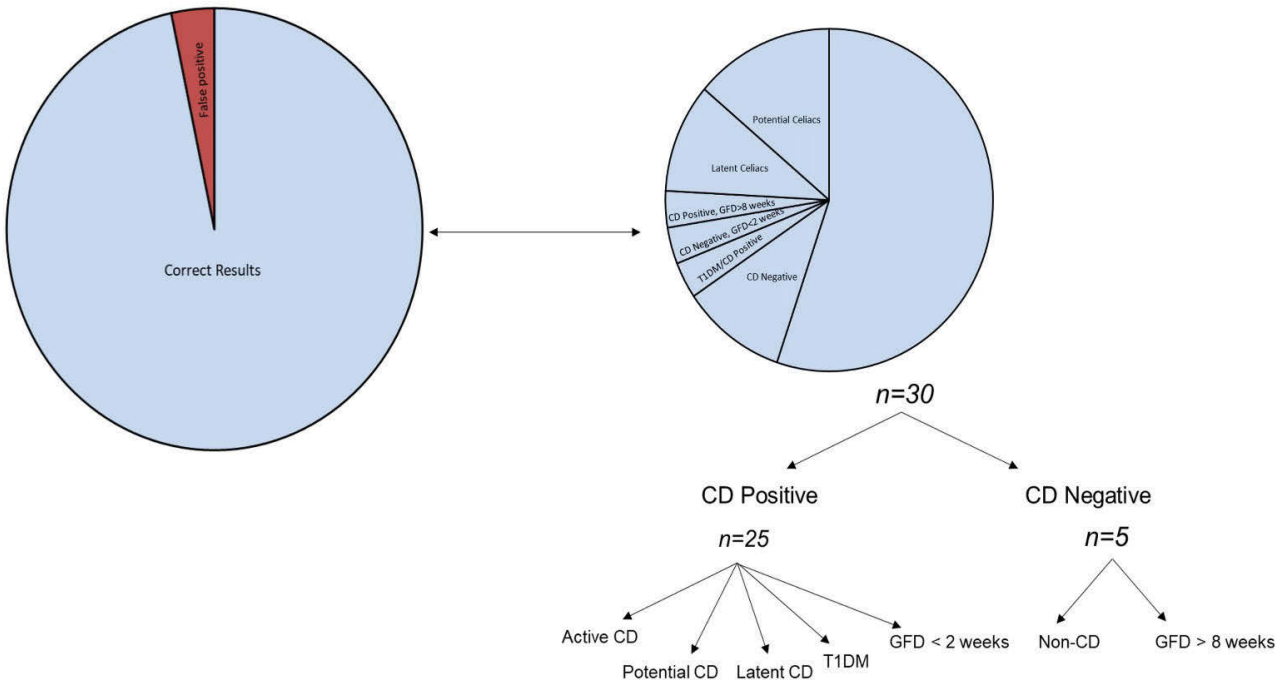

Figure 33: Representation of the distribution of clinical samples using AuNP-AGA Assay

In sixteen samples that were previously diagnosed with active CD all of them were identified as CD positive using the AuNP-AGA assay as well. These samples showed the formation of a precipitate, had a clear shift and a drop in UV-Vis absorbance values as well as a high colorimetric response value. The remaining samples were then classified into various sub-classes based on the analysis using the AuNP-Peptide-AGA assay as described below (refer Tables 21 and 22, Figure 33).

In the cohort of tested samples, there are two cases where the patients had previously been diagnosed with CD and therefore followed a gluten free diet (GFD). While one person had been on a GFD for more than 8 weeks (volunteer number n.11), the other person had been on a GFD for less than 2 weeks (volunteer number n.12). The AuNP-AGA diagnostic test distinguished the person following GFD > 8 weeks as negative for CD, while serum from the person who has been on GFD < 2 weeks formed a suspension (Table 21). Interestingly, the conventional serology test identified these two patients as negative suggesting that the nanoparticle test can detect true biopsy-confirmed cases even when traditional serology is negative. The analysis of these two exceptional patients using the AuNP-AGA method indicates that this diagnostic test can potentially also be used for monitoring patients on a GFD over time. More CD patients on GFD need to be tested in the future to confirm this result.

The sample cohort also contained serum from an individual who was suffering from Type 1 diabetes mellitus (T1DM); the diabetic person could be identified as positive for CD using biopsy. For patients with T1DM, the prevalence of CD in T1DM is reported to vary from 3% to 16%, [Volta et al. 2011], due to the common genetic background as well as the multiple environmental and immunological factors [Ventura et al. 2002]. In addition, most T1DM patients, particularly diabetic children, have an undiagnosed form of the disease characterised by the absence of both gastrointestinal and extra-intestinal signs and are often regarded as

asymptomatic. Therefore, the diagnosis for CD of diabetic patients is difficult and requires continuing careful clinical and serological follow-up [Holmes 2001].

The AuNP-AGA diagnostic test correctly identified the patient with T1DM as positive for CD, which matches with the previously conducted biopsy and serological profile of the patient. This result is important as it shows that the gliadin coated AuNPs can detect AGA in patients suffering from other autoimmune diseases. This is however, a single test result and needs to be further explored in larger clinical studies.

Three samples (volunteer numbers n.24, n.25, n.26, Table 22) with patchy/ irregular mucosal lesions, classified as a broad sub-type of potential or undiagnosed coeliac, demonstrated a clear precipitate using the AuNP-AGA test. The UV-Vis absorbance data supported the visual examination. These three samples were classified as positive for CD as these may be undiagnosed coeliac sufferers that have positive CD serology and display mild mucosal atrophy initially, that then develops with typical atrophy of small intestine mucosa [Kaukinen et al. 2001].

Four clinical samples (volunteer numbers n.27, n.28, n.29, n.30, Table 22) showed the formation of aggregated nanoparticles along with a drop in UV-Vis absorbance values. These samples showed mucosal inflammation with positive or low positive serology results. The AuNP-AGA test showed results similar to those found using the existing serological assays. These four cases have been identified as 'potential' CD positives, that is characterised by a normal villous architecture but demonstrate pathological findings such as increased $\gamma\delta^+$ intraepithelial lymphocytes as well as presence of gliadin specific antibodies, usually at low titres (<1:40) [Volta and Villanacci 2011]. Although, histology in general is considered the most reliable method of testing for CD, it has shown lowered predictive value in recognising "potential" CD cases. This situation requires an evaluation of serological markers for the

correct diagnosis of potential CD cases, which are then monitored for the appearance of pathological symptoms.

The cohort included four samples identified as negative for CD based on biopsy. Out of the four samples (volunteer numbers n.2, n.13, n.20 and n.21, Table 21), three samples were correctly identified as CD negative by AuNP-AGA diagnostic assay while, one sample (volunteer number n.20) showed the formation of aggregates and was identified as positive. The DGP-IgG serology titres for that sample however, indicate positive CD necessitating a clinical follow-up on the patient to confirm CD status. As intestinal biopsy has been used as the gold standard for CD confirmation, that one sample (volunteer number n.20) has been referred to as a false positive result.

Overall, the results for the clinical samples tested showed that 22 of the 23 samples gave the correct result based on previous biopsy and serology. In addition, there were 7 samples that were either potential or undiagnosed coeliac that all test positive for CD. Finally, there was one sample that may be a false positive giving an overall accuracy for this cohort of at least 96%.

In future work, AGA in serum as a biomarker for CD needs further validation in larger patient cohorts, particularly, in patients suffering from other autoimmune diseases. This is necessary not only to verify the diagnostic accuracy, but also to confirm specificity for the diagnosis of CD. The developed test looks very promising in that it is single step, carried out within 15-30 minutes and the results can be determined by eye not requiring any specialised equipment for signal reading. This gives this technology an advantage over the existing blood tests that need a sophisticated laboratory setting for analysis, which is time consuming and expensive. Finally, this assay may be useful for testing CD patients using saliva as a non-invasive, point of care test. Further work is required to test this possibility.

4.5 Conclusions

CD is a chronic disorder that damages the small intestine and is caused by consuming the protein gluten present in wheat and other cereals. Gliadin is one of the two major protein groups that comprises gluten and plays a significant role in causing the disease. In the present study, I have demonstrated the potential of gliadin coated AuNPs for detecting a biomarker for CD from serum. This was achieved by developing a methodology to coat the hydrophobic gliadin protein on the surface of AuNPs without causing aggregation.

The addition of AGA to gliadin coated AuNPs at levels associated with CD resulted in colour reduction and absorbance peak shift due to the aggregation of AuNPs. The gliadin coated AuNPs have been shown to detect AGA not only in quantitatively spiked samples but also in a small-scale study on real CD patients' samples. The analysis of the clinical samples demonstrated not only the ease of the test procedure, but also its very high accuracy. This study demonstrates the immense potential of AuNP-AGA based approach in that it can be used for pre-selecting CD sufferers which can then be confirmed by mucosal biopsy for CD as well as for monitoring the effectiveness of a gluten free treatment. The test method has potential to be adapted as a point-of-care test that will be useful in resource-limited laboratory settings for the screening to aid in early identification of CD.

CHAPTER V

A novel screening test for coeliac disease using peptide functionalised gold nanoparticles

5.1 Background

In this chapter, I present a novel screening test for CD based on the coating of gold nanoparticles with a peptide derived from gliadin, the protein that triggers CD. Peptide-functionalised nanoparticles (PFNs) are an emerging sensing element that have previously been used for effective drug delivery for treating brain tumours and for pancreatic cancer treatment as well as for enzyme studies. The gold nanoparticles were coated with a 17-mer peptide (QLQPFPQPQLPYPQPQC). The coating of the peptide to the AuNP was achieved through Avidin-Biotin interactions using Biotin-$(PEG)_{11}$-Maleimide as the linker.

The peptide coated gold nanoparticles were then converted into a serological assay. The peptide functionalised gold nanoparticle-based assay was tested on thirty patient serum samples in a blinded assessment and the results were compared with the previously run serological and pathological tests on these patients. This study demonstrates the potential of gold nanoparticle-peptide based approach to be adapted for developing a screening assay for diagnosis for CD.

This work is a part of the International patent PCT/AU2018/050125 that has been published with International Publication No. WO 2018/148801. This chapter is written in the form of a paper that has been published in the journal '*World Journal of Gastroenterology*'.

5.2 Introduction

Sensing platforms based on the optical properties of gold nanoparticles (AuNPs) for the molecular detection and recognition of disease biomarkers is an important research challenge. Colorimetric sensors based on AuNPs have been applied for detecting targets, such as metal ions [Lee et al. 2007, Hung et al. 2010, Chen et al. 2014, Chen et al. 2015], DNA, [Elghanian et al. 1997, Wang et al. 2016], protein conformations [Tsai et al. 2011] and enzyme activity [Wang et al. 2011], where they have demonstrated high sensitivity and effectiveness.

In recent years, newer designs of nanoparticles with enhanced and controlled surface chemistry are being explored for sensing applications. Peptide-functionalised nanoparticles (PFNs) are one such emerging sensing element. PFNs have previously been used for effective drug delivery for treating brain tumors and for pancreatic cancer treatment as well as for kinase inhibitor screening [Gao et al. 2014, Lee et al. 2013, Gupta et al. 2010, 2011]. Here the potential of PFNs as a colorimetric sensor for screening CD is demonstrated.

CD is a small intestine enteropathy affecting genetically susceptible individuals, following the consumption of wheat prolamins (gliadin) and other prolamins of cereals [Ludvigsson et al. 2013]. Population based studies have predicted a high prevalence rate for the disease, with a large number of CD sufferers remaining undiagnosed [Marsh et al. 2015]. The current diagnosis of CD is based on mucosal biopsy that remains the gold standard [Rostami et al. 2017]. Serological testing for gliadin-induced antibodies using an enzyme-linked immunosorbent assay is being widely applied [Dahlbom et al. 2016, Benkebil et al. 2013] and is usually the first line in clinical diagnosis for CD.

Gliadin antigenicity arises due to the higher content and repetitive arrangement of amino acids glutamine (~36 %) and proline (~17-23%) [Weiser 1996]. This acts as the substrate for the enzyme tissue transglutaminase (tTG: EC 2.3.2.13), resulting in deamidation and formation of

an irreversible isopeptidyl bond [Piper et al. 2002]. HLA-DQ molecules (HLA-DQ2/8) present the deamidated gliadin peptides (DGP) to mucosal $CD4^+$T cells leading to an immunostimulatory effect [Lundin et al. 1993]. Gluten reactive helper T cells support the activated $CD4^+$ T cells in the intestinal mucosa leading to the release of autoantibodies that act as the serological biomarkers [Sollid and Jabri 2013, Du Pre' and Sollid 2015].

Non-treated CD patients have been shown to have increased concentration of Anti-gliadin (AGA), tTG antibodies as well as Anti-DGP antibodies [Dieterich et al. 1998, Amarri et al. 2013]. A deamidated peptide sequence derived from α-gliadin amino acids 57-73 has also been identified as an immunogenic peptide sequence that can act as a trigger for CD [Anderson et al. 2000].

In this study, a screening test for CD using gold nanoparticles (AuNPs) coated with a peptide sequence derived from the gliadin protein is presented. A stable suspension (without any significant level of aggregation) of peptide coated AuNPs was established, which enables me to translate it to a serological assay. The sensitivity and specificity levels of the test using serum samples spiked with AGA was assessed. Furthermore, the assay was tested on thirty patient serum samples and it was found that the PFN-based assay could distinguish CD from non-CD patients.

This study highlights the potential of using immunodominant and biomarker specific peptide sequences that can be used for developing an efficient, easy to use screening test for pre-selecting CD cases, which can be then confirmed by mucosal biopsy for CD.

5.3 Materials and Methods

5.3.1 Reagents

20 nm citrate stabilised gold nanoparticles (AuNPs), bovine serum albumin (BSA), anti-gliadin antibody (AGA) from rabbit, IgG antibody from whole normal rabbit serum, 4-(2-

hydroxyethyl)-1-piperazineethanesulfonic acid (HEPES), Phosphate-Buffered Saline (PBS) were all obtained from Sigma-Aldrich (Australia). Poly (ethylene glycol) [*N*-(2-maleimidoethyl) carbamoyl] methyl ether 2-(biotinylamino) ethane (i.e. Biotin-PEG_{11}-Maleimide) and NeutrAvidin were all obtained from Thermo Fisher Scientific (Australia).

5.3.2 Peptide

Peptide (QLQPFPQPQLPYPQPQC) was synthesised from ChinaPeptides Co., Ltd. (China). The synthetic crude peptides were purified by reversed-phase liquid chromatography to give a satisfactory peptide sequence (~90% homogeneity by analytical HPLC) with the correct amino acid sequences and mass spectra. The peptide contained residues 57-72 of α-gliadin and was designated as follows: **Peptide**: QLQPFPQPQLPYPQPQC

Peptide (QLQPFPQPQLPYPQPQC) was coated on the surface of the AuNPs in two stages: first, coating with NeutrAvidin followed by a second step of binding of the peptide through a biotin-PEG-Maleimide linker molecule.

5.3.3 Preparation of the AuNPs coated with NeutrAvidin

300 µL of 20 nm AuNP were added dropwise to 200 µL of NeutrAvidin dissolved in 10mM HEPES (1 mg/mL) while vortexing. The tube was incubated for 60 minutes at room temperature with repeated vortexing. The solution was centrifuged for 30 minutes at 4500×g, supernatant discarded, and the pellet was re-suspended in 200 µL MilliQ water. The process was repeated twice after which the pellet was re-suspended in 200 µL HEPES buffer followed by centrifugation at 4500×g for 30 minutes using an Eppendorf® Microcentrifuge. The NeutrAvidin coated AuNPs were stored at 4°C.

Binding of Peptide to linker molecule

300 µL of 0.5 mg/mL peptide (QLQPFPQPQLPYPQPQC) dissolved in MilliQ water was added dropwise to 700 µL of 0.5 mg/mL Poly (ethylene glycol) [*N*-(2-maleimidoethyl) carbamoyl] methyl ether 2-(biotinylamino) ethane (i.e. Biotin-PEG-Maleimide) dissolved in MilliQ water, (M_n 5,400, MW 921 Da) having maleimide at the Ω-end and biotin at the α-end. This solution was left overnight at room temperature.

5.3.4 Preparation of the AuNPs coated with peptide using linker

The NeutrAvidin coated AuNPs were centrifuged at 4500×g for 30 minutes using an Eppendorf® Microcentrifuge, supernatant discarded, the pellet was re-suspended in 100 µL of the peptide-linker solution. The tube was incubated for 60 minutes at room temperature with repeated vortexing. The solution was centrifuged for 5 minutes at 4500×g, supernatant was discarded, and the pellet was re-suspended in 100 µL of MilliQ water. The peptide coated AuNPs were stored at 4°C for up to 4 weeks.

Dynamic Light Scattering (DLS)

The nanoparticle hydrodynamic radius was measured using Zetasizer Nano (Malvern Technologies, Inc.). Measurements were carried out at 25°C in disposable cuvettes using a sample volume of 500 µL. Each sample was measured in triplicates and the mean value was calculated.

Transmission Electron Microscopy (TEM)

High-resolution transmission electron microscopy (TEM) micrographs were obtained using a FEI Tecnai TEM 200V fitted with a Gatan (Pleasantville, CA) CCD camera. Samples were prepared by placing 2 µL of AuNP coated with peptide onto a carbon-coated TEM grid (Agar Scientific, UK) and the film allowed to air dry for 15 minutes.

UV-Vis Measurements

UV-Vis measurements were carried out using a Cary Series UV-Vis spectrophotometer (Agilent Technologies) using a standard 1 cm path-length quartz cuvette. Spectra were obtained from 200 nm to 800 nm. MilliQ water was used as the blank.

5.3.5 AGA Assay

The immunoassay used to assess the activity of AuNPs coated with the peptide with the antibodies is outlined below. Assay steps were performed at room temperature. Briefly, 150 µL of AuNPs coated with the peptide were added to 1.5 mL low protein binding Eppendorf® tubes. AGA (1 mg/mL) from rabbit was added to each of the tubes corresponding to concentrations ranging from 2 µg/mL to 20 µg/mL (i.e. 1 µL to 10 µL) to determine the specificity of the reaction between the peptide coated AuNPs and AGA. IgG from normal rabbit serum (1 mg/mL) was used as a control antibody and added to 150 µL of AuNPs coated with the peptide in concentrations ranging from 2 µg/mL to 20 µg/mL (i.e. 1 µL to 10 µL). MilliQ water was added to the tubes to bring the final volume in each Eppendorf tube up to 225 µL. The UV-Vis absorption spectra of solutions containing peptide coated gold nanoparticles and AGA at increasing dilutions (2 µg/mL, 4 µg/mL, 6 µg/mL, 8 µg/mL, 10 µg/mL, 12 µg/mL, 14

µg/mL, 16 µg/mL, 18 µg/mL and 20 µg/mL) were studied using a Cary Series UV-Vis spectrophotometer. Readings were taken in triplicate and the student's t-test was used to determine the p value.

AGA assay in spiked human serum

Normal human serum was diluted to 1:20 using 10 mM HEPES buffer. 75 µL of serum from the dilution was spiked with AGA at various dilutions comparable to that seen in patients with CD.

To prevent non-specific binding, 1 µl of 20% BSA dissolved in MilliQ water and was added to 150 µL of 20 nm AuNPs coated with peptide. The tubes were incubated for 30 minutes at room temperature. 75 µL of normal serum spiked with AGA at increasing dilutions of 2 µg/mL, 4 µg/mL, 6 µg/mL, 8 µg/mL and 10 µg/mL, 12 µg/mL, 14 µg/mL, 16 µg/mL, 18 µg/mL and 20 µg/mL was then added to AuNPs coated with the peptide. The tubes were then incubated for 30 minutes at room temperature.

AGA assay in clinical human serum

Anonymised patient samples were provided by Dr Jason Tye-Din from the Walter and Eliza Hall Institute of Medical Research (WEHI Institute, Melbourne Parkville, Australia). They were collected with informed consent and approval of Melbourne Health and WEHI Human Research Ethic Committees (2003.009 and 03/04) respectively. Ethical approval was also obtained from the University of Technology Sydney Research Ethics committee (UTS HREC ETH16-0841) before testing the clinical samples. The clinical samples consisted of 30 human serum samples that were analysed in a blinded assessment. No prior knowledge of the CD

status or any other clinical condition for any of the patient samples was known while testing. Samples were collected from patients with active CD (pre-treatment), treated CD (on a gluten free diet) and controls without CD. All cases of CD were medically diagnosed and based on typical small intestinal histology usually in conjunction with positive CD serology. The histological interpretation and the serology levels for each of the clinical sample tested using biopsy and the existing commercially available serology tests is presented in Tables 1 and 2.

Prior to testing, each human serum sample was diluted to 1:10, 1:20 and 1:50 using 10 mM HEPES buffer. 1 µl of 20% BSA dissolved in MilliQ water was added to AuNPs coated with the peptide to prevent non-specific binding. 75 µL of serum from each of the dilutions and the tubes were incubated for 15 minutes at room temperature before the absorbance was measured using a UV-Vis spectrophotometer.

Concentration of Immunoglobulins in clinical human serum

200 µL of each human serum sample was centrifuged at 3200×g or 15 minutes. The supernatant was removed, and the serum samples were diluted with 200 µL of 10mM PBS. An equal volume of saturated ammonium sulphate solution was added slowly to achieve a 33% saturated (v/v) final concentration with continuous stirring of the tubes. Samples were kept at 4°C for 30 minutes and then centrifuged again at 2500×g for 15 minutes. The supernatant was removed, and the pellet was re-suspended by adding 200 µL of 10mM PBS. The concentrated serum solution was stored at -20°C till further use.

Zeba^{TM} Spin desalting columns (Thermo Scientific^{TM}) were used for the desalting of the immunoglobulins from the concentrated serum solution according to the manufacturer's instructions. The final concentration of the total immunoglobulins was measured using the NanoDrop and stored at -20°C until further use.

5.3.6 Colorimetric Response Curve

A colorimetric response curve was plotted to represent the sensitivity values obtained for the different dilution values for both the AGA and the control antibody (IgG from rabbit serum). The assay sensitivity was determined based on the colorimetric response values calculated as Colorimetric Response = $I_{max\ at\ 527\ nm}$/ $I_{at\ 550\ nm}$, i.e. spectral absorbance value obtained at 527 nm - the wavelength where AuNP coated with the peptide show maximum absorbance by itself (no antibodies are added)- divided by the absorbance at 550 nm, where a shift in absorbance is observed following the interaction of the antibody to the AuNP coated with the peptide.

The assay sensitivity in spiked serum was calculated as Colorimetric Response = $I_{max\ at\ 580nm}/I_{at\ 527\ nm}$, i.e. absorbance value obtained at 580 nm. This is the wavelength where a shift in absorbance is observed following the interaction of the antibody to the AuNP coated with the peptide in serum divided by the maximum absorbance value of AuNP coated with the peptide in serum.

5.4 Results and Discussion

The hexapeptide sequence QXQPFP (X being P, Q and L) within gliadin was previously identified as the dominant epitope for IgA and IgG antibodies against deamidated gliadin peptides (a-DGP) [Osman et al. 2000]. This sequence overlaps with residues 57-62 of native α-gliadin and has been shown to occur with high specificity in sera from CD individuals [Piaggio et al. 1999, Aleanzi et al. 2001]. The 17-mer peptide sequence (QLQPFPQPQLPYPQPQC) used as the antigen in this study is a small, 2 kDa molecular weight hexapeptide containing sequence.

In order to use peptide to coat AuNPs and to develop an assay for AGA, the potential problem of aggregation of the coated nanoparticles prior to adding the AGA in the test needed to be overcome.

To ensure the peptide coating on AuNPs, a long chain PEG linker containing Maleimide at the Ω-end and Biotin group at the α-end was used. Following the reaction of maleimide group with the thiol (-SH) side chain of the cysteine amino acid in the peptide sequence, the biotinylated and PEGylated peptide was added to the NeutrAvidin coated AuNPs.

The coating of the peptide sequence to the colloidal AuNP using the Biotin-$(PEG)_{11}$-Maleimide linker is represented in the schematic below (Figure 34).

A

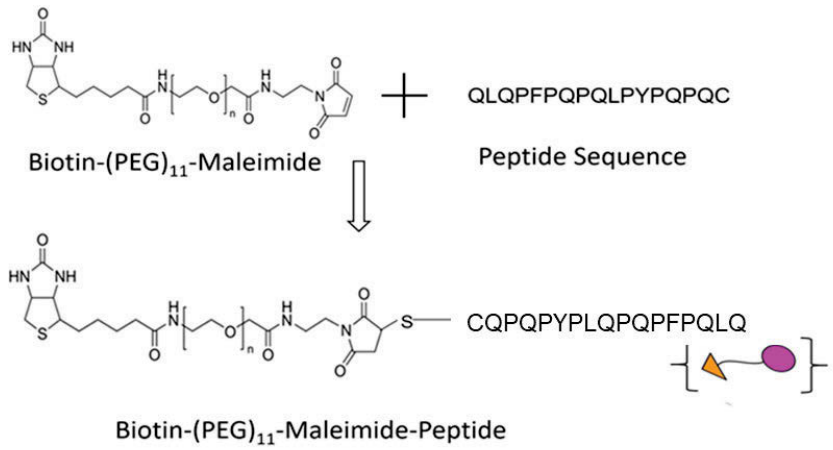

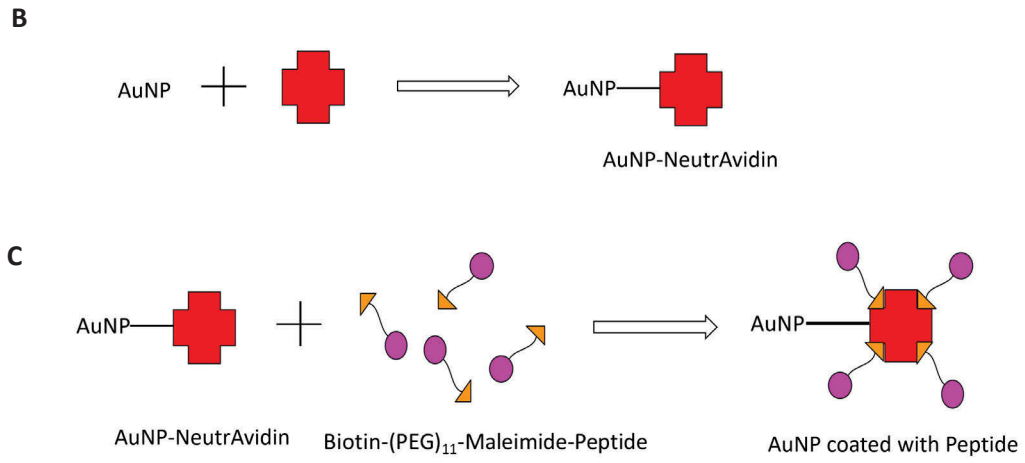

Figure 34: Schematic representation of preparation of peptide coated AuNPs. *(A) Maleimide groups of the linker reacted specifically with free (reduced) sulfhydryl's in the peptide sequence to form stable thio-ether bonds. (B) NeutrAvidin was coated on the surface of the AuNPs to obtain NeutrAvidin-AuNP particles. (C) The biotin end of the linker interacted with the NeutrAvidin-AuNPs resulting in the formation of peptide coated AuNPs.*

The coating of peptide onto the AuNPs surface was examined by UV-Vis measurements that are based on the observation of a change in the absorbance peak for the nanoparticle or a red-shift [Link and El-Sayed 1999]. It was observed that upon coating of the peptide onto the AuNPs, there was a shift in absorbance maximum from 525 nm to 527 nm (red-shift) (Figure 35). Also, any measurable decrease of absorbance at peak wavelength or increase of absorbance at long wavelengths (600-700 nm) was not observed. These results indicate that no strong AuNP-to-AuNP interactions took place after being coated with peptide and were stable in a dispersed colloidal state with minimal aggregation. In addition, a small peak at 210 nm was also observed following the binding of peptide to AuNPs, as indicated in previous studies on peptide coating [Slocik et al. 2011].

The absence of aggregation was confirmed using DLS, that showed an increase in hydrodynamic diameter from 20 nm to 28 nm following coating with peptide (Figure 35 B). The increase in hydrodynamic diameter is larger than that expected for a 2 kDa peptide and can be attributed to the larger molecular weight (68 kDa) NeutrAvidin that coated the AuNPs through the biotin-maleimide PEG linker. The hydrodynamic diameter of NeutrAvidin coated AuNPs is presented in Figure 36. Since the hydrodynamic radius in solution compares directly to the molar mass of the protein [Jans et al. 2009], in this case, being the peptide, NeutrAvidin as well as the linker, an increase in hydrodynamic radius to 28 nm can be correlated.

To directly observe the coating of peptide onto the surface of the AuNPs, high-resolution TEM imaging was used. The results showed the presence of a thin layer of material (< 1 nm) surrounding the nanoparticles (Figure 35 C (ii)), which was not observed on the surface of the uncoated nanoparticles (Figure 35 C (i)) [Jürgen's et al. 1999] that indicated peptide-linker-NeutrAvidin (peptide complex) coating. As the layer was very thin, peptide complex coated and uncoated AuNPs were incubated with AGA (12 µg/mL), wherein the peptide coated AuNPs aggregated (Figure 35 D (i, ii, iii) while uncoated AuNPs remained dispersed (Figure 35 D (iv, v, vi).

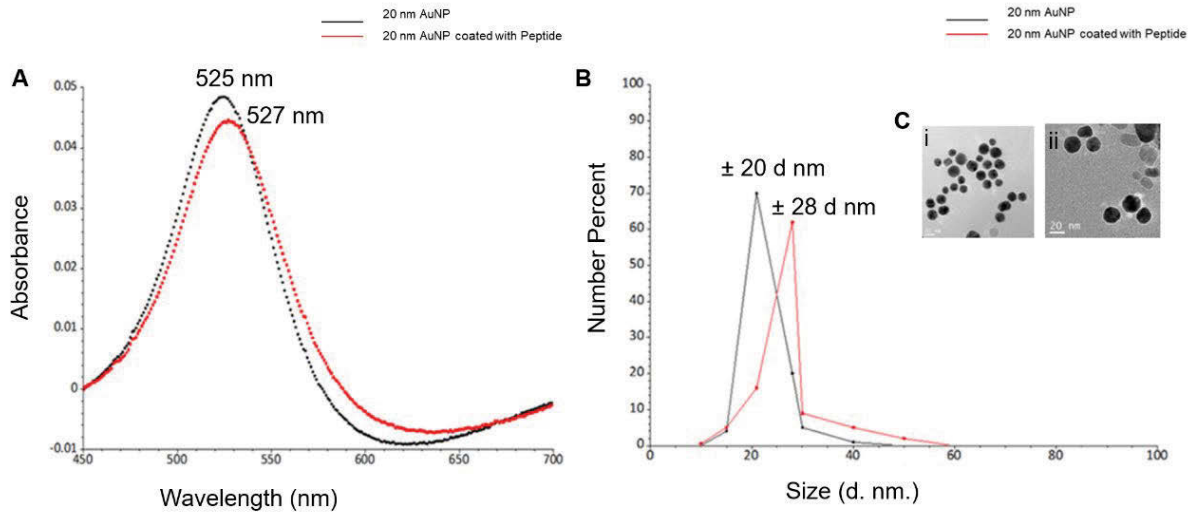

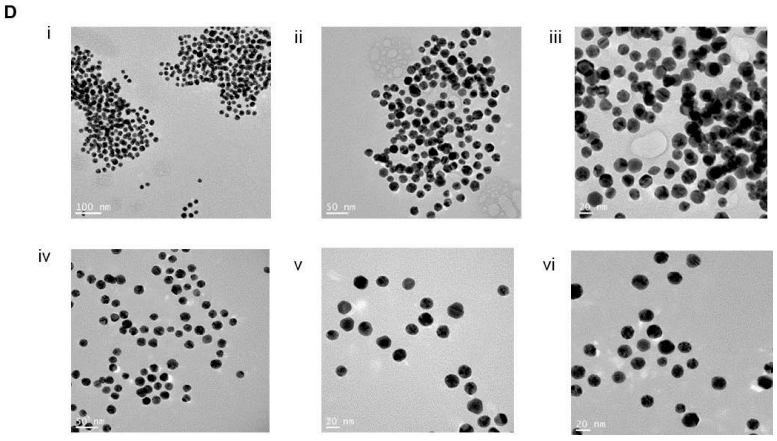

Figure 35: Characterisation of peptide coated AuNPs. *Characterisation of AuNP coated with peptide using a UV-Vis Spectrophotometer indicating a spectral red shift in wavelength from 525 nm (for 20 nm AuNP only) to 527 nm (for 20 nm AuNP coated with peptide). (B) Characterisation of AuNP coated with peptide using DLS that showed an increase in the hydrodynamic size of the uncoated vs coated particles from 20 nm to 28 nm respectively. (C) High resolution TEM images of (i) uncoated AuNPs, (ii) AuNPs coated with peptide showing a 'halo' layer surrounding the surface of the nanoparticles indicating coating of the gold with the peptide had occurred. In contrast, the 'halo' effect was not observed on the surface of the un-coated AuNPs. (D) High resolution TEM images following the incubation with AGA (12 µg/mL) (i, ii, iii) AuNPs coated with peptide showing aggregation confirming coating of peptide on AuNP (iv, v, vi) uncoated AuNPs remained dispersed.*

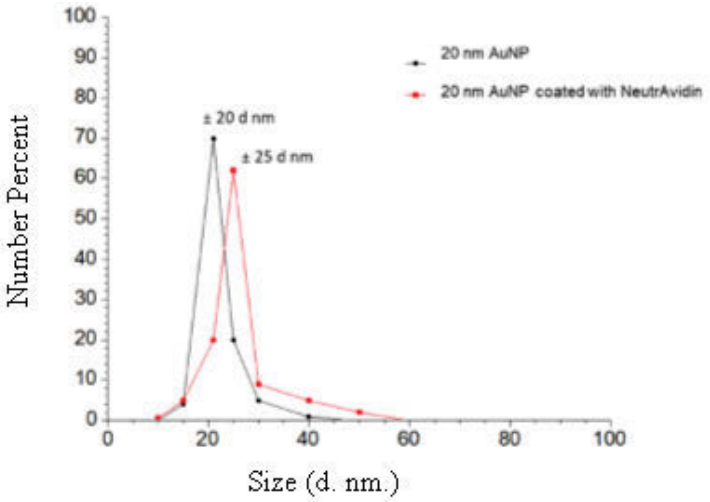

Figure 36: Characterisation of AuNP coated with NeutrAvidin using DLS that showed an increase in the hydrodynamic size of the uncoated vs coated particles from 20 nm to 25 nm respectively.

5.4.1 Incubation of Peptide-coated AuNPs with AGA

To assess the capability of peptide-coated AuNPs to detect AGA, serial dilutions of rabbit anti-gliadin IgG polyclonal antibody in a range that normally exists in human serum, was tested [O'Farrelly et al. 1983]. After 45 minutes incubation, a significant reduction in colour as well as a shift in absorbance from 527 nm to 550 nm was observed (Figure 37 A, B, Figure 38). The decrease in the absorbance peak indicated that in the presence of the AGA there was an increase in the intermolecular association of the peptide coated AuNPs. These inter-particle interactions caused aggregation, leading to precipitation and a drop-in absorbance.

To confirm the specificity of the interactions, normal IgG antibody with the peptide coated AuNPs as a control was tested, where it was observed that there is no significant reduction in colour or shift in the wavelength or aggregation of AuNPs. (Figure 37 A, B, Figure 39). At all the tested concentrations, the absorbance was significantly lower using AGA as compared to normal IgG ($p < 0.005$, Figure 37 B, Table 23).

These results obtained for the peptide coated AuNPs-AGA interaction are consistent with previous work, on the addition of specific analytes, such as metal ions, to citrate stabilised gold nanoparticles [Wang et al. 2008, Guo et al. 2011].

To confirm the sensitivity of the AGA toward peptide coated AuNPs, a colorimetric response for the assay was calculated (Figure 37 C). The colorimetric response reaches a maximum value at a concentration of 8 µg/mL of AGA meaning the highest sensitivity occurred at this concentration. This interaction of the peptide coated AuNPs with AGA resembles the precipitin reaction of antibody-antigen immune complexes. The near constant colorimetric response curve obtained for the control antibody as compared to the response curve obtained for AGA demonstrates the distinct sensitivity of the assay.

A

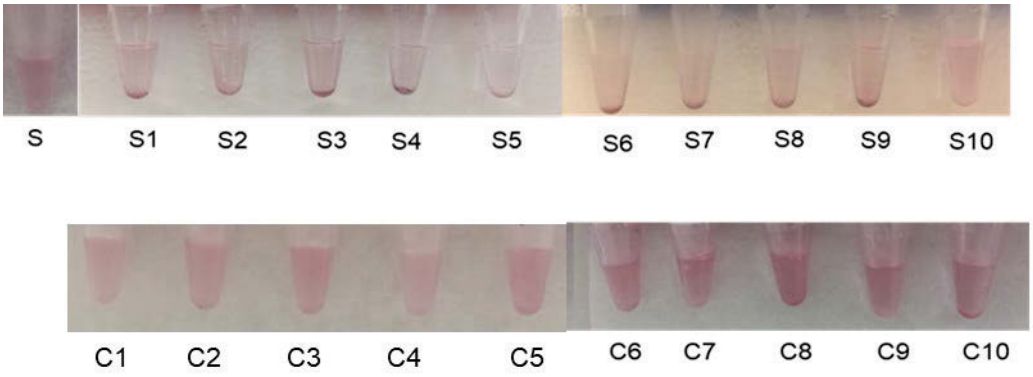

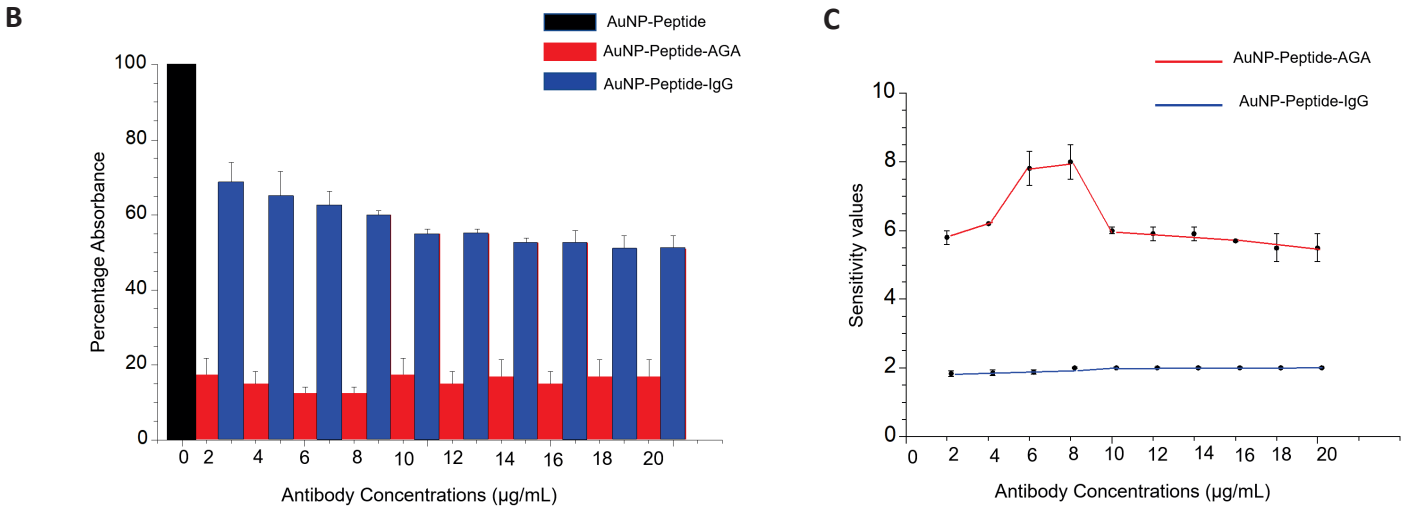

Figure 37: Testing peptide-coated AuNPs with AGA. *(A) Reduction in colour from red to translucent and absorbance was observed in the AuNP coated with peptide (S) and incubated with AGA at various dilutions (S1) 2 µg/mL, (S2) 4 µg/mL, (S3) 6 µg/mL, (S4) 8 µg/mL, (S5) 10 µg/mL), (S6) 12 µg/mL, (S7) 14 µg/mL, (S8) 16 µg/mL, (S9) 18 µg/mL and (S10) 20 µg/mL. No significant reduction in colour or shift in peak wavelength was observed in peptide coated AuNP incubated with control rabbit IgG at dilutions (C1) 2 µg/mL, (C2) 4 µg/mL, (C3) 6 µg/mL, (C4) 8 µg/mL, (C5) 10 µg/mL), (C6) 12 µg/mL, (C7) 14 µg/mL, (C8) 16 µg/mL, (C9) 18 µg/mL and (C10) 20 µg/mL. (B) Representation of specificity based on UV-Vis absorbance spectra for the antibody interactions at equal concentrations of AGA and control antibody (C) Colorimetric response curve plotted on AuNP coated with peptide following the addition of AGA at different dilutions.*

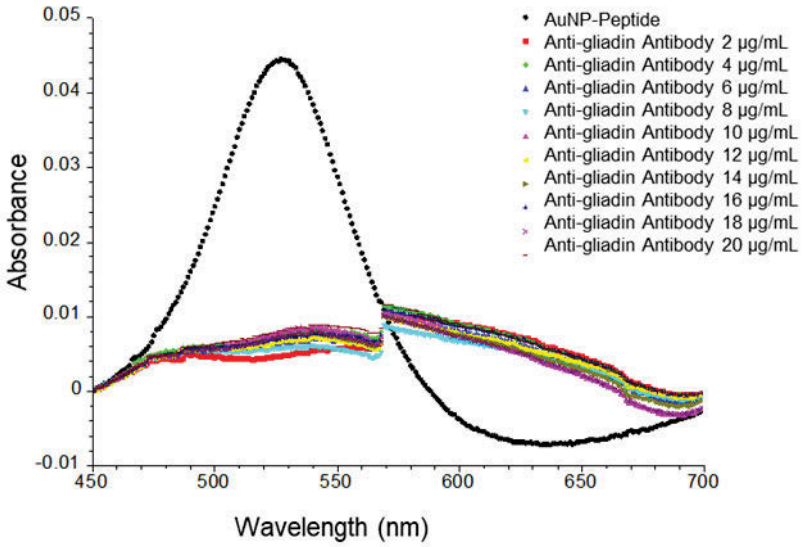

Figure 38: Incubation of AuNPs coated with peptide with AGA at various dilutions.

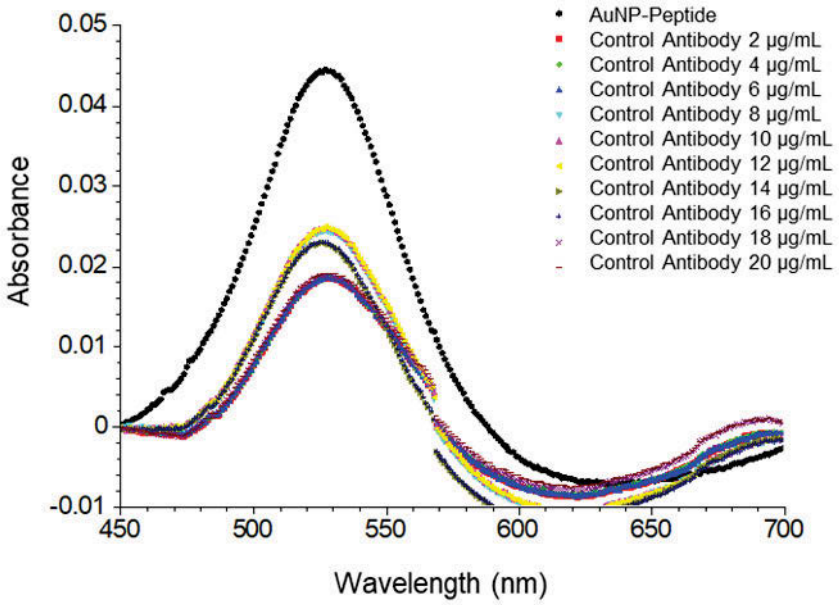

Figure 39: Incubation of AuNPs coated with peptide with control antibody at various dilutions.

Table 23: Shows the calculated p-value in AuNP coated with peptide in the presence of AGA antibody and the control antibody (IgG from rabbit serum) at dilutions 2-20 µg/mL.

Sample	Percentage Absorbance	t-test p-values
AuNP coated with Peptide	100.0	
Anti-gliadin antibody 2.0 µg/mL	17.5	0.0002
Control antibody 2.0 µg/mL	68.5	
Anti-gliadin antibody 4.0 µg/mL	15.0	0.0003
Control antibody 4.0 µg/mL	65.0	
Anti-gliadin antibody 6.0 µg/mL	12.5	0.0002
Control antibody 6.0 µg/mL	62.5	
Anti-gliadin antibody 8.0 µg/mL	12.5	0.0002
Control antibody 8.0 µg/mL	60.0	
Anti-gliadin antibody 10.0 µg/mL	17.5	0.001
Control antibody 10.0 µg/mL	55.0	
Anti-gliadin antibody 12.0 µg/mL	15.0	0.001
Control antibody 12.0 µg/mL	55.0	
Anti-gliadin antibody 14.0 µg/mL	17.0	0.002

Control antibody 14.0 µg/mL	52.5	
Anti-gliadin antibody 16.0 µg/mL	15.0	0.001
Control antibody 16.0 µg/mL	52.5	
Anti-gliadin antibody 18.0 µg/mL	17.0	0.0002
Control antibody 18.0 µg/mL	51.0	
Anti-gliadin antibody 20.0 µg/mL	17.0	0.0002
Control antibody 20.0 µg/mL	51.0	

5.4.2 Testing AGA in spiked serum

A variety of proteins, peptides as well as nucleic acids are constituents of human serum, making it a complex fluid. To reduce background binding, 1 µL of 20% BSA as a blocking agent was used, to lower the non-specific interaction with the peptide coated AuNPs. Spiked human serum containing 2-20 µg/mL AGA was incubated with the peptide coated AuNPs. The results showed an increase in aggregation and precipitation, which was easily detectable by eye, with a specificity up to a value of 2 µg/mL of AGA (Figure 40 A). A reduction in the colour of the solution from red to translucent was also observed. This change was supported by the increase in the colorimetric response reaching a maximum sensitivity at 8 µg/mL of AGA. The curve then begins to drop off at 10 µg/mL of AGA, however, it remains well above the control IgG level (Figure 40 B). In comparison, when normal rabbit IgG was added to the human serum, no precipitate formation or change in colour was observed. Normal serum itself did not show

any precipitate formation or change in absorbance with a constant response curve at all IgG concentrations.

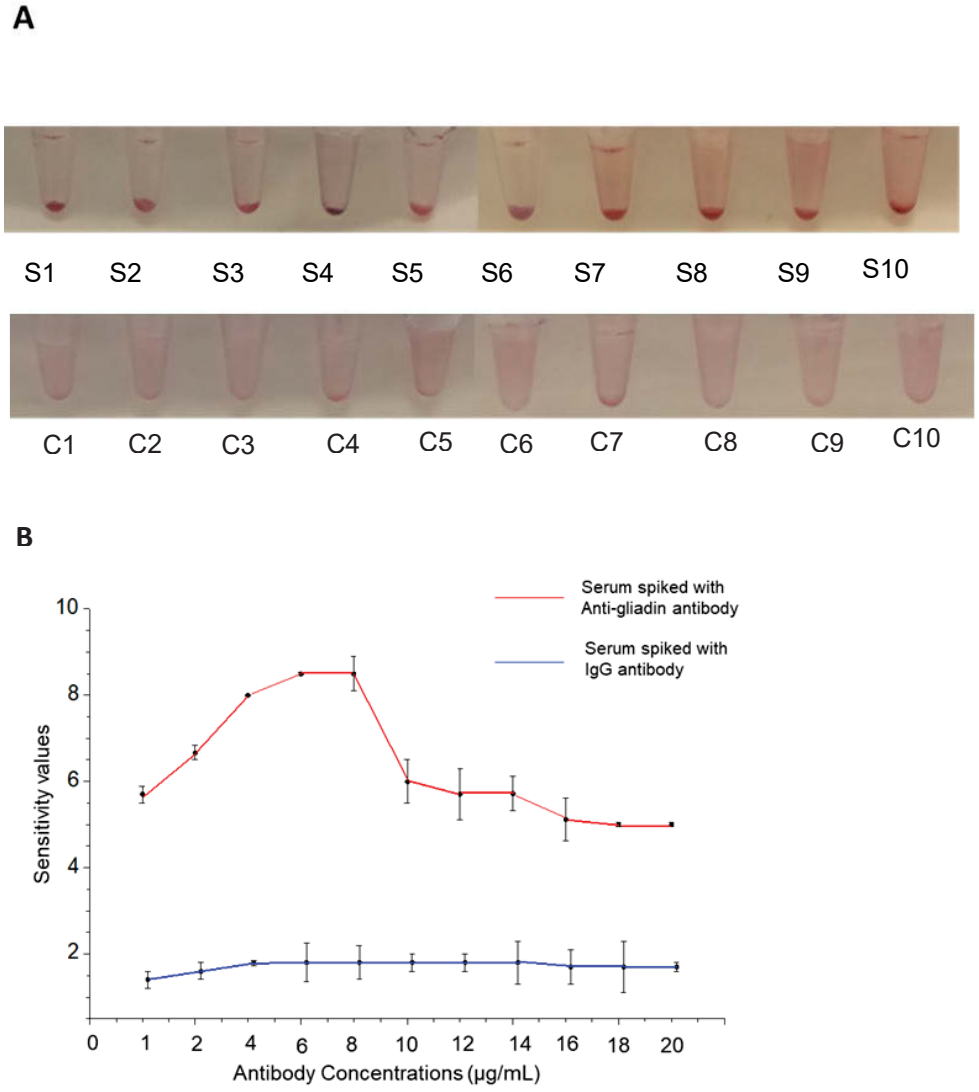

Figure 40: Detection of AGA in spiked human serum using the peptide-coated AuNPs.

(A) Reduction in colour from red to translucent as well as precipitate formation was observed in AuNP coated with peptide in the presence of AGA and serum at different concentrations (S1-S10). No reduction in colour from red to translucent or precipitate formation was observed in AuNP coated with peptide in the presence of control IgG and serum (C1-C10). (B) Colorimetric response curve plotted in AuNP coated with peptide in 1:20 diluted serum following the addition of AGA at different dilutions.

5.4.3 Testing clinical samples

Peptide-coated AuNPs were next tested in a selected set of human serum samples obtained from patients with CD or controls without CD. The main aim was to clearly distinguish the CD affected from the non-CD affected. To achieve that, serum was diluted with PBS, concentrated, purified and then allowed to react with AuNPs coated with peptide. This ensured that the range of the AGA in the sera fell in the peak sensitivity range (2-20 μg/mL).

The results for the 30 non-haemolytic, clinical samples were recorded after the visual examination of precipitate formation and determination of shift or change in absorbance values using a UV-Vis spectrophotometer. Based on the results observed by eye, the samples have been divided into three categories: clear precipitation, aggregation and colloidal suspension.

The assay sensitivity was determined based on the colorimetric response obtained for each serum sample and is calculated as Colorimetric Response = $I_{\text{max at 580 nm}}/I_{\text{at 527 nm}}$. Using this method, the calculated colorimetric response for normal serum (serum without AGA) is 1 and this acts as the cut-off value. Therefore, for the clinical samples, based on the spectral absorbance data, a value of ≤ 1 is indicated as negative for CD and a value above 1 is indicated as CD positive. Based on the observation and calculation of the colorimetric response curve, I have summarised the outcomes in Tables 24, 25 and Figure 41 along with the results reported using other serological methods, biopsy and histology.

Table 24. Comparison of the patient samples analysis using the AuNP-Peptide-AGA test with previously existing histology and serological* results

Volunteer	Histology	tTG-IgA	DGP-IgG	AuNP-Peptide-AGA Test
n.1	CD	1 (<4)	3 (<20)	CD Positive
n.2 ǂ	Non-CD	0.1 (0-6)	0.2 (0-6)	CD Positive
n.3	CD	>100 (<4)	33 (<20)	CD Positive
n.4	CD	121 (<20)		CD Positive
n.5	CD	>100 (<4)	>100 (<20)	CD Positive
n.6	CD	217 (<5)	>150 (<20)	CD Positive
n.7 ǂǂ	CD	13 (0-6)	23 (0-6)	CD Negative
n.8	CD	>100 (<5)	>100 (<20)	CD Positive
n.9	CD	11 (0-6)	1.4 (0-6)	CD Positive
n.10	CD	9 (<4)	97 (<20)	CD Positive
n.11	CD	18.2 (0<20)	3 (0.20)	CD Positive
n.12	CD	16 (0-20)	7 (<20)	CD Positive
n.13	Non-CD	4 (0-20)		Non-CD
n.14	CD	47 (<5)	86 (<5)	CD Positive
n.15 ǂǂ	CD	74 (0-20)		CD Negative
n.16	CD	145 (0-20)		CD Positive
n.17	CD	57 (<4)	93 (<20)	CD Positive
n.18	CD	149 (<20)	63 (<20)	CD Positive
n.19	CD	>100 (<4)	>100 (<20)	CD Positive

n.20 [ɪ]	Non-CD	3.8 (<6)	37 (<6)	CD Positive
n.21	Non-CD	<5 (<5)	<20 (<20)	Non-CD
n.22	CD	180 (0-6)	21 (0-6)	CD Positive
n.23	CD	20 (0-6)	8.1 (0-6)	CD Positive

* Serology tTG (Tissue transglutaminase), DGP (Deamidated gliadin peptides) results are indicated as IgA or IgG levels followed by normal reference ranges in brackets.

[ɪ] False positive based on histology and tTG antibody titre, [ɪɪ] False negative based on histology and tTG antibody titre

Table 25. Analysis of 7 samples with potential or undiagnosed CD using the Peptide-AuNP-AGA test as compared with previously existing serology*. Cases are separated into those showing histological observations of irregular/patchy mucosal lesions or those with mucosal inflammation resulting from an increase in $\gamma\delta^+$ IELs.

Volunteer	Histology	tTG-IgA	DGP-IgG	Peptide-AuNP-AGA
n.24	Mucosal lesions	5 (<20)	17 (<20)	CD Positive
n.25	Mucosal lesions	28 (0-6)	22 (0-6)	CD Positive
n.26	Mucosal lesions	4.8 (0-6)	22 (0-6)	CD Positive
n.27	Increased $\gamma\delta^+$ IELs	<5 (<5)	22 (<20)	CD Positive
n.28	Increased $\gamma\delta^+$ IELs	12 (0-6)	18 (0-6)	CD Positive
n.29	Increased $\gamma\delta^+$ IELs	11 (0-6)	13 (0-6)	CD Positive
n.30	Increased $\gamma\delta^+$ IELs	<5 (<5)	<20 (<20)	CD Positive

* Serology tTG (Tissue transglutaminase), DGP (Deamidated gliadin peptides) results are indicated as IgA or IgG levels followed by normal reference ranges in brackets.

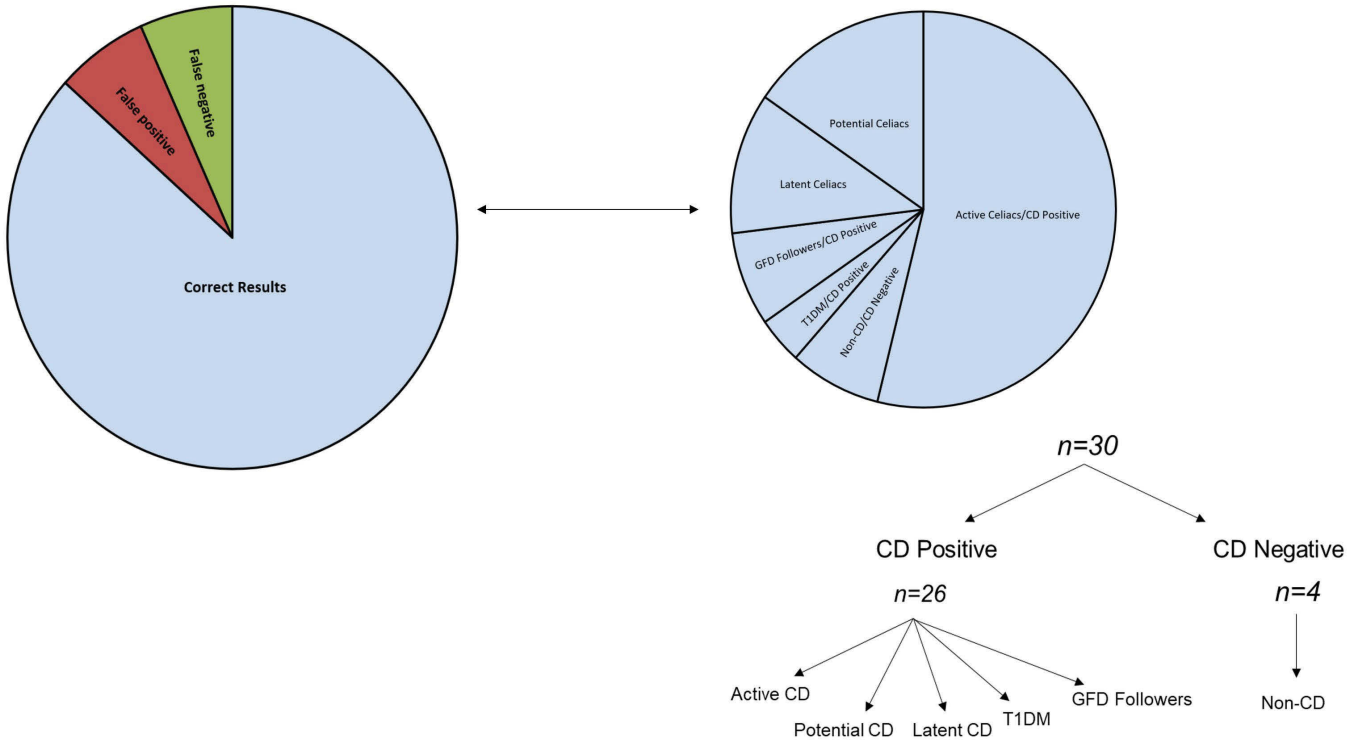

Figure 41: Representation of the distribution of clinical samples using AuNP-Peptide-AGA test

Out of these thirty samples, fourteen samples that were diagnosed with active CD with high antibody titres as shown by serology and intestinal damage as per biopsy were identified as CD positive using AuNP-Peptide-AGA assay as well (refer Table 24). These samples showed the formation of a precipitate and had a clear shift as well as drop in UV-Vis absorbance values as well as a high colorimetric response value. The remaining samples were then classified into various sub-classes based on the analysis using the AuNP-Peptide-AGA assay as described below (refer Tables 24 and 25, Figure 41).

The AuNP-Peptide-AGA assay could also correctly identify the patient suffering from another autoimmune disease, Type 1 Diabetes (T1DM), as positive for CD and this result matched with

the previously conducted biopsy and serology profile of the patient. In comparison, an existing commercially available point-of-care test, SimtomaX® blood drop (Augurix diagnostics) that uses a combination of three different peptides as the DGP antigens was found to be less specific in diagnosing CD in children suffering from T1DM [Bienvenu et al. 2012].

The elevated risks of patients with T1DM to develop CD arises because of multiple environmental and immunological factors and common genetic background [Volta et al. 2011]. The prevalence of CD in T1DM is reported high with a mean prevalence rate of 8% [Ventura et al. 2002] making regular monitoring of patients, particularly children with T1DM a necessity. AuNP-Peptide-AGA diagnostic assay shows improved specificity over the existing point-of-care test based on DGP. This test result shows immense potential of the assay in pre-selecting CD sufferers particularly those belonging to high-risk paediatric populations and, therefore, needs to be further explored in large clinical studies.

The cohort of tested samples included two cases where the patients had previously been diagnosed with CD and therefore followed a gluten free diet (GFD). While one person had been on a GFD for more than 8 weeks (volunteer number n.11), the other person had been on a GFD for less than 2 weeks (volunteer number n.12). While the conventional serology test identified these two patients as negative, the peptide-based assay obtained a positive for CD that is similar to the diagnosis based on mucosal biopsy.

A clear precipitate using the AuNP-Peptide-AGA assay was obtained for three samples (volunteer numbers n.24, n.25, n.26, Table 25) with patchy/ irregular mucosal lesions, classified as a broad sub-type of potential or undiagnosed coeliac. The UV-Vis absorbance data supported the visual examination. These three samples were classified as positive for CD as these may be undiagnosed coeliac sufferers that initially, display mild mucosal atrophy that

then develops to typical atrophy of small intestine mucosa along with a presentation of positive CD serology [Kaukinen et al. 2001].

Aggregation of nanoparticles along with a drop in UV-Vis absorbance values was demonstrated by four clinical samples (volunteer numbers n.27, n.28, n.29, n.30, Table 25). These samples had positive or low positive serology along with mucosal inflammation. The AuNP-Peptide-AGA assay showed results similar to those found using the existing serological assays. These four cases have been identified as 'potential' CD positives, a subtype of CD that displays a normal villous architecture but also shows clinical symptoms, such as increased $\gamma\delta^+$ intraepithelial lymphocytes along with the presence of gliadin specific antibodies, that are mostly at low titres (<1:40) [Volta et al. 2011]. Potential CD cases are often difficult to diagnose by histology and has a lowered predictive value in recognising such cases. Correct diagnosis for potential CD cases therefore necessitates an evaluation of both serological markers as well as pathological symptoms.

The cohort included four samples identified as negative for CD based on biopsy and existing serology tests (volunteer numbers n.2, n.13, n.20 and n.21, Table 24). Out of the four samples, two samples were correctly identified as CD negative by AuNP-Peptide-AGA assay while the other two samples showed the formation of aggregates and were identified as positive (volunteer numbers n.2 and n.20). As intestinal biopsy has been used as the gold standard for CD confirmation, these two samples have been referred to as a false positive.

Overall, upon comparing the results for the 30 clinical samples, while 26 samples showed comparable results with existing serology and histology, 2 false positive results and 2 false negative results were obtained using the AuNP-Peptide-AGA assay giving the AuNP-Peptide-AGA assay an overall accuracy of 86.6%.

5.5 Conclusions

CD is induced by the protein gliadin, present in wheat and some other cereals causing damage to the small intestine. In the present study, it was demonstrated that a peptide derived from gliadin in conjunction with AuNPs can be used as an efficient tool to detect a biomarker for CD from serum. This was achieved by developing a methodology to coat the small antigenic peptide on the surface of AuNPs without causing aggregation. A colour change and absorbance peak shift caused by the aggregation of AuNPs was observed following the addition of AGA to peptide coated AuNPs at levels associated with CD. The developed assay was confirmed to detect AGA not only in quantitatively spiked samples but also in a small-scale study on real non-haemolytic CD patients' samples.

The present study shows that this novel peptide functionalised AuNP based assay is useful for pre-selecting CD diseases particularly in high-risk paediatric populations that can be then confirmed by mucosal biopsy. The assay format has potential to be adapted as point-of-care test that would be useful in an exclusion diagnostic strategy as positive result would strengthen the possibility of CD that can be confirmed using intestinal biopsy.

CHAPTER VI

Conclusions

Gluten, a protein present in wheat and some other cereals such as rye and barley triggers CD, a chronic disorder that damages the small intestine. Of the two major groups that comprise gluten, namely gliadin and glutenin; gliadin plays the key role in inducing CD. The gliadin epitopes are recognised by the T cells that then activate the innate immune response by stimulating the release of $CD4^+$ T cells, CD8 T cells and natural killer (NK) cells. This leads to the release of pro-inflammatory cytokines and in turn damages the small intestine. The stimulation of $CD4^+$ T cells leads to lymphocyte B cell differentiation into plasma cells that causes the release and formation of specific anti-gliadin antibodies that are considered as the serological biomarker for CD.

The sensitivity of anti-gliadin antibodies for diagnosis for CD was based on the observed reduction in the titre levels of anti-gliadin antibody in a person diagnosed with CD who had been following a gluten free diet (Tucker et al. 1988). It was proposed that on a gluten containing diet, the IgA containing cells in the jejunum increased that in turn lead to an increase in circulating IgA. The circulating IgA anti-gliadin antibodies significantly decreased on compliance of a gluten free diet. The sensitivity values for anti-gliadin antibodies was confirmed using the ELISA assay (Rujner et al. 1996).

The current testing methods include mucosal biopsy, genetic testing of MHC Class II HLA DQ2/DQ8 alleles and serological testing that includes Anti-gliadin antibody (AGA), IgA endomysium antibody (EMA-IgA), IgA tissue transglutaminase antibody (tTG-IgA) and deamidated gliadin peptide (DGP). The analysis for these serological tests makes use of techniques such as ELISA, radioimmunoassay and fluorescent microscopy.

The review of the literature indicates that in spite of the reasonable results in terms of sensitivity and specificity of the existing tests, when applied on large public screenings, these

immunological assays even when combined with genetic testing, have a lowered predictive value for disease diagnosis. In addition, the challenges in developing a cheap and reliable diagnostic test for CD have been highlighted. Even the gold-standard mucosal biopsy has been found to have difficulties when testing in some individuals. There is an immediate need for an easy to use, cost effective, accurate and sensitive diagnostic assay for detecting CD.

Application of gold nanoparticles as sensors to help in the detection of biomarkers specific for CD is one novel method to aid early disease diagnosis. The concept of using gold–protein conjugates has previously found wide applicability as a colorimetric probe and has been used for analysing DNA, RNA, peptides, pregnancy testing in humans and detection of GLUT 1 in diabetic rats. A multidisciplinary research effort in immunology, molecular biology and nanotechnology may lead to pivotal discoveries in CD genetics, immunology and diagnostics that will ultimately solve this problem of diagnosis for CD. A promising new approach for CD detection was evaluated in this project using gold nanoparticles as the biosensor and gliadin as well as a peptide sequence derived from gliadin as the antigen. The CD detection is based on using the interaction of anti-gliadin antibody expressed in body fluids such as serum and protein gliadin as well as peptide sequence coated to gold nanoparticles. The test assay was validated on human serum sample cohort to determine the accuracy of the developed test methods.

6.1 CD diagnostic assay using gliadin and peptide coated AuNPs

AuNPs were successfully coated with gliadin as well as the peptide and were used to develop an efficient diagnostic test to detect CD specific biomarker, anti-gliadin antibody, from serum. To achieve a stable colloidal suspension of gliadin coated AuNPs, a novel methodology to solubilise and coat gliadin on AuNPs was developed. The gliadin coated gold nanoparticles

were characterised using UV-vis spectra, Dynamic Light Scattering (DLS) and Transmission Electron Microscopy (TEM). The peptide sequence was successfully coated to the AuNP and characterisation methods indicated that a stable colloidal suspension of the peptide coated AuNPs was achieved that was sustained by the high affinity biotin-avidin interactions. The UV-vis absorbance readings of gliadin/peptide coated AuNPs following interactions with AGA and IgG from rabbit serum (control antibody) were used to calculate the percentage absorbance values. The students t-test was used to compare the sets of quantitative data that were collected independently of one another to calculate the p value and determine statistical significance. The assay sensitivity was determined based on the colorimetric response values.

BSA is a water-soluble monomeric protein and was used as a control protein in the study. Adsorption of BSA on the AuNP took place due to electrostatic interactions as well as hydrogen bonding, hydrophobic and Van der Waal's interactions. The presence of a free thiol group on the external surface of BSA with the AuNP surface also support BSA conjugation to the AuNP surface [Shang et al. 2007]. In addition, BSA also showed an increased hydrodynamic diameter of BSA when coated to AuNPs as compared to gliadin adsorbed AuNPs. This can be attributed to the complete solubility that BSA shows in aqueous solution in addition to having a higher molecular weight as compared to gliadin, which is a hydrophobic protein with a much lower molecular weight. Subsequently, in the presence of water, while gliadin develops a tighter conformation with its amino acids directed towards the core, BSA shows a relaxed conformation. This results in a higher increase in the hydrodynamic diameter for AuNPs coated with BSA.

The absorbance spectra following the addition of an affinity purified, polyclonal anti-gliadin antibody raised in rabbit to AuNPs coated to gliadin as well as peptide was observed using the UV-Vis absorbance spectroscopy. Upon addition of anti-gliadin antibody there was a broadening of the SPR band as well as a reduction in colour from red to translucent with

precipitation. The decrease in absorbance was accompanied by a red shift; the wavelength of light increased, and it shifted to the red end of the spectrum. The interactions between the gliadin/peptide coated AuNPs were assisted by the flexible arms of the IgG antibody which shows a Y-shape structure, and each of the antibody arms can bind to two individual nanoparticles at a given time. This lead to a decrease in the inter-particle distance between the nanoparticles and facilitated their interaction. Similar results as observed for the AuNP-gliadin – anti-gliadin interaction were obtained with previous work by Lee et al. [2008] who studied the changes in the stability ratio of gold nanoparticle aggregates after the addition of benzyl mercaptan. The presence of benzyl mercaptan, lead to aggregation of gold nanoparticles that caused a decrease in the intensity and a red shift in the characteristic surface plasmon band at 520 nm. In comparison, when the gliadin/peptide coated AuNPs were spiked with a non-specific antibody, rabbit serum IgG antibody, no significant change in colour or shift in the wavelength or size of the absorbance peak was observed.

The clinical accuracy of the gliadin coated AuNPs was determined using a selected, varied set of thirty human serum samples obtained from patients with CD or controls without CD. The results for the thirty clinical samples were recorded after the visual examination of precipitate formation and the determination of a shift or change in absorbance values using a UV-Vis spectrophotometer. The assay sensitivity was determined based on the colorimetric response values obtained for each serum sample.

Following testing and analysis, an overall accuracy of 96% was obtained using the AuNP-gliadin-AGA assay, while when using the AuNP-Peptide-AGA assay an overall accuracy of 86.6% was obtained. This level of accuracy is in the range required for a serological test and is similar to the accuracy levels of the existing serological assay. On comparing the AuNP-Peptide assay with the AuNP-gliadin assay, the gliadin-based assay seems to be more sensitive. However, both the approaches seem promising for development as a point-of-care test. This is

because both approaches are based on the formation of a precipitate as well as a reduction in colour for a positive sample in the presence of a CD specific auto-antibody, thereby, eliminating the need for secondary antibody. One-step detection would be particularly useful in aiding large-scale screening of the general population, particularly in the pre-selection of young CD sufferers which can be then confirmed by mucosal biopsy. A positive result would strengthen the possibility of CD while a negative test would help avoid unnecessary intestinal biopsy thereby reducing the economic burden on healthcare resources resulting in cost savings.

6.2 Summary and Future Work

In the present study, I have demonstrated the potential of the highly antigenic protein gliadin coated AuNPs for detecting a biomarker for CD from serum. Results obtained have demonstrated that following the addition of the biomarker, anti-gliadin antibody to gliadin coated AuNPs at levels associated with CD, resulted in colour reduction from pink to translucent and absorbance peak shifted due to the aggregation of AuNPs.

The difference in the accuracy levels for the gliadin based AuNP assay as compared to the peptide-based assay, might be because an auto-antibody- anti-gliadin antibody, is detected in the assay. The auto-antibodies differ from synthesised antibodies in that they can recognise multiple epitopes as well as structural diversities. As a result, anti-gliadin antibody can recognise not only the critical epitope portions of the antigen that are composed of backbone atoms but side-chain carbons such as those made from aromatic amino acids [Peng et al. 2014], leading to increased specificity with gliadin. In addition, gliadin solubilisation using the solvents might have played a driving factor in forming direct hydrogen bonding across paratope-epitope interactions, thereby involving four-fifth of surface atoms and improving the AuNP-gliadin interactions with anti-gliadin antibody.

The results obtained in this work, demonstrate the great potential of the AuNP based approach to be developed as a CD detection test and can have a huge market as it has been reported that the CD shows 'iceberg characteristics' i.e. there are far greater number of undiagnosed cases than the diagnosed cases. This project is a stepping stone in the development of a diagnostic device for CD detection using functionalised AuNPs. The findings produced here show promising potential for future research in an effort to meet the need to develop easier and pain free coeliac detection methods.

The existing criteria for diagnosis for CD require four components of testing, including serological testing of two auto-antibodies namely tTG and anti-EMA along with genetic testing for HLA DQ2/8 genes followed by biopsy. The existing serological tests face the problem of inter-observer variability as significant differences exist among the serological tests particularly with regard to assay methodology and interpretation, the ELISA based assays are however more objective as compared to immunofluorescence methods. This limits the potential of the existing tests for development as a point-of -care test. On the other hand, the AuNP based assay developed in this study demonstrates great potential to be developed as a point-of-care test that would be useful in an exclusion based diagnostic strategy as well as for monitoring gluten free treatment.

After developing the serum based AuNP assay, the next step would be to validate the assay in real patient saliva samples. Disease detection based on saliva analysis is currently being used for a number of infectious and malignant diseases, hereditary disorders, autoimmune diseases and endocrine disorders as well as the evaluation of therapeutic drug levels. The analysis of these disorders and diseases is based on ELISA, polymerase chain reaction (PCR) methodology or its advancements such as multiplex PCR. The method studied here brings together the specificity of the antibody and the physical properties of gold nanoparticles. Such an assay would be particularly useful for investigating CD in young children as it is a non-invasive and

pain free method for CD detection. In this direction, I have already obtained promising results using spiked saliva samples wherein anti-gliadin IgG antibody was added at concentrations represented in CD sufferers to the saliva. Normal saliva meaning the saliva of a person not suffering from CD was used as a control. A shift of the absorbance peak to a lower absorbance level was observed following the addition of saliva containing anti-gliadin antibodies to gliadin coated AuNPs. The decrease in absorbance suggested strong AuNP-AuNP interactions in the presence of anti-gliadin antibody in saliva. As the saliva was diluted prior to testing, other proteins and constituents of saliva do not seem to disrupt the interactions. Visual examination of the tubes also indicated aggregation of the particles. These results are consistent with those obtained for the AuNP-gliadin-anti-gliadin interactions that took place in spiked serum. Further optimisation of the test method is being carried out to improve assay sensitivity, this would involve coating of gliadin to different sized nanoparticles such as the smaller sized 10 nm AuNPs. Following optimisation, the next step would be assay validation of the AuNP-saliva based assay using saliva from patients with CD as well as from non-CD individuals. The saliva sample cohort would be assembled from a varied, diverse set of individuals to enable a non-biased study.

Following testing of real saliva samples and validation of the results, the next step would be to develop a prototype of the point-of-care device to allow for testing for CD in clinics. The design prototype of the device is presented below. Saliva would be collected at the top end of the device, and would flow towards the gliadin coated gold nanoparticles, indicated by red colour. A positive test would be indicated by a colour change or precipitation that would be observable by naked eye. A negative test would however, remain red with no observable precipitation.

Prototype design: Proposed design of prototype for testing CD using saliva.

As compared to the current methodologies in use, mainly, blood-based testing; the saliva-based test would be non-invasive, have a quicker result turnaround, and has lower manufacturing costs with a greater potential for use as a take home test. Such a test would be particularly useful for testing individuals and would be a first in the direction of pain-free testing for CD.

Bibliography

Ludvigsson, J.F., Leffler, D.A., Bai, J.C., Biagi, F., Fasano, A., Green, P.H.R., Hadjivassiliou, M., Kaukinen, K., Kelly, C.P., Leonard, J.N., Aslaksen, L., Murray, J.A., Sanders, D.S., Walker, M.M., Zingone, F. & Ciacci, C. 2013, 'The Oslo definitions for celiac disease and related terms'. Gut, vol. 62, pp. 43-52.

Lionetti, E., Gatti, S., Pulvirenti, A. & Catassi, C. 2015, 'Celiac disease from a global perspective', Best Pract Res Clin Gastroenterol vol. 29, pp. 365-379.

Oliveira, R.P., Sdepanian, V.L., Barreto, J.A., Cortez, A.J.P., Carvalho, F.O., Bordin, J.O., de Camargo, S., Maria, A. da Silva P., Francy, R., Kawakami, E., de Morais, M.B. & Fagundes-Neto, U. 2007, 'High prevalence of celiac disease in Brazilian blood donor volunteers based on screening by IgA antitissue transglutaminase antibody', Eur J Gastroenterol Hepatol, vol. 19, pp. 43-49.

Gomez, J.C., Selvaggio, G.S., Viola., M., Pizarro, B., la Motta, G., de Barrio, S., Castelletto, R., Echeverrı´a, R., Sugai, E., Vazquez, H., Maurin˜o, E., & Bai, J.C. 2001, 'Prevalence of celiac disease in Argentina: screening of an adult population in the La Plata area', Am J Gastroenterol, vol. 96, pp. 2700-2704.

Hovell, C.J., Collett, J.A., Vautier, G. Cheng, A.J., Sutanto, E., Mallon, D.F., Olynyk, J.K. & Cullen, D.J. 2001, 'High prevalence of celiac disease in a population-based study from Western Australia: a case for screening'?, Med J Aust, vol. 175, pp. 247-250.

Sood, A., Midha, V., Sood, N., Kaushal, V. & Puri, H. 2001, 'Increasing incidence of celiac disease in India', Am J Gastroenetrol, vol. 96, pp. 2804-2805.

Ramakrishna, B.S., Makharia, G.K., Chetri, K., Dutta, S., Mathur, P., Ahuja, V., Amarchand, R., Balamurugan, R., Chowdhury, S.D., Daniel, D., Das, A., George, G., Gupta, S.D., Krishnan, A., Prasad, J.H., Kaur, G., Pugazhendhi, S., Pulimood, A., Ramakrishna, K. & Verma, A.K. 2016, 'Prevalence of Adult Celiac Disease in India: Regional Variations and Associations', Am J Gastroenetrol, vol. 111(1), pp. 115-123.

Kang, J.Y., Kang, A.H.Y., Green, A. & Ho, K.Y. 2013, 'Systematic review: worldwide variation in the frequency of celiac disease and changes over time', Aliment Pharmacol Ther, vol. 38, pp. 226-245.

Lohi, S., Mustalahti, K., Kaukinen, K., Laurila, K., Collin, P., Rissanen, H., Lohi, O., Bravi, E., Gasparin, M., Reunanen, A., & Maki, M. 2007, 'Increasing prevalence of celiac disease over time', Ailment Pharmacol Ther, vol. 26, pp. 1217-1225.

Kivela, L., Kaukinen, K., Lahdeaho, M-L., Huhtala, H., Ashorn, M., Ruuska, T., Hiltunen, P., Visakorpi, J., Maki, M., & Kurppa, K. 2015, 'Presentation of Celiac Disease in Finnish Children Is No Longer Changing: A 50-Year Perspective', J Pediatr, vol. 167, pp. 1109-1115.

Rautava, S., Ruuskanen, O., Ouwehand, A., Salminen, S., & Isolauri, E. 2004, 'The hygiene hypothesis of atopic disease-an extended version', J Pediatr Gastroenterol Nutr, vol. 38, pp. 378-88.

Khoo, U.Y., Proctor, I.E. & MacPherson, A.J. 1997, 'CD^{4+} T cell down regulation in human intestinal mucosa: evidence for intestinal tolerance to luminal bacterial antigens', J Immunol vol. 158, pp. 3626-3634.

Canova, C., Zabeo, V., Pitter, G., Romor, P., Baldovin, T., Zanotti, R. & Simonato, L. 2014, 'Association of maternal education, early infections, and antibiotic use with celiac disease: a population-based birth cohort study in northeastern Italy', Am J Epidemiol, vol. 180, pp. 76–85

Stene, L.C., Honeyman, M.C., Hoffenberg, E.J., Haas, J.E., Sokol, R.J., Emery, L., Taki, I., Norris, J.M., Erlich, H.A., Eisenbarth, G.S. & Rewers M. 2006, 'Rotavirus infection frequency and risk of celiac disease autoimmunity in early childhood: a longitudinal study', Am J Gastroenterol, vol. 101, pp. 2333–2340.

Riddle, M.S., Murray, J.A., Cash, B.D., Pimentel, M. & Porter, C.K. 2013, 'Pathogen-specific risk of celiac disease following bacterial causes of foodborne illness: a retrospective cohort study,' Dig Dis Sci, vol. 58, pp. 3242–3245.

Kemppainen, K.M., Lynch, K.F., Liu, E., Lönnrot, M., Simell, V., Briese, T., Koletzko, S., Hagopian, W., Rewers, M., She, J-X., Simell, O., Toppari, J., Ziegler, A-G., Akolkar, B., Krischer, J.P., Lernmark, Å, Hyöty, H., Triplett, E.W. & Agardh, D. for the TEDDY Study Group. 2017, 'Factors that increase risk of celiac disease autoimmunity after a gastrointestinal infection in early life', Clin Gastroenterol Hepatol, vol. 15, pp. 694–702.

Rubio-Tapia, A., Ludvigsson, J.F., Brantner, T.L., Murray, J.A. & Everhart, J.E. 2012, 'The prevalence of celiac disease in the United States', Am J Gastroenetrol, vol. 107, pp. 1538-1544.

Lionetti, E. & Catassi, C. 2011, 'New clues in celiac disease epidemiology, pathogenesis, clinical manifestations, and treatment', Int Rev Immunol, vol. 30, pp. 219-231.

Catassi, C. & Fasano, A. 2014, 'The new epidemiology of celiac diease', J Pediatr Gastroenterol Nutr, vol. 59(Suppl.1), pp. S7-9.

Catassi, C., Anderson, R.P, Hill, I.D., Koletzko, S., Lionetti, E., Mouane, N., Schumann, M. & Yachcha, S.K. 2012, 'World perspective on celiac disease', J Pediatr Gastroenterol Nutr, vol. 55, pp. 494-499.

Oberhuber, G., Granditsch, G., & Vogelsang, H. 1999, 'The histopathology of celiac disease: time for a standardised report scheme for pathologists', Eur J Gastroentrology, vol. 11, pp. 1185-1194.

Marsh, M.N., Vincenzo, V & Srivastava, A. 2015, 'Histology of gluten related disorders', Gastroenterol Hepatol Bed Bench, vol. 8, pp. 171-177.

Mohamed, B.M., Feighery, C., Coates, C., O'Shea, U., Delaney, D., O'Brian, S., Kelly, J. & Abuzakouk, M. 2008, 'The absence of a mucosal lesion on standard histological examination does not exclude diagnosis of celiac disease', Dig Dis Sci, vol. 53, pp. 52-61.

Corazza, G.R., Villanacci, V., Zambelli, C., Milione, M., Luinetti, O., Vindigni, C.C., Albarello, L., Bartolini, D. & Donato, F. 2007, 'Comparison of the interobserver reproducibility with different histologic criteria used in celiac disease', Clin Gastroenterol Hepatol, vol. 5, pp. 838-843.

Corazza, G.R. & Villanacci, V. 2005, 'Coeliac disease', J Clin Pathol, vol. 58, pp. 573-574.

Lebwohl, B., Sanders, D.S. & Green, P.H.R. 2018, 'Coeliac Disease', Lancet, vol. 391, pp. 70–81.

Hadjivassiliou, M., Sanders, D.S., Woodroofe, N. Williamson, C. & Grünewald R.A. 2008, 'Gluten ataxia', Cerebellum (2008) 7: 494.

Tonutti, E. & Bizzaro, N. 2014, 'Diagnosis and classification of celiac disease and gluten sensitivity', Autoimmun Rev, doi:10.1016/j.autrev.2014.01.043.

Auricchio, S., Mazzacca, G., Tosi, R. & Deritis, G. 1988, 'Coeliac disease as a familial condition: identification of asymptomatic coeliac patients within family groups', Gastroenterol Int, vol. 1, pp. 25.

Ferguson, A., Arranz, E. & O'Mahony, S. 1993, 'Clinical and pathological spectrum of coeliac disease-active, silent, latent, potential', Gut, vol. 34, pp. 150-151.

Weinstein, W.M. 1974, 'Latent celiac sprue', Gastroenterology, vol. 66, pp. 489-493.

Freeman, H.J. 2008, 'Refractory celiac disease and sprue-like intestinal disease', World J Gastroenterol, vol. 14, pp. 828-830.

Freeman, H.J. 2010, 'Risk factors in familial forms of celiac disease', World J Gastroenterol, vol. 16, pp. 1828-1831.

Woychik, J.H., Boundy, J.A. & Dimler, R.J. 1961, 'Starch gel-electrophoresis of wheat gluten proteins with concentrated urea', Arch Biochem Biophys, vol. 94, pp. 477-482.

Bushuk, W. & Zillman, R.R. 1978, 'Wheat cultivar identification by gliadin electrophoregrams: 1. Apparatus, method, and nomenclature', Can J Plant Sci, vol. 58, pp. 505-515.

Metakovsky, E.V., Branlard, G., Chernakov, V.M.R. Upelneik, V.P. & Redaelli, R. & Pogna, N.E. 1997, 'Recombinant mapping of some chromosome 1A-, 1B-, 1D-, and 6B-controlled gliadins and low molecular weight glutenin subunits in common wheat', Theor Appl Genet, vol. 94, pp. 788-795.

Anderson, O.D., Dong, L., Huo, N. & Gu, Y.Q. 2012, 'A New Class of Wheat Gliadin Genes and Proteins', Plos One, vol. 7, pp. 12.

Kasarda, D.D., Okita, T.W., Bernardin, J.E., Baecker, P.A., Nimmo, C.C., Lew, E.J., Dietler, M.D. & Greene, F.C. 1984, 'Nucleic acid (cDNA) and amino acid sequences of α-type gliadins from wheat (*Triticum aestivum*)', Proc Natl Acad Sci, vol. 81, pp. 4712-4716.

Anderson, O.D. & Greene, F.C. 1997, 'The α-gliadin gene family. DNA and protein sequence variation, subfamily structure, and origins of pseudogenes', Theor Appl Genet, vol. 95, pp. 59-65.

Noma, S., Kawaura, K., Hayakawa, K., Abe, C., Tsuge, N. & Ogihara, Y. 2016, 'Comprehensive molecular characterization of the α/β gliadin multigene family in hexaploid wheat', Mol Genet Genomics, vol. 291, pp. 65-77.

Camarca, A., Anderson, R.P., Mamone, G., Fierro, O., Facchiano, A., Costantini, S., Zanzi, D., Sidney, J., Auricchio, S., Setta, A., Troncone, R. & Gianfrani, C. 2009, 'Intestinal T cell responses to gluten peptides are largely heterogenous: implications for a peptide-based therapy in celiac disease', J Immunol, vol. 182, pp. 4158-4166.

Qi, P.F., Wei, Y.M., Ouellet, T., Chen, Q., Tan, X., & Zheng, Y.L. 2009, 'The γ-gliadin multigene family in common wheat (*Triticum aestivum*) and its closely related species', BMC Genomics, vol. 10, pp. 168.

Vader, L.W., Kooy, Y., Van Veelan, P. L., De Ru A, Harris, D., Benckhuijsen, W., Pen, S., Mearin, M.L., Drijfhout, J.W. & Koning, F. 2002, 'The gluten response in children with celiac disease is directed toward multiple gliadin and glutenin peptides', Gastroenterology, vol. 122, pp. 1729-3177.

Kruppa, K. 2012, 'Endomysial antibodies predict celiac disease irrespective of the titers or clinical presentation', World J Gastroenterol, vol. 18, pp. 2511-2516.

Kagnoff, M.F. 2002, 'Coeliac disease pathogenesis: the plot thickens', Gastroenterology, vol. 123, pp. 939–943.

Fasano, A. 2011, 'Zonulin and its regulation of intestinal barrier function: The biological door to inflammation, autoimmunity, and cancer', Physiol Rev, vol. 91, pp. 151-175.

Lammers, K.M., Lu, R., Brownley, J., Lu, B., Gerard, C., Thomas, K., Rallabhandi, P., Shea-Donohue, T., Tamiz, A., Alkan, S., Netzel-Arnett, S., Antalis, T., Vogel, S.N. & Fasano, A. 2008, 'Gliadin induces an increase in intestinal permeability and zonulin release by binding to the chemokine receptor CXCR3', Gastroenterology, vol. 135, pp. 194-204.

Schumann, M., Richter, J.F., Wedell, I., Moos, V., Zimmermann-Kordmann, M., Schneider, T., Daum, S., Zeitz, M., Fromm, M. & Schulzke, J.D. 2008, 'Mechanisms of epithelial translocation of the alpha (2)-gliadin-33 mer in celiac sprue', Gut, vol. 57, pp. 747-754.

Matysiak-Budnik, T., Moura, I.C., Arcos-Fajardo, M., Lebreton, C., Ménard, S., Candalh, C., Ben-Khalifa, K., Dugave, C., Tamouza, H., van Niel, G., Bouhnik, Y., Lamarque, D., Chaussade, S., Malamut, G., Cellier, C., Cerf-Bensussan, N., Monteiro, R.C. & Heyman, M.

2008, ‘Secretory IgA mediates retrotraanscytosis of intact gliadin peptides via the transferrin receptor in celiac disease’, J Exp Med, vol. 205, pp. 143-154.

Di Sabatino, A., & Corazza, G.R. 2009, ‘Coeliac disease’, Lancet, vol. 373, pp. 1480-93.

Sollid, L.M. & Jabri, B. 2013, ‘Triggers and drivers of autoimmunity: lessons from celiac disease’, Nat Rev Immunol, vol. 13, pp. 294-302.

Bulfone-Paus, S., Ungereanu, D., Pohl, T., Lidner, G., Paus, R., Ruckert, R., Adams, G. G., Rowe, A. J., Harding, S. E., Hans Krause & Ulrich, K. 1997, ‘Interleukin-15 protects from lethal apoptosis in vivo’, Nat Med, vol. 3, pp. 1124-1128.

Waldmann, T.A. 2006, ‘The biology of interleukin-2 and interleukin-15; implications for cancer therapy and vaccine design’, Nat Rev Immunol, vol. 6, pp. 595-601.

Bodd, M., Ráki, M., Tollefsen, S., Fallang, L.E., Bergseng, E., Lundin, K.E. & Sollid, L.M. 2010, ‘HLA-DQ2-restricted gluten-reactive T cells produce IL-21 but not IL-17 or IL-22’, Mucosal Immunol, vol. 3, pp. 594-601.

Peluso, I., Fantini, M.C., Fina, D., Caruso, R., Boirivant, M., MacDonald, T.T., Pallone, F. & Monteleone, G. 2007, ‘IL-21 counteracts the regulatory T cell-mediated suppression of human CD4+ T lymphocytes’, J Immunol, vol. 178, pp. 732-739.

Hüe, S., Mention, J-J., Monteiro, R.C., Zhang, S., Cellier, C., Schmitz, J., Verkarre, V., Fodil, N., Bahram, S., Cerf-Bensussan, N. & Caillat-Zucman, S. 2004, ‘A direct role for NKG2D/MICA interaction in villous atrophy during celiac disease. Immunity, vol. 21, pp. 367-377.

Meresse, B., Curran, S.A., Ciszewski, C., Orbelyan, G., Setty, M., Bhagat, G., Lee, L., Tretiakova, M., Semrad, C., Kistner, E., Winchester, R.J., Braud, V., Lanier, L.L., Geraghty, D.E., Green, P.H., Guandalini, S. & Jabri, B. 2006, ‘Reprograming of CTLs into natural killer-like cells in celiac disease’, J Exp Med, vol. 203, pp. 1343-1355.

Griffin, M., Casadio, R. & Bergamini, C.M. 2002, ‘Transglutaminase: nature’s biological glues’, Biochem J, vol. 368(Pt2), pp. 377-396.

Ikura, K., Nasu, T., Yokota, H., Tsuchiya, Y., Sasaki, R. & Chiba, H. 1988, ‘Determination of amino- and carboxyl-terminal sequences of guinea pig liver transglutaminase: evidence for amino-terminal processing’, Biochemistry, vol. 27, pp. 2898-2905.

Folk, J.E. & Gross, M.J. 1971, ‘Mechanism of action of guinea pig liver transglutaminase VIII active site studies with ‘reporter’ group-labeled halomethyl ketones’, Biol Chem, vol. 246, pp. 6683-6691.

Thomazy, V. & Fesus, L. 1989, ‘Differential expression of tissue transglutaminase in human cells. An immunohistochemical study’, Cell Tissue Res, vol. 255(1), pp. 215-224.

Sabatino, A.D., Vanoli, A., Giuffrida, P., Luinetti, O., Solcia, E. & Corazza, G.R. 2012, ‘The function of tissue transglutaminase in celiac disease’, Autoimmun Rev, vol. 11, pp. 746-753.

Evans, D.F., Pye, G., Bramley, R., Clark, A.G., Dyson, T.J. & Hardcastle, J.D. 1988, ‘Measurement of gastrointestinal pH profiles in normal ambulant human subjects’, Gut, vol. 29, pp. 1035-1041.

Dieterich, W., Esslinger, B., & Schuppan, D. 2003, ‘Patho mechanisms in celiac disease’, Int Arch Allergy Immunol, vol. 132, pp. 98-108.

Sjostorm, H., Lundin, K.E.A., Molberg, O., Korner, R., McAdam, S.N., Anthosen, D., Quartsen, H., Noren, O., Roepstorff, P., Thorsby, E. & Sollid, L.M. 1998, ‘Identification of a gliadin T cell epitope in celiac disease: general importance of gliadin deamidation of intestinal T cell recognition’, Scan J Immunol, vol. 48, pp. 111-115.

Piper, J.L., Gray, G.M. & Khosla, C. 2002, ‘High selectivity of human tissue transglutaminase for immunoactive gliadin peptides: implications for coeliac sprue’, Biochemistry, vol.41, pp. 386-393.

Dieterich, W., Laag, E., Schopper, H., Volta, U., Ferguson, A., Gillett, H., Riecken, E.O. & Schuppan, D. 1998, ‘Autoantibodies to tissue transglutaminase as predictors of celiac disease’, Gastroenterology, vol. 115, pp. 1317-1321.

Sollid, L.M. 2000, ‘Molecular basis of celiac disease’, Annu Rev Immunol, vol. 18, pp. 53-81.

Du Pre’, M.F. & Sollid L.M. 2015, ‘T-cell and B-cell immunity in celiac disease’, Best Pract Res Clin Gastroenterol, vol. 29, pp. 413-423.

Bronstein, H.D., Haeffner, L.J. & Kowlessar, O.D. 1966, ‘Enzymatic digestion of gliadin: the effect of the resultant peptides in adult celiac disease’, Clin Chim Acta, vol. 14, pp. 141-155.

Weiser, H. 1996, ‘Relation between gliadin structure and celiac toxicity’, Acta Paediatr Suppl, vol. 412, pp. 3-9.

Shan, L., Molberg, O., Parrot, I., Hausch, F., Filiz, F., Gray, G.M., Sollid, L.M. & Khosla, C. 2002, 'Structural basis for gluten intolerance in celiac disease', Science, vol. 297, pp. 2275-2279.

Qi, P.F., Chen, Q., Oullet, T., Wang, Z., Le, C-X., Wei, Y-M., Lan, X-J. & Zheng, Y-L. 2013, 'The molecular diversity of α-gliadin genes in the tribe *Triticea*', Genetica, vol. 141, pp. 303-310.

Ravelli, A.M., Tobanelli, P., Minelli, L., Villanacci, V. & Cestari, R. 2001, 'Endoscopic features of celiac disease in children', Gastrointest Endosc, vol. 54, pp. 736-742.

Bao, F., Green, P.H. & Bhagat, G. 2012, 'An update on celiac disease histopathology and the road ahead', Arch Pathol Lab Med, vol. 136, pp. 735-745.

Castillo, N.E., Theethira, T.G. & Leffler, D.A. 2015, 'The present and the future in diagnosis and management of celiac disease', Gastroenterol Rep, vol. 3(1), pp. 3-11.

Hardy, M.Y. & Tye-Din, J.A. 2016, 'Celiac disease: a unique model for investigating broken tolerance in autoimmunity', Clin Transl Immunology, doi:10.1038/cti.2016.58.

Greco, L., Romino, R., Coto, I., Di Cosmo, N., Percopo, S., Maglio, M., Paparo, F., Gasperi, V., Limongelli, M.G., Cotichini, R., D'Agate, C., Tinto, N., Sacchetti, L., Tosi, R. & Stazi, M.A. 2002, 'The first large population-based twin study of celiac disease', Gut, vol. 50, pp. 624-628.

Howell, M.D., Austin, R.K., Kelleher, D., Nepom, G.T. & Kagnoff, M.F. 1986, 'An HLA-D region restriction length polymorphism associated with celiac disease', J Exp Med, vol. 169, pp. 345-350.

Olivares, M., Neef, A., Castillejo, G., Palma, G.D., Varea, V., Capilla. A., Palau, F., Nova, E., Marcos, A., Polanco, I., Ribes-Koninckx, C., Ortigosa, L., Izquierdo, L. & Sanz, Y. 2015, 'The HLA-DQ2 genotype selects for early intestinal microbiota composition in infants at high risk of developing celiac disease', Gut, vol. 64, pp. 406-417.

Rioux, J.D., & Abbas, A.K. 2005, 'Paths to understanding the genetic basis of autoimmune disease', Nature, vol. 435, pp. 584-589.

Lundin, K.E.A., Scott, H., Hansen, T., Paulsen, G., Halstensen, T.S., Fausa, O., Thorsby, E. & Sollid, L.M. 1993, 'Gliadin-specific, HLA-DQ (alpha1*0501, beta1*0201) restricted T cells

isolated from the small intestinal mucosa of celiac disease patients', J Exp Med, vol. 178, pp. 187-96.

Costantini, S., Rossi, M., Colonna, G. & Facchiano, A.M. 2005, 'Modelling of HLA-DQ2 and its interaction with gluten peptides to explain molecular recognition in celiac disease', J Mol Graph Model, vol. 23, pp. 419-431.

Henderson, K.N., Tye-Din, J.A., Reid, H.H., Chen, Z., Borg, N.A., Beissbarth, T., Tatham, A., Mannering, S.I., Purcell, A.W., Dudek, N.L., van Heel, D.A., McCluskey, J., Rossjohn, J. & Anderson, R.P. 2007, 'A Structural and Immunological Basis for the Role of Human Leukocyte Antigen DQ8 in Celiac Disease', Immunity, vol. 27, pp. 23-34.

Broughton, S.E., Petersen, J., Theodossis, A., Scally, S.W., Loh, K.L., Thompson, A., van Bergen, J., Kooy-Winkelaar, Y., Henderson, K.N., Beddoe, T., Tye-Din, J.A., Mannering, S.I., Purcell, A.W., McCluskey, J., Anderson, R.P., Koning, F., Reid, H.H. & Rossjohn, J. 2012, 'Biased T Cell Receptor Usage Directed against Human Leukocyte Antigen DQ8-Restricted Gliadin Peptides Is Associated with Celiac Disease', Immunity, vol. 37, pp. 611-621.

Hadithi, M., von Blomberg, B.M., Crusius, J.B., Bloemena, E., Kostense, P.J., Meijer, J.W., Mulder, C.J., Stehouwer, C.D. & Peña, A.S. 2007, 'Accuracy of serologic tests and HLA-DQ typing for diagnosing celiac disease', Ann Intern Med, vol. 147, pp. 294-302.

Husby, S., Koletzko, S., Korponay-Szabó, I.R., Mearin, M.L., Phillips, A., Shamir, R., Troncone, R., Giersiepen, K., Branski, D., Catassi, C., Lelgeman, M., Mäki, M., Ribes-Koninckx, C., Ventura, A., Zimmer, K.P., ESPGHAN Working Group on Coeliac Disease Diagnosis & ESPGHAN Gastroenterology Committee. 2012, 'European Society for Pediatric Gastroenterology, Hepatology, and Nutrition guidelines for the diagnosis of celiac disease', J Pediatr Gastroenterol Nutr, vol. 54, pp. 136-160.

Hall, E.H. & Crowe, S.E. 2011, 'Environmental and lifestyle influences on disorders of the large and small intestine: implications for treatment', Dig Dis, vol. 29, pp. 249–254.

Fukunaga, M., Ishimura, N., Fukuyama, C., Daisuke, I., Nahoko, I., Asuka A., Akihiko O., Tomoko M., Shunji I., Riruke M., Kyoichi A. & Yoshikazu K. 2017, 'Celiac disease in non-clinical populations of Japan', J Gastroenterol, vol. 53, pp. 2018-214.

Dubois, P.C., Trynka, G., Franke, L., Hunt, K.A., Romanos, J., Curtotti, A., Zhernakova, A., Heap, G.A., Adány, R., Aromaa, A., Bardella, M.T., van den Berg, L.H., Bockett, N.A., de la Concha, E.G., Dema, B., Fehrmann, R.S., Fernández-Arquero, M., Fiatal, S., Grandone, E., Green, P.M., Groen, H.J., Gwilliam, R., Houwen, R.H., Hunt, S.E., Kaukinen, K., Kelleher, D., Korponay-Szabo, I., Kurppa, K., MacMathuna, P., Mäki, M., Mazzilli, M.C., McCann, O.T., Mearin, M.L., Mein, C.A., Mirza, M.M., Mistry, V., Mora, B., Morley, K.I., Mulder, C.J., Murray, J.A., Núñez, C., Oosterom, E., Ophoff, R.A., Polanco, I., Peltonen, L., Platteel, M., Rybak, A., Salomaa, V,. Schweizer, J.J., Sperandeo, M.P., Tack, G.J., Turner, G., Veldink, J.H., Verbeek, W.H., Weersma, R.K., Wolters, V.M., Urcelay, E., Cukrowska, B., Greco, L., Neuhausen, S.L., McManus, R., Barisani, D., Deloukas, P., Barrett, J.C., Saavalainen, P., Wijmenga, C. & van Heel, D.A. 2010, 'Multiple common variants for celiac disease influencing immune gene expression', Nature genetics, vol. 42(4), pp. 295-302.

Abraham, G., Rohmer, A., Tye-Din, J.A. & Inoye, M. 2015, 'Genomic prediction of celiac disease targeting HLA-positive individuals. Genome Med, vol. 7, pp. 3-11.

Ploski, R., Thorsby, J.E. & Sollid, L.M. 1993, 'On the HLA-DQ (alpha 1*0501, beta 1*0201)-associated susceptibility in celiac disease: a possible gene dosage effect of DQB1*0201', Tissue Antigens, vol. 41, pp. 173–177.

Noble, J.A., Valdes, A.M., Lane, J.A., Green, A.E. & Erlich, H.A. 2006, 'Linkage disequilibrium with predisposing DR3 haplotypes accounts for apparent effects of tumor necrosis factor and lymphotoxin-alpha polymorphisms on type 1 diabetes susceptibility', Hum Immunol, vol. 67, pp. 999–1004.

Miller, F.W., Waite, K.A., Biswas, T. & Plotz, P.H. 1990, 'The role of an autoantigen, histidyl-tRNA synthetase, in the induction and maintenance of autoimmunity', Proc Natl Acad Sci, vol. 87, pp. 9933-9937.

O'Farrelly, C., Kelly, J., Hekkens, W., Bradley, B., Thompson, A., Feighery, C. & Weir, D.G. 1983, 'α Gliadin antibody levels: a serological test for coeliac disease', Br Med J (Clin Res Ed), vol. 286, pp. 2007-2010.

Savilahati, E., Viander, M., Perkkio, M., Vainio, E., Kalimo, K. & Renuala, T. 1983, 'IgA antigliadin antibodies: a marker of mucosal damage in childhood coeliac disease', The Lancet, vol. 1, pp. 320-322.

Tucker, N.T., Barghuthy, F.S., Prihoda, T.J., Kumar, V., Lerner, A. & Lebenthal, E. 1988, 'Antigliadin antibodies detected by enzyme- linked immunosorbent assay as a marker of childhood coeliac disease', J Pediatr, vol. 113, pp. 286-289.

Bodé, S., Weile, B., Krasilnikoff, P.A. & Gudmand-Høyer, E. 1993, 'The Diagnostic Value of the Gliadin Antibody Test in Celiac Disease in Children: A Prospective Study', J Pediatr Gastroenterol Nutr, vol. 17, pp. 260-264.

Lerner, A., Kumar, V. & Iancu, T.C. 1994, 'Immunological diagnosis of childhood celiac disease: comparison between antigliadin, antireticulin and antiendomysial antibodies', Clin Exp Immunol, vol. 95, pp. 78-82.

Chartrand, L.J., Aglunik, J. & Vanounou, T. 1997, 'Effectiveness of anti-gliadin antibodies as a screening test for celiac disease in children', Can Med Assoc J, vol. 157, pp. 527-533.

Lagerqvist, C., Ingrid, D., Tony, H., Jidell, E., Juto, P., Olcén, P., Stenlund, H., Hernell, O. & Ivarsson, A. 2008, 'Antigliadin Immunoglobulin A best in finding celiac disease in children younger than 18 Months of age', J Pediatr Gastroenterol Nutr, vol. 47, pp. 428-435.

Pereira, S.V., Raba, J. & Messina, G.A. 2010, 'IgG anti-gliadin determination with an immunological microfluidic system applied to the automated diagnostic of the celiac disease', Anal Bioanal Chem, vol. 396, pp. 2921-2927.

Ladinser, B., Rossipal, E. & Pittschieler, K. 1994, 'Endomysium antibodies in celiac disease: an improved method,' Gut, vol. 35, pp. 776-78.

Picarelli, A. 1999, '31-43 amino acid sequence of the α-gliadin induces anti-endomysial antibody production during in vitro challenge', Scand J Gastroenterol, vol. 34, pp. 1099-1102.

Rostami, K., Kerckhaert, J., Tiemessen, R., von Blomberg, M.E., Meijer, J.W.R. & Mulder, C.J.J. 1994, 'Sensitivity of antiendomysium and antigliadin antibodies in untreated celiac disease: disappointing in clinical practice: Sensitivity of IgA EMA and AGA in Celiac Disease', Am J Gastroenterol, vol. 94, pp. 888-894.

Leffler, D.A. & Schuppan. D. 2010, 'Update on serologic testing in celiac disease', Am J Gastroenterol, vol. 105, pp. 2520-2524.

Bruce, S.E., Bjarnason, I. & Peter, I. 1985, 'Human jejunal transglutaminase: demonstration of activity, enzyme kinetics and substrate specificity with special relation to gliadin and celiac disease', Clin Sci, vol. 68, pp. 573-579.

Hill, P.G. & Holmes, G.K. 2008, 'Celiac disease: a biopsy is not always necessary for diagnosis', Aliment Pharmacol Ther, vol. 27, pp. 572-577.

Vivas, S., Ruiz de Morales, J.G., Riestra, S., Arias, L., Fuentes, D., Alvarez, N., Calleja, S., Hernando, M., Herrero, B., Casqueiro, J & Rodrigo, L. 2009, 'Duodenal biopsy may be avoided when high transglutaminase antibody titres are present', World J Gastroenterol, Vol. 15, pp. 4775-4780.

Tortara, R., Imperatore, N. & Capone, P. 2014. 'The presence of anti-endomysial antibodies and the level of anti-tissue transglutaminase can be used to diagnose adult celiac disease without duodenal biopsy', Aliment Pharmacol Ther, vol. 40, pp. 122-129.

Dahlbom, I., Nyberg, B.I., Bernston, L., & Hansson, T. 2016, 'Simultaneous detection of IgA and IgG antibodies against tissue transglutaminase: the preferred pre-biopsy test in childhood celiac disease', Scand J Clin Lab Invest, vol. 76, pp. 208-216.

Sblattero, D., Berti, I., Trevisiol, C., Marzari, R., Tommasini, A., Bradbury, A., Fasano, A., Ventura, A. & Not, T. 2000, 'Human recombinant tissue transglutaminase ELISA: An innovative diagnostic assay for celiac disease', Am J Gastroenterol, vol. 95, pp. 1253-1257.

Lock, R.J., Gilmour, J.E.M. & Unsworth, D.J. 1999, 'Anti-tissue transglutaminase, anti-endomysium and anti-R1-reticulin autoantibodies: the antibody trinity of celiac disease', Clin Exp Immunol, vol. 116, pp. 258–262.

Lewis, N.R. & Scott, B.B. 2010, 'Meta-analysis: deamidated gliadin peptide antibody and tissue transglutaminase antibody compared as screening tests for celiac disease', Aliment Pharmacol Ther, vol. 31, pp. 73-81.

Dahlbom, I., Korponay-Szabo, I.R., Kovacs, J.B., Szalai, Z., Mäki, M. & Hansson, T. 2010, 'Prediction of clinical and mucosal severity of celiac disease and dermatitis herpetiformis by quantification of IgA/IgG serum antibodies to tissue transglutaminase', J Pediatr Gastroenterol Nutr, vol. 50, pp. 140-146.

Volta, U., Granito, A., Fiorini, E., Parisi, C., Piscaglia, M., Pappas, G., Muratori, P. & Bianchi, F.B. 2008, 'Usefulness of antibodies to deamidated gliadin peptides in celiac disease diagnosis and follow-up', Dig Dis Sci, vol. 53, pp. 1582-1588.

Dahle, C., Hagman, A., Ignatova, S. & Ström, M. 2010, 'Antibodies against deamidated gliadin peptides identify adult celiac disease patients negative for antibodies against endomysium and tissue transglutaminase', Aliment Pharmacol Ther, vol. 32, pp. 254-260.

Barbato, M., Maiellaa, G., Di Camillo, C., Guida, S., Valitutti, F., Lastrucci, G., Mainiero, F. & Cucchiara, S. 2011, 'The anti-deamidated gliadin peptide antibodies unmask celiac disease in small children with chronic diarrhea', Dig Liver Dis, vol. 43, pp. 465-469.

Amarri, S., Alvisi, P., Giorgio, R.D., Gelli, M.C., Cicola, R., Tovoli, F., Sassatelli, R., Caio, G. & Volta, U. 2013, 'Antibodies to deamidated gliadin peptides: An accurate predictor of coeliac disease in infancy', J Clin Immunol, vol. 33, pp. 1027-1030.

Schwertz, E., Kahlberg, F., Sack, U., Richter, T., Stern, M., Conrad, K., Zimmer, K.P. & Mothes, T. 2004, 'Serologic assay based on gliadin-related nonapeptides as a highly sensitive and specific diagnostic aid in celiac disease', Clin Chem, vol. 50, pp. 2370-2375.

Agardh, A. 2007, 'Antibodies against synthetic deamidated gliadin peptides and tissue transglutaminase for the identification of childhood celiac disease', Clin Gastroenterol Hepatol, vol. 5, pp. 1276-1281.

Ankelo, M., Kleimola, V., Simell, S., Simell, O., Knip, M., Jokisalo, E., Tarkia, M., Westerlund, A., He, Q., Viander, M., Ilonen, J. & Hinkkanen, A.E. 2007, 'Antibody responses to deamidated gliadin peptide show high specificity and parallel antibodies to tissue transglutaminase in developing celiac disease', Clin Exp Immunol, vol. 150, pp. 285-293.

Rashtak, S., Ettore, M.W., Homburger, H.A. & Murray, J.A. 2008, 'Comparative usefulness of deamidated gliadin antibodies in the diagnosis of celiac disease', Clin Gastroenetrol Hepatol, vol. 6, pp. 426-432.

Basso, D., Guariso, G., Fogar, P., Meneghel, A., Zambon, C.F., Navaglia, F., Greco, E., Schiavon, S., Rugge, M. & Plebani, M. 2008, 'Antibodies against Synthetic Deamidated Gliadin Peptides for Celiac Disease Diagnosis and Follow-Up in Children', Clin Chem, vol. 55, pp. 150-157.

Sugai, E., Moreno, M.L., Hwang, H.J., Cabanne, A., Crivelli, A., Nachman, F., Vázquez, H., Niveloni, S., Argonz, J., Mazure, R., La Motta, G., Caniggia, M.E., Smecuol, E., Chopita, N., Gómez, J.C., Mauriño, E. & Bai, J.C. 2010, 'Celiac disease serology in patients with

different pretest probabilities: is biopsy avoidable?', World J Gastroenterol, vol. 16, pp. 3144-3152.

Volta, U., Giorgio, R. De., Granito, A., Stanghellani, V., Barbara, G., Avoni, P., Liguori, R., Petrolini, N., Fiorini, E., Montagna, P., Corinaldesi, R. & Bianchi, F.B. 2006, 'Anti-ganglioside antibodies in coeliac disease with neurological disorders', Dig Liver Dis, vol. 38(3), pp. 183 – 187.

Yuki, N., Susuki, K., Koga, M., Nishimoto, Y., Odaka, M., Hirata, K., Taguchi, K., Miyatake, T., Furukawa, K., Kobata, T. & Yamada, M. 2004, 'Carbohydrate mimicry between human ganglioside GM1 and Campylobacter jejuni lipooligosaccharide causes Guillain–Barré syndrome', Proc Natl Acad Sci, vol. 101(31), pp. 11404-11409.

Alaedini, A. & Latov, N. 2006 'Transglutaminase-independent binding of gliadin to intestinal brush border membrane and GM1 ganglioside', J Neuroimmunol, vol. 177, pp. 167-172.

Cinova, J., De Palma, G., Stepankova, R., Kofronova, O., Kverka, M., Sanz, Y. & Tuckova, L. 2011, 'Role of Intestinal Bacteria in Gliadin-Induced Changes in Intestinal Mucosa: Study in Germ-Free Rats', Plos One, vol. 6 (1), pp. 1-10. DOI: 0.1371/journal.pone.0016169.

Elena, F. V., Heather, J. G. & Bana, J. 2015, 'Novel players in coeliac disease pathogenesis: role of the gut microbiota', Nat Rev Gastroenterol Hepatol, vol. 12 (9), pp. 497-506.

Alaedini, A., Okamoto, H., Briani, C., Wollenberg, K., Shill, H.A., Bushara, K.A., Sander, H.W., Green, P.H.R, Hallett, M. & Latov, N. 2007, 'Immune Cross-Reactivity in Celiac Disease: Anti-Gliadin Antibodies Bind to Neuronal Synapsin I', J Immunol, vol. 178 (10), pp. 6590-6595; DOI: https://doi.org/10.4049/jimmunol.178.10.6590

Bustos, R., Kolen, E.R., Braiterman, L., Baines, A.J., Gorelick, F.S. & Hubbard, A.L. 2001, 'Synapsin I is expressed in epithelial cells: localization to a unique trans-Golgi compartment', J Cell Sci, vol. 114, pp. 3695-3704.

Anderson, R.P., van Heel, D.A., Tye-Din, J.A., Barnardo, M., Salio, M., Jewell, D.P. & Hill, A.V. 2005, 'T cells in peripheral blood after gluten challenge in celiac disease', Gut, vol. 54, pp. 1217-1223.

Brottveit, M., Ráki, M., Bergseng, E., Fallang, L.E., Simonsen, B., Løvik, A., Larsen, S., Løberg, E.M., Jahnsen, F.L., Sollid, L.M. & Lundin, K.E. 2011, 'Assessing possible celiac disease by an HLA-DQ2-gliadin tetramer test', Am J Gastroenterol, vol. 106, pp. 1318-1324.

Goletti, D., Vincenti, D., Carrara, S., Butera, O., Bizzoni, F., Bernardini, G., Amicosante, M. & Girardi, E. 2005, 'Selected RD1 peptides for active tuberculosis diagnosis: comparison of a gamma interferon whole-blood enzyme-linked immunosorbent assay and an enzyme-linked immunospot assay', Clin Diagn Lab Immunol, vol. 12, pp. 1311-1316.

Ruhwald, M., Bjerregaard-Anderson, M., Rabna, P., Kofoed, K., Eugen-Olsen, J. & Ravn P. 2007, 'CXCL10/IP-10 release is induced by incubation of whole blood from tuberculosis patients with ESAT-6, CFP10 and TB7.7', Microbes Infect, vol. 9, pp. 806-812.

Lalvani, A., Meroni, P.L., Millington, K.A., Modolo, M.L., Plebani, M., Tincani, A., Villalta, D., Doria, A. & Ghirardello, A. 2008, 'Recent advances in diagnostic technology: applications in autoimmune and infectious diseases', Clin Exp Rheumatol, vol. 26, pp. S62-S66.

Anderson, R.P., Degano, P., Godkin, A.J., Jewell, D.P. & Hill, A.V. 2000, 'In vivo antigen challenge in celiac disease identifies a single transglutaminase-modifed peptide as the dominant A-gliadin T cell epitope', Nat Med, vol. 6, pp. 337-342.

Tye-Din, J.A., Stewart, J.A., Dromey, J.A., Beissbarth, T., van Heel, D.A., Tatham, A., Henderson, K., Mannering, S.I., Gianfrani, C., Jewell, D.P., Hill, A.V.S., McCluskey, J., Rossjohn, J. & Anderson, R.P. 2010, 'Comprehensive, quantitative mapping of T cell epitopes in gluten in celiac disease', Sci Transl Med, 2:41ra51.

Ontiveros, N., Tye-Din, J.A., Hardy, M.Y. & Anderson, R.P. 2014, 'Ex-vivo whole blood secretion of interferon (IFN)-γ and IFN-γ-inducible protein-10 measured by enzyme-linked immunosorbent assay are as sensitive as IFN-γ enzyme-linked immunospot for the detection of gluten-reactive T cells in human leucocyte antigen (HLA)-DQ2.5+-associated celiac disease', Clin Exp Immunol, vol. 175, pp. 305–315.

Lehmann, P.V. & Zhang, W. 2012, 'Unique strengths of ELISPOT for T cell diagnostics', Methods Mol Biol, vol. 792, pp. 3-23.

Nauntofte, B., Tenevuo, Jo & Lagerlof, F. 2003, 'Secretion and composition of saliva. In: Fejerskov O, Kidd E, editors. Dental Caries: The disease and its clinical management', Oxford: Blackwell Munlsgard, pp. 7-29.

Lowry, O. H., Rosebrough, N. J., Farr, A. L., & Randall, B. J. 1951, 'Protein measurement with the Folin phenol reagent', J Biol Chem, vol. 193, pp. 265.

Gronbald, E.A. 1982, Concentration of immunoglobulins in human whole saliva: effect of physiological stimulation. Acta Odontol Scand, vol. 40, pp. 87-95.

Salazer, C., Nagadia, R., Pandit, P., Cooper-White, J., Banerjee, N., Dimitrova, N., Coman, W.B. & Punyadeera, C. 2014, 'A novel saliva-based micro-RNA biomarker panel to detect head and neck cancers', Cell Oncol, vol. 37, pp. 331-338.

Baldini, C., Giusti, L., Ciregia, F., Da Valle, Y., Giacomelli, C., Donadio, E., Sernissi, F., Bazzichi, L., Giannaccini, G., Bombardieri, S. & Lucacchini, A. 2011, 'Proteomic analysis of saliva: a unique tool to distinguish primary Sjogren's syndrome from secondary Sjogren's syndrome and other sicca syndromes', Arthritis Res Ther, vol. 13(6):R194.

Jacobs, R., Maasdorp, E., Malherbe, S., Loxton, A.G., Stanley, K., van der Spuy, G., Walzl, G. & Chegou, N.N. 2016, 'Diagnostic potential of novel salivary host biomarkers as candidates for the immunological diagnosis of tuberculosis disease and monitoring of tuberculosis treatment response', Plos One, doi:10.1371:1-13.

Sueki, A., Matsuda, K., Yamaguchi, A., Uehara, M., Sugano, M., Uehara, T. & Honda, T. 2016, 'Evaluation of saliva as a diagnostic materials for influenza virus infection by PCR-based assay', Clinica Chimica Acta, vol. 453:71-74.

Slavin, H.C. 1998, 'Toward molecularly based diagnostics for the oral cavity', J Am Dent Assoc, vol. 129, no. 11, pp. 38-1143.

Scully, C. 1997, 'HIV topic update: salivary testing for antibodies', Oral Dis, vol. 3, pp. 212-215.

Chen, D.X., Schwatrz, P.E. & Li, F.Q. 1990, 'Saliva and serum CA 125 assays for detecting malignant ovarian tumours', Obststet Gynecol, vol. 75, pp. 701-704.

Navarro, M.A., Mesia, R., Diez-Gilbert, O., Rueda. A., Ojeda, B. & Alonso, M.C. 1997, 'Epidermal growth factor in plasma and saliva of patients with active breast cancer and breast cancer patients in follow-up compared with healthy women', Breast Cancer Res Treat, vol. 42, pp. 83-86.

Hakeem, V., Fifield, R., Al-Bayaty, H.F., Walker, D.M., Williams, J. & Jenkins, H.R. 1992, 'Salivary IgA antigliadin antibody as a marker for celiac disease', Arch Dis Child, vol. 67, pp. 724-727.

Lenander-Lumikari Ihalin, R. & Lahteenoja, H. 2000, 'Changes in whole saliva in patients with celiac disease', Arch Oral Biol, vol. 45(5), pp. 347-354.

Wang, D., Zhou, J. Q. & Zhao, M. P. 2010, 'A simple and rapid competitive enzyme-linked immunosorbent assay (cELISA) for high- throughput measurement of secretory immunoglobulin A (sIgA) in saliva', Talanta, vol. 82, pp. 432-436.

Tonutti, E., Visentini, D., Picierno, A., Bizzaro, N., Villalta, D., Tozzoli, R., Kodermaz, G., Carroccio, A., Lacono, G., Teresi, S., Chiusa, S. M. L. & Brusca, I. 2009, 'Diagnostic efficacy of the ELISA test for the detection of deamidated anti-gliadin peptide antibodies in the diagnosis and monitoring of coeliac disease', J Clin Lab Anal, vol. 23, pp. 165-171.

Bonamico, M., Nenna, R., Montuori, M., Luparia, R.P., Turchetti, A., Mennini, M., Lucantoni, F., Masotti, D., Magliocca, F.M., Culasso, F. & Tiberti, C. 2011, 'First salivary screening of celiac disease by detection of anti-transglutaminase autoantibody radioimmunoassay in 5000 Italian primary schoolchildren', J Pediatr Gastroenterol Nutr, vol. 52(1), pp. 17-20.

Adornetto, G., Fabiani, L., Volpe, G., De Stefano, A., Martini, S., Nenna, R., Lucantoni, F., Bonamico, M., Tiberti, C. & Moscone, D. 2015, 'An electrochemical immunoassay for the screening of celiac disease in saliva samples', Anal Bioanal Chem, vol. 407, pp. 7189-7196.

Actis, A.B., Perovic, N.R., Defagó, D., Beccacece, C & Eynard, A.R. 2005, 'Fatty acid profile of human saliva: a possible indicator of dietary fat intake', Arch Oral Biol, vol. 50, pp. 1-6.

Benkebil, F., Combescure, C., Anghel, S.I., Besson Duvanel, C. & Schäppi, M.G. 2013, 'Diagnostic accuracy of a new point-of-care screening assay for celiac disease', World J Gastroenterol, vol. 19, pp. 5111-5117.

Bienvenu, F., Duvanel, C.B., Seignovert, C., Rouzairea, P., Lachauxb, A. & Bienvenua, J. 2012, 'Evaluation of a point-of-care test based on deamidated gliadin peptides for celiac disease screening in a large pediatric population', Eur J Gastroenterol Hepatol, DOI: 10.1097/meg.0b013e3283582d95.

Watanabe, C., Komoto, S., Hokari, R., Kurihara, C., Okada, Y., Hozumi, H., Higashiyama, M., Sakuraba, A., Tomita, K., Tsuzuki, Y., Kawaguchi, A., Nagao, S., Ogata, S. & Miura, S. 2014, 'Prevalence of serum celiac antibody in patients with IBD in Japan', J Gastroenterol, vol. 49, pp. 825-834.

Wungjiranirun, M., Kelly, C.P. & Leffler, D.A. 2016, 'Current status of celiac disease drug development,' Am J Gastroenterol, vol. 111, pp. 779-786.

Soler, M., Estevez, M.C., Moreno Mde, L., Cebolla, A. & Lechuga, L.M. 2016, 'Label-free SPR detection of gluten peptides in urine for non-invasive celiac disease follow-up', Biosens Bioelectron, vol. 79, pp. 158-164.

Comino, I., Fernández-Bañares, F., Esteve, M., Ortigosa, L., Castillejo, G., Fambuena, B., Ribes-Koninckx, C., Sierra, C., Rodríguez-Herrera, A., Salazar, J.C., Caunedo, Á., Marugán-Miguelsanz, J.M., Garrote, J.A., Vivas, S., Lo Iacono, O., Nuñez, A., Vaquero, L., Vegas, A.M., Crespo, L., Fernández-Salazar, L., Arranz, E., Jiménez-García, V.A., Antonio Montes-Cano, M., Espín, B., Galera, A., Valverde, J., Girón, F.J., Bolonio, M., Millán, A., Cerezo, F.M., Guajardo, C., Alberto, J.R., Rosinach, M., Segura, V., León, F., Marinich, J., Muñoz-Suano, A., Romero-Gómez, M., Cebolla, Á. & Sousa, C. 2016, 'Fecal gluten peptides reveal limitations of serological tests and food questionnaires for monitoring gluten-free diet in celiac disease patients', Am J Gastroenterol, vol. 111, pp. 1456-1465.

Rohrman, B.A. & Richards-Kortum, R.R. 2012, 'A paper and plastic device for performing recombinase polymerase amplification of HIV DNA', Lab Chip, vol. 12, pp. 3082–3088.

Fu, E., Liang, T., Spicar-Mihalic, P., Houghtaling, J., Ramachandran, S. & Yager, P. 2012, 'Two-dimensional paper network format that enables simple multistep assays for use in low-resource settings in the context of malaria antigen detection', Anal Chem, vol. 84, pp. 4574–4579.

Veigas, B., Jacob, J.M., Costa, M.N., Santos, D.S., Viveiros, M., Inácio, J., Martins, R., Barquinha, P., Fortunato, E. & Baptista, P.V. 2012, 'Gold on paper–paper platform for Au-nanoprobe TB detection', Lab Chip, vol. 12, pp. 4802–4808.

Fasano, A. & Catassi, C. 2001, 'Current approaches to diagnosis and treatment of celiac disease: an evolving spectrum', Gastroenterology, vol. 120, pp. 636-651.

Jin, R.C., Cao, Y.W., Mirkin, C.A., Kelly, K.L., Schatz, G.C. & Zheng, J.G. 2001, 'Photoinduced conversion of silver nanospheres to nanoprisms', Science, vol. 294, pp. 1901–1903.

Shimoni, O. & Valenzuela, S.M. 2017, 'Gold Nanoparticles with Organic Linkers for Applications in Biomedicine', Nanotechnology in Biology and Medicine, CRC press.

Turkevich, J., Stevenson, P.C. & Hillier, J. 1951, 'A study of the nucleation and growth processes in the synthesis of colloidal gold', Discuss. Faraday Soc, vol. 11, pp. 55–75.

Sanvicens, N. & Marco, M.P. 2008, 'Multifunctional nanoparticles-properties and prospects for their use in human medicine', Trends Biotechnol, vol. 26, pp. 425-433.

El-Sayed, M.A. 2001, 'Some interesting properties of metals confined in time and nanometer space of different shapes', Acc Chem Res, vol. 34, pp. 257-264.

Daniel, M.C. & Astruc, D. 2004, 'Gold nanoparticles: assembly, supramolecular chemistry, quantum-size related properties, and applications toward biology, catalysis, and nanotechnology', Chem Rev, vol. 104, pp. 293-346.

Jensen, T.R., Malinsky, M.D., Haynes, C.L. & Van Duyne, R.P. 2000, 'Nanosphere Lithography: Tunable Localized Surface Plasmon Resonance Spectra of Silver Nanoparticles', J Phys Chem B, vol. 104 (45), pp. 10549-10556.

Mie, G. 1908, Ann. Phys. (Weinheim, Ger), vol. 25, pp. 377.

Mock, J.J., Smith, D.R. & Schultz, S. 2003, 'Local refractive index dependence of plasmon resonance spectra from individual nanoparticles', Nano Lett, vol. 3(4), pp. 485-491.

Willets, K.A. & Duyne, R.P. Van. 2007, 'Localised surface plasmon resonance spectroscopy and sensing', Annu Rev Phys Chem, pp. 267-297.

Homola, J. Yee, S.S & Gauglitz, G. 1999, 'Surface plasmon resonance sensors: review', Sens Actuators, vol. 54, pp. 3-15.

Eustis, S. & El-Sayed, M.A. 2006, 'Why gold nanoparticles are more precious than pretty gold: Noble metal surface plasmon resonance and its enhancement of the radiative and nonradiative properties of nanocrystals of different shapes', Chem Soc Rev, vol, 35, pp. 209-217.

Lee, T.M.H. 2008, 'Over-the-counter biosensors: past, present, future', Sensors, vol. 8, pp. 5535–5559.

Wijaya, E., Lenaerts, C., Maricot, S. & Mastanin, J. 2011, 'Surface plasmon resonance-based biosensors: from the development of different SPR structures to novel surface functionalization strategies', Curr Opin Solid State Mater Sci, vol. 15, pp. 208-224.

Jain, P.K., Lee K.S., El-Sayed, I.H. & El-Sayed, M.A. 2006, 'Calculated absorption and scattering properties of gold nanoparticles of different size, shape and composition: applications in biological imaging and biomedicine', J Phys Chem B, vol. 110, pp. 7238–7248

Haes, J., Haynes, C.L. & Van Duyne, R.P. 2001, 'Nanosphere lithography: Self-assembled photonic and magnetic materials', Mater Res Soc Symp 636, D4.8.

Bohren, C.F. & Huffman, D.R. 1998, 'Absorption and Scattering of Light by Small Particles'

Wiley-Interscience.

Pissuwan, D., Cortie, C.H., Valenzuela, S.M. & Cortie, M.B. 2007, 'Gold nanosphere-antibody conjugates for hyperthermal therapeutic applications', Gold Bulletin, vol. 40 (2), pp. 121-129.

Su, K.H., Wei, Q. H. & Zhang, X. 2003, 'Interparticle coupling effects on plasmon resonances of nanogold particles', Nano Lett, vol. 3 (8), pp. 1087-1090.

Lundqvist, M., Stigler, J., Elia, G., Lynch, I., Cedervall, T. & Dawson, K.A. 2008, 'Nanoparticle size and surface properties determine the protein corona with possible implications for biological impacts', Proc Natl Acad Sci, vol. 105, pp. 14265–14270.

Deng, Z.J., Liang, M., Monteiro, M., Toth, I. & Minchin, R.F. 2011, 'Nanoparticle-induced unfolding of fibrinogen promotes Mac-1 receptor activation and inflammation', Nat Nanotechnol, vol. 6, pp. 39–44.

Huang, R., Carney, R.P., Stellacci, F. & Lau, B.L.T. 2013, 'Protein–nanoparticle interactions: the effects of surface compositional and structural heterogeneity are scale dependent', Nanoscale, vol. 5, pp. 6928–6935.

Feliu, N., Walter, M. V., Montanez, M. I., Kunzmann, A., Hult, A., Nystrom, A., Malkoch, M. & Fadeel, B. 2012, 'Stability and biocompatibility of a library of polyester dendrimers in comparison to polyamidoamine dendrimers', Biomaterials, vol. 33, pp. 1970–1981.

Lesniak, A., Campbell, A., Monopoli, M.P., Lynch, I., Salvati, A., & Dawson, K.A. 2010, 'Serum heat inactivation affects protein corona composition and nanoparticle uptake', Biomaterials, vol. 31, pp. 9511–9518.

Mahmoudi, M., Abdelmonem, A.M., Behzadi, S., Clement, J.H., Dutz, S., Ejtehadi, M.R., Hartmann, R., Kantner, K., Linne, U., Maffre, P., Metzler, S., Moghadam, M.K., Pfeiffer, C.,

Rezaei, M., Ruiz-Lozano, P., Serpooshan, V., Shokrgozar, M.A., Nienhaus, G. U. & Parak, W.J. 2013, 'Temperature: The "Ignored" Factor at the NanoBio Interface', ACS Nano, vol. 7, pp. 6555–6562.

Gebauer, J.S., Malissek, M., Simon, S., Knauer, S.K., Maskos, M., Stauber, R.H., Peukert, W., & Treuel, L. 2012, 'Impact of the Nanoparticle–Protein Corona on Colloidal Stability and Protein Structure', Langmuir, vol. 28 (25), pp. 9673-9679.

Tenzer, S., Docter, D., Rosfa, S., Wlodarski, A., Kuharev, J., Rekik, A., Knauer, S.K., Bantz, C., Nawroth, T., Bier, C., Sirirattanapan, J., Mann, W., Treuel, L., Zellner, R., Maskos, M., Schild, H., & Stauber, R.H. 2011, 'Nanoparticle Size Is a Critical Physicochemical Determinant of the Human Blood Plasma Corona: A Comprehensive Quantitative Proteomic Analysis', ACS Nano, vol. 5, pp. 7155–7167.

del Pino, P., Pelaz, B., Zhang, Q., Maffre, P., Nienhaus, G.U. & Parak, W.J. 2014, 'Protein corona formation around nanoparticles- from the past to the future', Mater Horiz, vol. 1, pp. 301-313.

Silvia, H., De P., Lacerda, Park, J.J., Meuse, C., Pristinski, D., Becker, M.L., Karim, A., & Douglas, J.F. 2009, 'Interaction of gold nanoparticles with common human blood proteins', ACS Nano, vol. 4, pp. 365-379.

Jung, S. Y., Lim, S. M., Albertorio, F., Kim, G., Gurau, M. C., Yang, R. D., Holden, M. A., & Cremer, P. S. 2003, 'The Vroman effect: a molecular level description of fibrinogen displacement', J Am Chem Soc, vol. 125, pp. 12782–12786.

Lynch, I., Cedervall, T., Lundquist, M., Cabaleiro-Lago, C., Linse, S. & Dawson, K.A. 2007, 'The nanoparticle-protein complex as a biological entity: a complex fluids and surfaces challenge for the 21st century. Adv Colloidal Interface Sci. 134-135. 167-174.

Sperling, R.A. & Parak, W. 2010, 'Surface modification, functionalization and bioconjugation of colloidal inorganic nanoparticles', Phil Trans Math Phys Eng Sci, vol. 368, pp. 1333-1383.

Verma, A. & Stellaci, F. 2010, 'Effect of surface properties on nanoparticle-cell interactions', Small, vol. 6, pp. 12-21.

Link, S. & El-Sayed, M.A. 2003, 'Optical properties and ultrafast dynamics of metallic nanocrystals', Annu Rev Phys Chem, vol. 54, pp. 331-366.

Lin, S.-Y., Chen, C.-H., Lin, M.-C. & Hsu, H.-F. 2005, 'A co-operative effect of bifunctionalised nanoparticles on recognition: sensing alkali ions by crown and carboxylate moieties in aqueous media', Anal Chem, vol. 77, pp. 4821-4828.

Chai, F., Chungang Wang, C., Wang, T., Li, L., & Su, Z. 2010, 'Colorimetric Detection of Pb^{2+} Using Glutathione Functionalized Gold Nanoparticles', ACS Appl Mater Interfaces, vol. 2 (5), 1466-1470. DOI: 10.1021/am100107k.

Wang, A., Guo, H., Zhang, M., Zhou, D., Wang, R., & Feng, J. 2013, 'Sensitive and selective colorimetric detection of cadmium (II) using gold nanoparticles modified with 4-amino-3-hydrazino-5-mercapto-1,2,4-triazole', Microchimica Acta, vol. 180, pp. 1051-1057.

Elghanian, R., Storhoff, J. J., Mucic, R. C., Letsinger, R.L. & Mirkin, C.A. 1997, 'Selective colorimetric detection of polynucleotides based on the distance-dependent optical properties of gold nanoparticles', Science, vol. 277, pp. 1078-1081.

Watanabe, S., Seguchi, H., Yoshida, K., Kifune, K., Tadaki, T. & Shiozaki, H. 2005, 'Colorimetric detection of fluoride ions in an aqueous solution using a thioglucose-capped gold nanoparticle', Tetrahedron Lett, vol. 46 (51), pp. 8827-8829.

Otsuka, H., Akiyama, Y., Nagasaki, Y. & Kataoka, K.J. 2001, 'Quantitative and Reversible Lectin-Induced Association of Gold Nanoparticles Modified with α-Lactosyl-ω-mercapto-poly (ethylene glycol)', Am Chem Soc, vol. 123, pp. 8226-8230.

Duncan, C., Hone, Alan, H., Haines & David, A. R. 2003, 'Rapid, Quantitative Colorimetric Detection of a Lectin Using Mannose-Stabilized Gold Nanoparticles', Langmuir, vol. 19, pp 7141–7144.

Niikura, K., Nagakawa, K., Ohtake, N., Suzuki, T., Matsuo, Y., Sawa, H., & Ijiro, K., 2009 'Gold Nanoparticle Arrangement on Viral Particles through Carbohydrate Recognition: A Non-Cross-Linking Approach to Optical Virus Detection', Bioconjugate Chem, vol., 20 (10), pp. 1848-1852. DOI: 10.1021/bc900255x.

Zhang, J., Liu, B., Liu, H., Zhang, X. & Tan, W. 2013, 'Aptamer-conjugated gold nanoparticles for bioanalysis', Nanomedicine, vol. 8, pp. 983-993.

Huang, C-C., Huang, Y-F., Cao, Z., Tan, W. & Chang, H-T. 2005, 'Aptamer-Modified Gold Nanoparticles for Colorimetric Determination of Platelet-Derived Growth Factors and Their Receptors', Anal Chem, 2005 77 (17), 5735-5741. DOI: 10.1021/ac050957q

Huang, C-C., Huang, Y-F., Cao, Z., Tan, W. & Chang, H-T. 2007, 'Aptamer-Functionalized Gold Nanoparticles for Turn-On Light Switch Detection of Platelet-Derived Growth Factor,' Anal Chem, vol. 79 (13), pp. 4798-4804. DOI: 10.1021/ac0707075

Thanh, N.T.K. & Rosenzweig, Z. 2002, 'Development of an aggregation-based immunoassay for anti-protein A using gold nanoparticles', Anal Chem, vol. 74, pp. 1624–1628.

Laromaine, A., Koh, L., Murugesan, M., Ulijn, R.V. & Stevens, M.M. 2007, 'Protease-Triggered Dispersion of Nanoparticle Assemblies', JACS, vol. 129 (14), pp. 4156-4157. DOI: 10.1021/ja0706504

Huang, S.H. 2007, 'Gold nanoparticle- based immunochromatographic assay for the detection of Staphylococcus aureus', Sens Actuators B Chem, vol. 127, pp. 335-340.

Zhou, S.H., Cui, S.J., Chen, C.M., Zhang, F.C., Li, J., Zhou, S., Oh, J.S. & Virol, J. 2009, 'Development and validation of an immunogold chromatographic test for on-farm detection of PRRSV', Methods, vol. 160, pp. 178-189.

Li, X.M., Luo, P.J., Tang, S.S., Beier, R.C., Wu, X.P., Yang, L.L., Li, Y.W. & Xiao, X.L. 2011, 'Development of an immunochromatographic strip test for rapid detection of melamine in raw milk, milk products and animal feed', J Agric Food Chem, vol. 59, pp. 6064-6070.

Su, J., Zhou, Z., Li, H. & Liu, S. 2014, 'Quantitative detection of human chorionic gonadotropin antigen via immunogold chromatographic test strips', Anal Method, vol. 6, pp. 450.

Wang, H-Y., Wei, Y-M., Ze, H-Y & Zheng, Y-L. 2007, 'Isolation and Analysis of α-Gliadin Gene Coding Sequences from Triticum durum', Agri Sci China, vol. 6, pp. 25-32.

Dohlman, J.G., Lupas, A. & Carson, M. 1993, 'Long charge-rich α-helices in systemic autoantigens', Biochem Biophys Res Commun, vol. 195, pp. 686-696.

Tsai, De-Hao, DelRio, F. W., Keene, A. M., Tyner, K. M., MacCuspie, R. I., Cho, T. J., Zachariah, M. R. & Hackley, V. A. 2011, 'Adsorption and confirmation of serum albumin protein on gold nanoparticles investigated using dimensional measurements and in situ spectroscopic methods', Langmuir, vol. 27, pp. 2464-2477.

Kendall, C., Ionescu-Matiu, I. & Dreesm, G. R. 1983, 'Utilization of the Biotin-Avidin System to Amplify the Sensitivity of the Enzyme-Linked Immunosorbent Assay (ELISA)', J Immunol Methods, vol. 56, pp. 329-339.

Weber, P.C., Ohlendorf, D.H., Wendoloski, J.J. & Salemme, F.R. 1989, 'Structural origins of high-affinity biotin binding to streptavidin', Science, vol. 243, pp. 85-88.

Sastry, M., Lala, N., Patil, V., Chavan, S.P. & Chittiboyina, A.G. 1998, 'Optical absorption study of the Biotin-Avidin Interaction on colloidal silver and gold particles', Langmuir, vol. 14, pp. 4138-4142.

Gill, S.C. & von Hippel, P.H. 1989, 'Calculation of protein extinction coefficients from amino acid sequence data. Anal Biochem, vol. 182, pp. 319–326.

Pace, C.N. & Vajdos, F. & Gray, T. 1995, 'How to measure and predict the molar absorption coefficient of a protein', Protein Sci, vol. 4, pp. 2411–2423.

Berne, B. J. & Pecora, R. 1976, 'Dynamic light scattering: with applications to chemistry, biology, and physics', Wiley: New York, 1976.

Jain, P. K., Lee, K. S., El-Sayed, I. H. & El-Sayed, M.A. 2006, 'Calculated absorption and scattering properties of gold nanoparticles of different size, shape, and composition: applications in biological imaging and biomedicine', J Phys Chem B, vol. 110, pp. 7238–7248.

Hühn, D., Kantner, K., Geidel, C., Brandholt, S., De Cock, I., Soenen, S. J., Rivera, G. P., Montenegro, J.M., Braeckmans, K., Müllen, K., Nienhaus, G.U., Klapper, M. & Parak, W. J. 2013, 'Polymer-coated nanoparticles interacting with proteins and cells: focusing on the sign of the net charge', ACS Nano, vol. 7, pp. 3253–3263.

Rogers, S.O. & Bendich, A.J. 1989, 'Extraction of DNA from plant tissues', In: Gelvin S.B., Schilperoort R.A., Verma D.P.S. (eds) Plant Molecular Biology Manual. Springer, Dordrecht.

Baldwin, A.D. & Kiick, K.L. 2011, 'Tunable Degradation of Maleimide–Thiol Adducts in Reducing Environments', Bioconjug Chem, vol. 22, pp. 1946–1953.

Williams, D.B. & Carter, C.B. 1996, 'The transmission electron microscope', In: Transmission Electron Microscopy. Springer, Boston, MA.

Oliver, R.M. 1973, 'Negative stain electron microscopy of protein macromolecules', Meth Enzymol, vol. 27, pp. 616–672.

Jürgen's, L., Nichtl, A. & Werner, U. 1999, 'Electron density imaging of protein films on gold-particle surfaces with transmission electron microscopy', Cytometry, vol. 37, pp. 87-92.

Janeway, C.A., Travers, P.A., Walport, M. & Shlomchik, M.J. 2001. Immunobiology. New York: Garland Publishing.

Davies, R.D. & Chacko, S. 1993, 'Antibody structure', Acc Chem Res, vol. 26, pp. 421-427.

Amit, A.G., Mariuzza, R. A., Phillips, S. E. & Poljak, R. J. 1986, 'Three-dimensional structure of an antigen-antibody complex at 2.8 A resolution', Science, vol. 233, (4765), pp. 747-753.

Kumar, A.A., Hennek, J.W., Smith, B.S., Kumar, S., Beattie, P., Jain, S., Rolland, J.P., Stossel, T.P. & Whitesides, G.M. 2015, 'From the Bench to the Field in Low-Cost Diagnostics: Two Case Studies', Angew Chemie, vol. 54, pp. 5836-5853.

Tye-Din, J.A., Cameron, D.J., Daveson, A.J., Day, A. S., Dellsperger P., Hogan, C., Newnham, E.D., Shepherd, S.J., Steele, R.H., Wienholt, L. & Varney, M.D. 2015, 'Appropriate clinical use of human leukocyte antigen typing for coeliac disease: An Australasian perspective', Intern Med J, vol. 45(4), pp. 441-450.

Kaur, A., Shimoni, O. & Wallach, M. 2017, 'Celiac disease: from etiological factors to evolving diagnostic approaches', J Gastroenterol, vol. 52(9), pp. 1001-1012. https://doi.org/10.1007/s00535-017-1357-7.

Laderman, E.I., Whitworth, E., Dumaual, E., Jones, M., Hudak, A., Hogrefe, W., Carney, J. & Groen, J. 2008, 'Rapid, sensitive, and specific lateral-flow immunochromatographic point-of-care device for detection of herpes simplex virus type 2-specific immunoglobulin G antibodies in serum and whole blood', Clin Vaccine Immunol, vol. 15(1), pp. 159–163.

Lindhardt, C., Schönenbrücher, H., Slaghuis, J., Bubert, A. & Ossmer, R. 2009, 'Singlepath salmonella. Performance tested method 060401', JAOAC Int 2009, vol. 92(6), pp. 1885–1889.

Rong-Hwa, S., Shiao-Shek, T., Der-Jiang, C. & Yao-Wen, H. 2010, 'Gold nanoparticle-based lateral flow assay for detection of *staphylococcal* enterotoxin B', Food Chem, vol. 118(2), pp. 462–466.

Su, J., Zhou, Z., Li, H. & Liu, S. 2014, 'Quantitative detection of human chorionic gonadotropin antigen via immunogold chromatographic test strips', Anal Method, vol. 6, pp. 450-455.

Alkaladi, A., Abdelazim, A.M. & Afifi, M. 2014, 'Antidiabetic Activity of Zinc Oxide and Silver Nanoparticles on Streptozotocin-Induced Diabetic Rats', Int J Mol Sci, vol. 15(2), pp. 2015-2023. DOI:10.3390/ijms15022015.

Biagini, R.E., Sammons, D.L., Smith, J.P., MacKenzie, B.A., Striley, C.A.F., Snawder, J.H., Robertson, S.A. & Quinn, C.P. 2006, 'Rapid, sensitive, and specific lateral-flow immunochromatographic device to measure anti-anthrax protective antigen immunoglobulin G in serum and whole blood', Clin Vaccine Immunol, vol. 13(5), pp. 541–546. DOI: 10.1128/cvi.13.5.541-546.2006.

Tippkötter, N., Stückmann, H., Kroll, S., Winklemann, G., Udo, N., Scheper, T. & Roland, U. 2009, 'A semi-quantitative dipstick assay for microcystin', Anal Bioanal Chem, vol. 394(3), pp. 863-869. DOI:10.1007/s00216-009-2750-8

Li, Q., Liu, L., Chen, W., Peng, C., Wang, L. & Xu, C. 2009, 'Gold nanoparticle-based immunochromatographic assay for the detection of 7-aminoclonazepam in urine', Int J Environ Anal Chem, vol. 89(4), pp. 261–268. DOI: 10.1080/03067310802538493

Abadie, V., Sollid, L.M., Barreiro, L.B. & Jabri, B. 2011, 'Integration of Genetic and Immunological Insights into a Model of Celiac Disease Pathogenesis', Annu Rev Immunol, vol. 29(1), pp. 493-525.

Malamut, G., El Machhour, R., Montcuquet, N., Martin-Lannerée, S., Dusanter-Fourt, I., Verkarre, V., Mention, J-J., Rahmi, G., Kiyono, H., Butz, E.A., Brousse, N., Cellier, C., Cerf-Bensussan, N., & Meresse, B. 2010, 'IL-15 triggers an antiapoptotic pathway in human intraepithelial lymphocytes that is a potential new target in coeliac disease-associated inflammation and lymphomagenesis,' J Clin Invest, vol. 120(6), pp. 2131-2143.

Lee, J., Han, M. & Mirkin, C. 2007, 'Colorimetric Detection of Mercuric Ion (Hg^{2+}) in Aqueous Media using DNA-Functionalized Gold Nanoparticles', Angew Chemie, vol. 119, pp. 4171-4174.

Wang, Q., Liu, R., Yang, X., Wang, K., Zhu, J., He, L. & Li Q. 2016, 'Surface plasmon resonance biosensor for enzyme-free amplified microRNA detection based on gold nanoparticles and DNA super sandwich', Sens Actuators B Chem, vol. 223, pp. 613-620.

Slocik, J.M., Govorov, A.O. & Naik, R.R. 2011, 'Plasmonic circular dichroism of peptide-functionalized gold nanoparticles', Nano Lett, vol. 11(2), pp. 701-705. DOI: 10.1021/nl1038242.

Huang, C-C., Huang, Y-F., Cao, Z., Tan, W. & Chang, H-T. 2005, 'Aptamer-modified gold nanoparticles for colorimetric determination of platelet-derived growth factors and their receptors', Anal Chem, vol. 77 (17), pp. 5735-5741. DOI: 10.1021/ac050957q.

Brewer, S.H., Glomm, W.R., Johnson, M.C., Knag, M. K. & Franzen, S. 2005, 'Probing BSA binding to citrate-coated gold nanoparticles and surfaces', Langmuir, vol. 21(20), pp. 9303-9307. DOI: 10.1021/la050588t

Watson, J.C. & Thompson, W.F. 1986, 'Purification and restriction endonuclease analysis of plant nuclear-DNA', Method Enzymol, vol. 118, pp. 57-75.

Link, S. & El-Sayed, M.A. 1999, 'Size and temperature dependence of the plasmon absorption of colloidal gold nanoparticles', J Phys Chem B, vol. 103(21), pp. 4212-4217.

Jans, H., Liu, X., Austin, L., Maes, G. & Huo, Q. 2009, 'Dynamic light scattering as a powerful tool for gold nanoparticle bioconjugation and biomolecular binding studies', Anal Chem, vol. 81(22), pp. 9425-9432.

Al-Bayaty, H.F., Aldred, M.J., Walker, D.M., Newcombe, R.G., Smith, P.M. & Ciclitira, P.J. 1989, 'Salivary and serum antibodies to gliadin in the diagnosis of celiac disease', J Oral Pathol Med, vol. 18, pp. 578-581.

Volta, U., Tovoli, F. & Caio, G. 2011, 'Clinical and immunological features of celiac disease in patients with type 1 diabetes mellitus', Expert Rev Gastroenterol Hepatol, vol. 5, pp. 479-487.

Ventura, A., Magaz`u, G., Gerarduzzi, T. & Greco, L. 2002, 'Coeliac disease and the risk of autoimmune disorders', Gut, vol. 51, pp. 897.

Holmes, G.K. 2001, 'Coeliac disease and Type 1 diabetes mellitus- The case for screening', Diabet Med, vol. 18, pp. 169-177.

Kaukinen, K., Mäki, M., Partanen, J., Sievänen, H. & Collin, P. 2001, 'Celiac disease without villous atrophy revision of criteria called for', Dig Dis Sci, vol. 46(4), pp. 879-887.

Volta, U. & Villanacci, V. 2011, 'Celiac disease: diagnostic criteria in progress', Cell Mol Immunol, vol. 8, pp. 96-102.

Lee, J.S., Han, M.S. & Mirkin, C.A. 2007, 'Colorimetric Detection of Mercuric Ion (Hg^{2+}) in Aqueous Media using DNA-Functionalized Gold Nanoparticles', Angewandte Chemie, vol. 119, pp. 4171-4174.

Hung, Y.L., Hsiung, T.M., Chen, Y.Y., Huang, Y.F. & Huang, C.C. 2010, 'Colorimetric Detection of Heavy Metal Ions Using Label-Free Gold Nanoparticles and Alkanethiols', J Phys Chem C, vol. 114 (39), pp. 16329-16334.

Chen, G.H., Chen, W.Y., Yen, Y.C., Wang, C.W., Chang, H.T. & Chen, C.F. 2014, 'Detection of Mercury (II) Ions Using Colorimetric Gold Nanoparticles on Paper-Based Analytical Devices', Anal Chem, vol. 86 (14), pp. 6843-6849.

Chen, W., Cao, F., Zheng, W., Tian, Y., Xianyu, Y., Xu, P., Zhang, W., Wang, Z., Deng, K. & Jiang, X. 2015, 'Detection of the nanomolar level of total Cr[(iii) and (vi)] by functionalized gold nanoparticles and a smartphone with the assistance of theoretical calculation models', Nanoscale, vol. 7, pp. 2042-2049.

Wang, Q., Liu, R., Yang, X., Wang, K., Zhu, J., He, L. & Li, Q. 2016, 'Surface plasmon resonance biosensor for enzyme-free amplified microRNA detection based on gold nanoparticles and DNA supersandwich,' Sens Actuators B Chem, vol. 223, pp. 613-620.

Wang, J., Wu, Li., Ren, J. & Qu, X. 2011, 'Visualizing Human Telomerase Activity with Primer-Modified Au Nanoparticles', Small, vol. 8 (2), pp. 259-264.

Gao, H., Xiong, Y., Zhang, S., Yang, Z., Cao, S. & Jiang, X. 2014, 'RGD and Interleukin-13 Peptide Functionalized Nanoparticles for Enhanced Glioblastoma Cells and Neovasculature Dual Targeting Delivery and Elevated Tumor Penetration', Mol Pharm, vol. 11 (3), pp. 1042-1052.

Lee, G.Y., Qian, W.P., Wang, L., Wang, Y.A., Staley, C.A., Satpathy, M., Nie, S., Mao, H. & Yang, L. 2013, 'Theranostic Nanoparticles with Controlled Release of Gemcitabine for Targeted Therapy and MRI of Pancreatic Cancer', ACS Nano, vol. 7 (3), pp. 2078-2089.

Gupta, S., Andresen, H., Ghadiali, J.E. & Stevens, M.M. 2010, 'Kinase-Actuated immunoaggregation of Peptide-Conjugated Gold Nanoparticles', Small, vol. 6 (14), pp. 1509-1513.

Gupta, S., Andresen, H. & Stevens, M.M. 2011, 'Single-step kinase inhibitor screening using a peptide-modified gold nanoparticle platform', Chem Commun, vol. 47(8), pp. 2249-2251.

Rostami, K., Marsh, M.M., Johnson, M.W., Mohaghegh, H., Heal, C., Holmes, G., Ensari, A., Aldulaimi, D., Bancel, B., Bassotti, G., Bateman, A., Becheanu, G., Bozzola, A., Carroccio, A., Catassi, C., Ciacci, C., Ciobanu, A., Danciu, M., Derakhshan, M.H., Elli, L., Ferrero, S., Fiorentino, M., Fiorino, M., Ganji, A., Ghaffarzadehgan, K., Going, J.J., Ishaq, S., Mandolesi, A., Mathews, S., Maxim, R., Mulder, C.J., Neefjes-Borst, A., Robert, M., Russo, I., Rostami-Nejad, M., Sidoni, A., Sotoudeh, M., Villanacci, V., Volta, U., Zali, M.R. & Srivastava, A. 2017, 'ROC-king onwards: intraepithelial lymphocyte counts, distribution & role in coeliac disease mucosal interpretation', Gut, vol. 66, pp. 2080-2086.

Osman, A.A., Gunnel, T., Dietl, A., Uhlig, H.H., Amin, M., Fleckenstein, B., Richter, T. & Mothes, T. 2000, 'B cell epitopes of gliadin', Clin Exp Immunol, vol. 121, pp. 248-254.

Piaggio, M.V., Demonte, A.M., Sihufe, G., Garcilazo, S., Esper, M.C., Waggener, M. & Aleanzi, M. 1999, 'Serological diagnosis of celiac disease: anti-gliadin peptide antibodies and anti-tissue transglutaminase', Medicina, vol. 59, pp. 693-697.

Aleanzi, M., Demonte, A.M., Esper, C., Garcilazo S. & Waggener, M. 2001, 'Celiac disease: antibody recognition against native and selectively deamidated gliadin peptides', Clin Chem, vol. 47, pp. 2023-2028.

Wang, Z., Lee, J.H. & Lu, Y. 2008, 'Label-free colorimetric detection of lead ions with a nanomolar detection limit and tunable dynamic range by using gold nanoparticles and DNAzyme', Adv Mater, vol. 20(17), pp. 3263-3267.

Guo, Y., Wang, Z., Qu, W., Shao, H. & Jiang, X. 2011, 'Colorimetric detection of mercury, lead and copper ions simultaneously using protein-functionalised gold nanoparticles', Biosens Bioelectron, vol. 26(10), pp. 4064-4069.

Rujner, J., Socha, J., Barra, E., Gregorek, H., Madalinski, K., Wozniewicz, B. & Giera, B. 1996, 'Serum and salivary antigliadin antibodies and serum IgA anti-endomysium antibodies as a screening test for coeliac disease', Acta Paediatr, vol. 85, pp. 814-817.

Shang, L., Wang, Y. Z., Jiang, J. G., Dong & S. J. 2007, 'pH dependent protein conformational changes in albumin: gold nanoparticle bioconjugates: a spectroscopic study', Langmuir, vol. 23, pp. 2714-2721.

Lee, K., Kim, T., Lee, C.H. & Joo, S. W. 2008, 'Kinetics of gold nanoparticle aggregation: experiments and modeling', J Colloid Interface Sci, vol. 318, pp. 238-243.

Peng, H-P., Lee, K.H., Jian, J-W. & Yanga, A-S. 2014, ‘Origins of specificity and affinity in antibody–protein interactions’, Proc Natl Acad Sci, vol. 111, pp. E2656–E2665.